Hamburg University of Applied Sciences

Faculty Life Sciences

Plastic recycling: technical and economical evaluation of two different recycle loops

Master thesis

Process Engineering, M.Sc.

Submitted by

Diego Luna Victoria Torres

[redacted]

Hamburg

01.08.2023

Evaluator: Prof. Dr. Marc Hölling (HAW Hamburg)

Evaluator: Dr. Andrea Stooß (AFRY Deutschland GmbH)

This Master thesis was supervised and written in cooperation with the company AFRY Deutschland GmbH

Confidential Clause

The presented master thesis with the title: "Plastic recycling: technical and economical evaluation of two different recycle loops" is based on internal, confidential data and information of the company AFRY Deutschland GmbH. This work may only be available to the first and second reviewers and authorized members of the board of examiners. Any publication and duplication of this master thesis – even in part – is prohibited.

An exception of this arrangement requires the expressed permission of the company AFRY Deutschland GmbH.

_____ _____

Place, Date Signature

Affidavit

I hereby declare that this master thesis has been written only by the undersigned and without any assistance from third parties. I confirm that no sources have been used in the preparation of this thesis other than those indicated in the thesis itself.

_____ _____

Place, Date Signature

Abstract

In this work, two different recycling loops for plastic waste are investigated regarding technical and economic aspects. The aim of the processes is to produce light olefins (ethylene and propylene), which serve as feedstock for the production of polyolefins. The loops are referred as chemical recycling and combustion loop.

The chemical recycling loop consist of the pyrolysis of plastic waste with a product recovery section, in which the pyrolysis gas is treated to yield the olefin product. The combustion loop involves a more complex process, consisting of the incineration of plastic waste, with a subsequent flue gas cleaning process and a carbon capture unit, in which the CO_2 of the flue gas is captured to produce methanol through CO_2 hydrogenation. Afterwards, the crude methanol product is further processed in a methanol to olefins (MTO) unit, in which the olefin products are recovered after a hydrocarbon fractionation process.

The loops are compared regarding product yield, CO_2 footprint and capital cost of the equipment. The comparison is performed in base of the results of a process simulation, which is carried out with the help of process simulation software (EBSILON, DWSIM). The system boundary of the process comprises the unit operations from the input of the prepared plastic waste feed in the first unit of the loop (pyrolysis reactor/combustion chamber) up to the ethylene and propylene outlet in the product recovery section.

The results show that the combustion loop provides a better product yield and a lesser carbon footprint that the pyrolysis loop, with a selectivity of 79 wt.% compared to the 49 wt.% of the chemical recycling loop. The gap between the product yields becomes especially noticeable when the propylene yields are compared, then the combustion loop produces almost twice the amount of propylene that the chemical recycling loop. Regarding the ethylene yield and the produced CO_2, although the combustion loop performance is better, the results lie on a similar range.

However, when it comes to the capital cost and the energy demand, it comes out that the combustion loop requires much higher investments costs and amounts of energy. The results show that the combustion loop requires 52 times the power demand and 3 times the investment of the chemical recycling loop. The biggest issue in the combustion loop is the hydrogen demand for the CO_2 hydrogenation. This demand is covered by a Electrolyzer, which is the most expensive and simultaneously the most energy consuming unit in the loop.

Table of Contents

List of Figures

List of Tables

List of Symbols

Symbol	Description	Unit
a	Fitting parameter for reboiler heat duty (CCU)	-
A	First Arrhenius parameter for frequency factor	-
b	Fitting parameter for reboiler heat duty (CCU)	-
B	Second Arrhenius parameter for frequency factor	$\frac{\mathrm{J}}{\mathrm{mol}}$
D	Diameter	ft, m
d	Particle diameter	m
E	Pollutant concentration	$\frac{\mathrm{mg}}{\mathrm{Nm}^3}$
F	Factor for pressure vessel calculation	-
G	Carrier gas molar flow (CCU)	$\frac{\mathrm{kmol}}{\mathrm{h}}$
H	Column height	m, ft
k_1	Arrhenius frequency factor	$\frac{\mathrm{mol}^4}{{\mathrm{kg}_{\mathrm{cat}}}^4 \cdot \mathrm{s}^4 \cdot \mathrm{bar}}$
k_2	Arrhenius frequency factor	$\frac{\mathrm{mol}}{\mathrm{kg}_{\mathrm{cat}} \cdot \mathrm{s}}$
k_3	Arrhenius frequency factor	$\frac{\mathrm{mol}}{\mathrm{kg}_{\mathrm{cat}} \cdot \mathrm{s} \cdot \mathrm{bar}^{0.5}}$
k_4	Arrhenius frequency factor	$\frac{\mathrm{mol}}{\mathrm{kg}_{\mathrm{cat}} \cdot \mathrm{s} \cdot \mathrm{bar}}$
k_5	Arrhenius frequency factor	$\frac{\mathrm{mol}^2}{{\mathrm{kg}_{\mathrm{cat}}}^2 \cdot \mathrm{s}^2 \cdot \mathrm{bar}}$
K	Equilibrium constant	-
l	Combustion Air flow	$\frac{\mathrm{kg}}{s}, \frac{\mathrm{m}^3}{s}$
L	Pure solvent molar flow (CCU)	$\frac{\mathrm{kmol}}{\mathrm{h}}$
LG	molar liquid to solvent ratio (CCU)	-
$\dot{m}$	mass flow	$\frac{\mathrm{kg}}{s}$
n	number of stages/ number of trays	-
O	Reference O_2 concentration	Vol%

p	Pressure	bar
P	Power	kW
Q	Heat flow	kW
r	Reaction rate	$\frac{\mathrm{mol}}{\mathrm{kg_{cat}} \cdot \mathrm{s}}$
R	Universal gas constant	$\frac{\mathrm{J}}{\mathrm{mol} \cdot \mathrm{K}}$
T	Temperature	K
u	Gas velocity	$\frac{\mathrm{m}}{s}$
X	Molar solvent CO2 loading	-
x	Molar fraction	-
Y	Molar carried gas CO2 loading	-
α	Specific molar CO2 loading	-
ΔH	Specific heat, specific enthalpy	$\frac{\mathrm{kJ}}{\mathrm{kg}}$
ΔL	Length, length difference	m
Δp	Pressure difference, pressure drop	Pa
ε	Performance number	-
η	Efficiency	-
ϑ	Temperature	°C
λ	Air to fuel ratio	-
μ	Dynamic viscosity	$\mathrm{Pa} \cdot \mathrm{s}$
Π	Multistage compression ratio	-
ρ	Density	$\frac{\mathrm{kg}}{\mathrm{m^3}}$
ψ	Porosity	-

Indices:

Symbol	Description
0	Index 0, reference value
$\mathrm{amb.}$	Ambient temperature, ambient reference value
B	Reference value
c	Pressure vessel factor for cost calculation
cat	Catalyst
$\mathrm{CO_2, abs.}$	Absorbed CO2
$\mathrm{cold, out}$	Cold fluid outlet
cool	Cooling
$\mathrm{el.}$	Electrical
eq	Equation
$\mathrm{hot, in}$	Hot fluid inlet
i	Index
lean	Lean MEA solution
M	Measured value
ME	Methanol
min	Minimum
n	Number of stages
$\mathrm{pl.}$	Plastic feed
$\mathrm{py.}$	Pyrolysis
R	Reactor, reaction.
$\mathrm{Reb.}$	Reboiler
rich	Rich MEA solution

RS	Refrigeration system
RWGS	Reverse water gas shift reaction
th	Theoretical value

1 Introduction

Since the last century, plastics have become one of the most important materials for humankind. In fact, plastics are used in so many fields in daily life, that it is almost impossible to imagine living without plastic. The fields of application for plastics, also known as polymers, go from daily life products such as clothing, packing and toys to industrial products such as cars, ships, aircraft, telecommunications and even products in the medical branch, for example medical implants [1, p. 2].

The versatility of polymers relies on their mechanical, thermal, and chemical properties, like having a low density at solid state (suitable to produce light weight objects), a low thermal and electrical conductivity (good for insulation purposes) and being easily module into the desired shapes. Furthermore, plastic are low-cost materials and have a good chemical resistance and low degradation rates, which makes then a highly durable material [2, p. 1]. However, the last of these properties turns out to be huge disadvantage when it comes to the disposal of plastic waste.

Due to the lower degradation rate of polymers, plastic disposal has become a huge problem for the environment. Plastic waste can not only be found in Landfills, but also in the nature. Specially the contamination of the sea causes a lot of damage, not only in the environment, but also possibly to human health, for example in the case of microplastics. As the plastic demand is increasing and a suitable replacement for this material may be very difficult [2, p. 16], the recycling path to mitigate the environmental impact of plastics becomes constantly more relevant (see Figure 1).

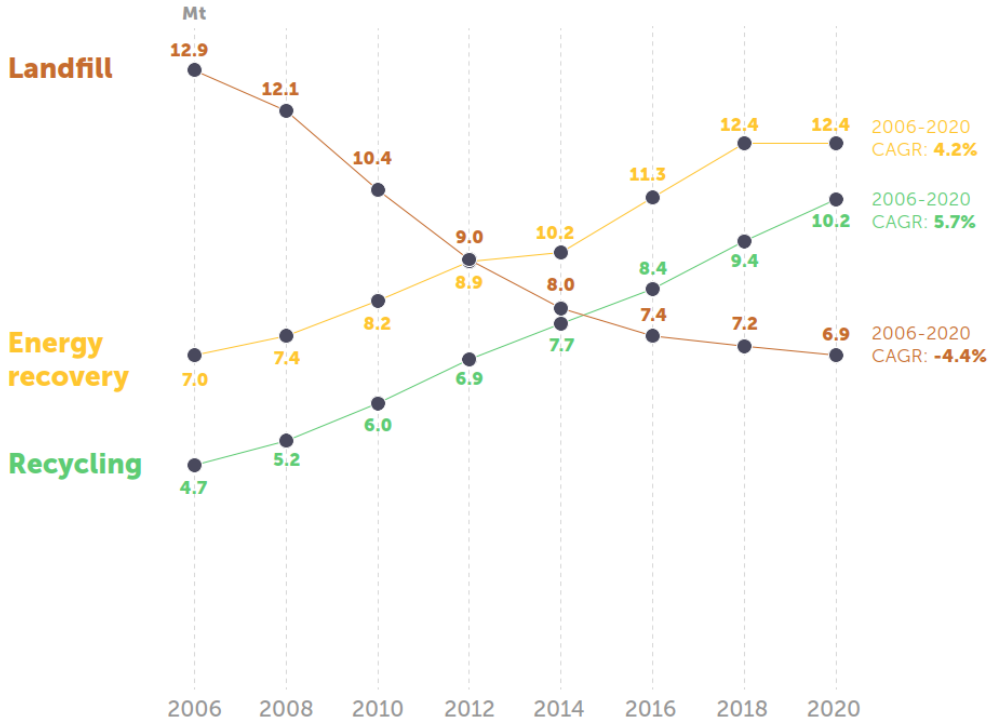

Figure 1: Evolution of post-consumer plastics waste treatment in million tons (Mt) per year in the European Union [3, p. 26].

There are many ways to reduce the plastic waste production. Reducing the consumption or reusing the plastic products to expand their lifespan are possible ways. Although these measures help to mitigate the damage caused by plastic waste, further measures are

still required. As plastics can be considered an important source of valuable chemicals (mainly hydrocarbons) and energy [2, p. 15], chemical recycling and energy recovery could become feasible recycling methods.

In this work, two recycling loops for plastics are investigated. The first one is the chemical recycling loop, in which valuable chemicals can be recovered from plastic waste through thermal degradation. The second one is the combustion loop, in which plastic waste is burned to recover energy. Additionally, the flue gas from the combustion is further processed to obtain valuable chemical products (CO_2 utilization). In both cases, the obtained compounds can be used as feedstock for producing new plastics.

The aim of this master thesis is to perform a technical and economical evaluation of two different recycling loops (chemical recycling loop and combustion loop) for polyolefins. A process flow model for the two different loops will be developed, including mass and energy balances for the later comparison with the help of simulation software, conversions rates and further data from the literature. For the process model, a polyolefin mixture will be considered as feedstock.

Additionally, the possible impact on the environment is considered, for example the CO_2-Footprint of the implemented processes. Furthermore, the technology readiness level (TRL) of each process is investigated to evaluate which of the technologies is more likely to be applied in the near future. Finally, a cost estimation of the processes is required to evaluate which of the technologies is economically more suitable.

2 Theoretical Background of Plastics and Plastic Recycling

The aim of this chapter is to present basic concepts of plastics and plastic recycling. Furthermore, the technical background of the processes implemented in the investigated recycle loops will be explained. These concepts serve as a base to build the process models for the technical analysis and to estimate costs for the economical evaluation.

2.1 Classification of Hydrocarbons

For most plastics, the raw material from which the feedstock for the polymerization process (monomers) is obtained are hydrocarbon gases gained from the petrochemical industry. Moreover, in the process of plastic feedstock recycling, for example the process of thermal degradation, the obtained product is usually a mixture of different hydrocarbons [4, pp. 6-4]. As a consequence of this, an overview about the different types of hydrocarbons that can be found in such mixtures is presented in this chapter.

The hydrocarbons that can generally be found in petroleum refining process, for example fluid catalytic cracking, are classified into paraffins, olefins, naphthenes and aromatics [5, p. 48]. The chemical structure of propane (paraffins), ethylene (olefins) and benzene (aromatics) are depicted in Figure 2.

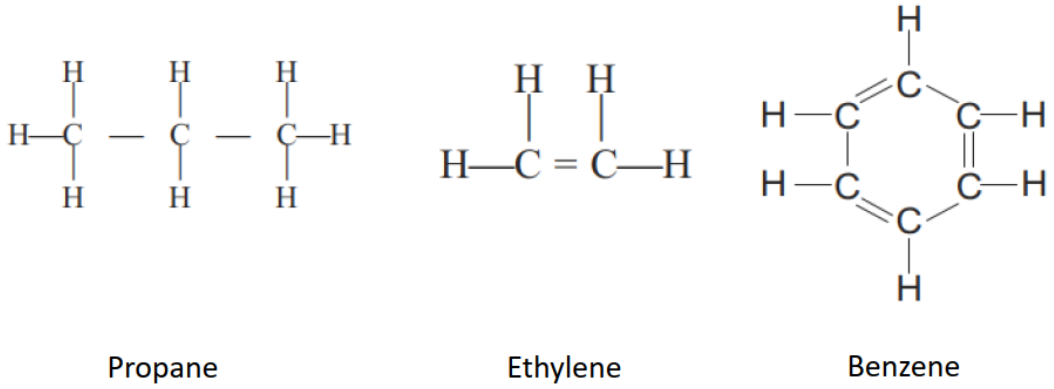

Figure 2: Chemical structure of propane (paraffins), ethylene (olefins) and benzene (aromatics) [5, pp. 49-51].

As presented in Figure 2, hydrocarbons are basically molecules composed of carbon atoms chains bounded with hydrogen atoms in different shapes. According to their chemical structure, different chemical, physical or thermal properties arise.

2.1.1 Paraffins

Also known as alkanes, paraffins are single-bounded hydrocarbon chains with different lengths. The general chemical formula for paraffins, which counts the amount of carbon and hydrogen atoms present in the molecule, is C_nH_{2n+2}. Paraffins are described as "saturated hydrocarbons", then all possible carbon bounds are completely occupied with hydrogen atoms. Common examples for paraffines are methane, ethane, and propane, with methane being the simplest alkene [6, p. 24].

2.1.2 Olefins

Olefins, also named alkenes, are unsaturated hydrocarbons. In contrast to paraffins, not all possible bounds in the carbon atoms are filled with hydrogen, but with double carbon bounds. Olefins have the chemical formula C_nH_{2n}. The simplest of the olefins is ethylene. Other examples are propylene, 1-buten and 1-penten [6, p. 53].

2.1.3 Naphthenes and Aromatics

Contrary to paraffins and olefins, naphthenes and aromatics are not hydrocarbon chains, but have a cyclic or a ring shape. Naphthenes are saturated hydrocarbon rings with the formula C_nH_{2n}. Aromatics are molecules that contain at least one unsaturated resonance stabilized benzene ring (see Figure 2). Aromatics have chemical formula C_nH_{2n-6}. Common examples for aromatics are benzene and toluene [5, pp. 50-51].

2.2 Monomer Production

The process to obtain plastics from raw materials begins with the petroleum and the petrochemical industry, in which the monomers are gained in polymer grade quality to be further processed via polymerization into the final product. The petrochemical industry produces not only plastics, but several chemicals derived from petroleum, such as rubbers, fibres, paints, solvents, and detergents [7, p. 101].

Petroleum is processed in a refinery and separated through fractional distillation into different products, such as liquified petroleum gas (LPG), naphtha, kerosene, diesel, and several oils (see Figure 3).

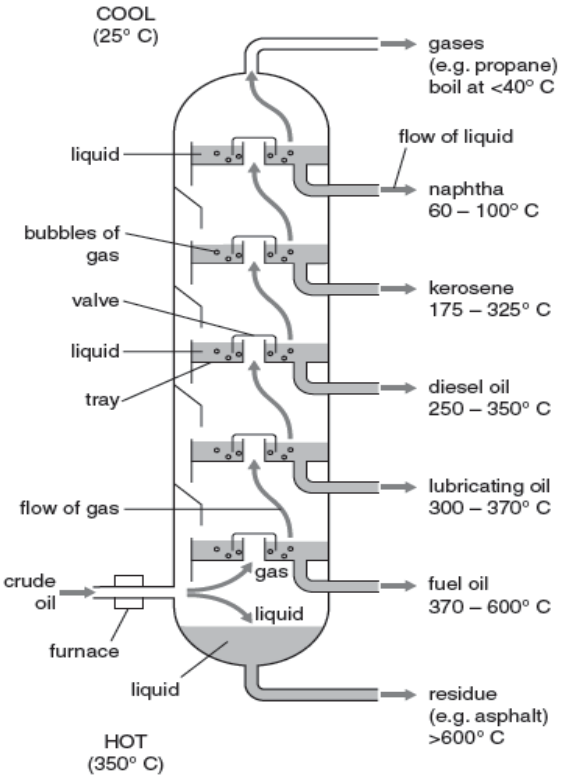

Figure 3: Overview on the fractional distillation of crude oil [8, p. 3].

The products are separated thermally due to their different boiling points, with the light boiling fractions, such as LPG or Naphtha accumulating at the top of the column and the high boiling components, such as the distillation residue and heavy oils, accumulating in the bottom of the column. Additionally, the heavy petroleum fractions can be further upgraded into lighter distillates by a fluid catalytic cracking unit (FCCU) [9, p. 75].

The different obtained petroleum fractions are mostly employed as fuels or chemical feedstocks for other processes. In case of the petrochemical industry, natural gas and refinery products are the most important source of raw materials. The overall process for monomers production in the petrochemical industry is presented in Figure 4.

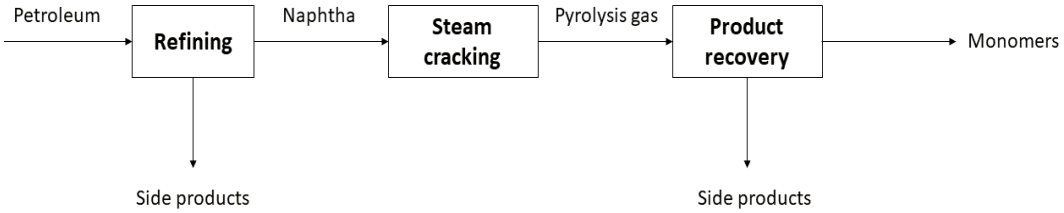

Figure 4: Overview on the monomer production in the petrochemical industry.

To produce olefins, the most widely used feedstock is naphtha obtained from petroleum refineries [7, p. 101 ff.], which is converted into lighter hydrocarbons through a process named cracking (sometimes also called steam cracking or pyrolysis). In the case of ethylene, the cracking of naphtha is the most employed production path worldwide [10, p. 43].

Additionally, other feedstocks such as natural gas liquids (ethane, propane, and n-butane), gas oils or whole crude oils can also be processed in industrial cracking units. In the case of the USA, as a result of the availability of low-price natural gas in Canada and the Artic regions of North America, ethane and propane are preferred as raw materials for olefin production [11, p. 614].

As an alternative to thermal cracking, olefins can be produced through other routes using nonoil feedstocks, such as the methanol to olefins process (MTO)(see chapter 2.2.2), which employs methanol, sometimes mixed with water, as a raw material to produce basic petrochemicals through a catalytic reaction [12, p. 1922].

2.2.1 Steam Cracking

Steam cracking is the most employed process for the production of olefins, using naphtha or natural gas liquids as feedstock. Basically, this technology consists of the endothermic dehydrogenation of saturated hydrocarbons to produce mainly ethylene, propylene, and other byproducts such as C4-hydrocarbons (butane, butene, etc.), and pyrolysis gasoline rich in BTX-aromatics (benzene, toluene and xylene) [13, p. 66 ff.].

In conventional cracking plants, the feedstock is mixed with steam, which is known as "dilution steam", and introduced in a furnace. In the cracking furnace, the mixture is heated to temperatures about 850 to 950 °C for gaseous feedstock and 750 °C for heavy feedstocks at pressures about 1.7 to 2.5 bars. The required heat is provided by gas or oil-fired burners. The ratio of steam to hydrocarbon can vary from 0.2 to 1 kg steam per kg hydrocarbon feed [13, p. 66].

In addition to the cracking furnace, steam cracking plants are composed of several unit operations, starting from the cracked gas at the furnace outlet to the purified final

products. An overview of a conventional cracking plant for the production of Ethylene is depicted in Figure 5.

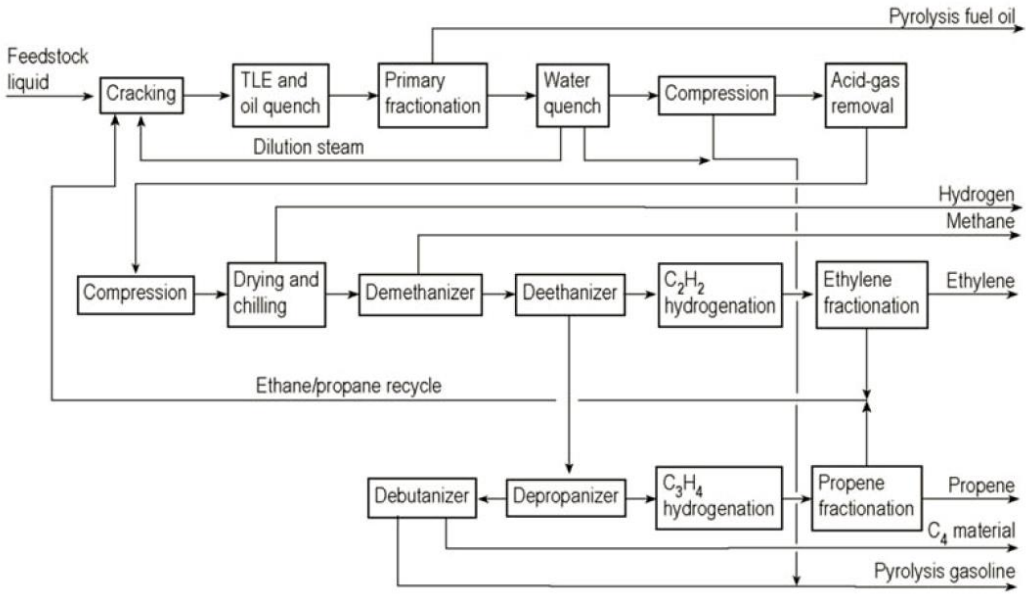

Figure 5: Overview of a cracking plant for the production of ethylene [14, p. 504].

After the hot pyrolysis gas leaves the cracking furnace, it needs to be rapidly quenched (fast cooling) to avoid undesired reactions that would otherwise lead to loss of ethylene and propylene. This is achieved by transfer line exchangers (TLE), which are steam generators located at the outlet of the furnace.

The pyrolysis gas in the TLE is cooled down through indirect cooling to temperatures about 650 to 400 °C. The heat recovered in the TLE is used to produce high pressure steam, which can be further employed to drive the compressors in other parts of the plant. The TLE is followed by additional heat exchangers in which temperatures drop down to 300 °C [15, p. 429].

Afterwards, the cooled pyrolysis gas goes into the primary fractionation, in which it is further cooled down by direct quenching with pyrolysis oil to temperatures around 100 °C [14, p. 500]. In this section, an oil fraction with high boiling components is separated from the gas stream (see pyrolysis fuel oil in Figure 5). The heat recovered from this quenching section can be used to generate steam for other parts of the plant. The obtained pyrolysis oil is employed as fuel for the plant or to produce coke or carbon black [14, p. 499].

The next unit operation is the water quench tower. In this part, the pyrolysis gas is cooled down to temperatures about 37-48 °C by recirculating quench water [16, p. 16]. A part of the recirculating water is separated from the loop and pretreated with filters and coalescers to separate oil impurities from the quench water before being feed to the steam stripper, in which the dissolved volatile compounds in the water are recovered and feed back to the pyrolysis gas stream (see Figure 6).

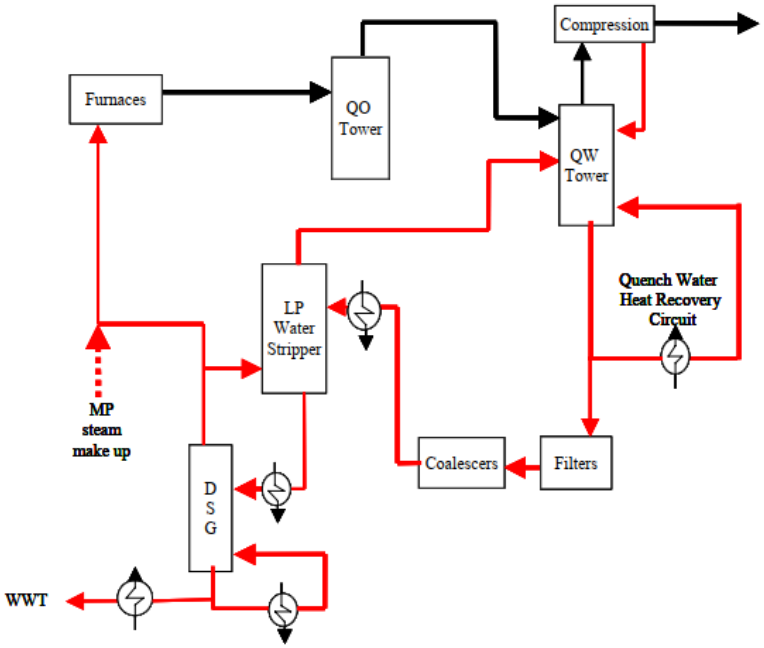

Figure 6: Overview on the loop of the quench water column, steam stripper (water stripper) and the dilution steam generator on an ethylene plant (red line represents the steam/water stream, black line depicts the pyrolysis gas stream) [17, p. 2].

The recovered water at the bottom of the steam stripper heads to the dilution steam generator, forming a closed loop between the furnace and the quench water column. A part of the generated dilution steam is recycled to the steam stripper, while the other remaining part is used as a feed for the furnace. Middle pressure steam at 14 barg and 260 °C is condensed to generate the dilution steam. A small part of this overheated steam (MP steam make up in Figure 6) is mixed with the dilution steam to raise its temperature slightly above superheated before being headed to the furnace [17, p. 2].

After most of the dilution steam is recovered in the quench water tower, the gas enters the compression stage (see Figure 5). Here, the pyrolysis gas undergoes several compression stages (usually 4 to 5 stages) with intermediate cooling with cooling water [14, p. 502]. After every intermediate cooling step, condensate is removed and treated to recover hydrocarbons and water. Some of the recovered liquids, especially the ones condensing in the first compression stages, are fed back to the water quench system for water and hydrocarbons recovery (see Figure 5).

Between the compression stage 3 and 4 (or 4 and 5), an acid gas removal is carried out to remove carbon dioxide and hydrogen sulfide from the pyrolysis gas stream. This is usually done with a caustic washer using a NaOH solution. Carbon dioxide is removed because it can freeze in the further cryogenic processes in the plant. Moreover, it is absorbed into the ethylene stream, which can damage the product quality. Hydrogen sulfide is also a potential product contaminant. However, this component is also corrosive and can poison the catalyst used in the further processes downstream the plant (e.g., Acetylene hydrogenation or polymerization processes) [14, p. 502].

Afterwards the final compression stage, the pyrolysis gas enters a drying unit, in which the remaining moisture is removed to prevent water freezing in the refrigeration system. The drying is mostly carried out with molecular sieves, alumina, or silica gel packed towers [11, p. 624]. Subsequently, the dried gas enters the refrigeration system, in which the gas is cooled down to temperatures about -140 to -160 °C, which allows to

separate the hydrocarbons from hydrogen through partial condensation before entering the cryogenic distillation units [14, p. 506].

The last unit operations in the ethylene plant are the distillation units for hydrocarbon recovery. This section consists of six columns in which different hydrocarbon fractions are recovered [11, p. 624] [14, p. 506 ff.]:

- Demethanizer: in this column, a methane rich stream containing hydrogen and carbon monoxide residues is separated from the other hydrocarbons and gained at the top of the column.
- Deethanizer: the C2-fraction (ethylene and ethane) is separated from the main stream and obtained at the top of the column.
- C2-splitter: this column separates ethylene from ethane, gaining ethylene at the top and ethane at the bottom of the column.
- Depropanizer: C3-components (propylene and propane) are obtained at the top of the column.
- C3-splitter: in this unit operation, propylene and propane are separated, with propylene at the top and propane at the bottom of the column.
- Debutanizer: in this column, the remaining C4-fraction is recovered at the top of column. Pyrolysis gasoline, rich in BTX-aromatics, is obtained at the bottom of the column.

Additionally, a removal of acetylenic compounds present in the gas stream is required. In the case of acetylene, it is a contaminant which damage the catalyst in polymerization units [18, p. 8]. In case no acetylene product is desired, a selective catalytic hydrogenation unit is employed to convert acetylene into ethylene using the recovered hydrogen from the refrigeration system [14, p. 512 ff.].

There are mainly three configurations for acetylene hydrogenation in an ethylene plant: raw-gas, front-end and tail-end hydrogenation. These configurations are presented in Figure 7, with scripts 1, 2 and 3 representing the raw-gas, front-end and tail-end configuration respectively.

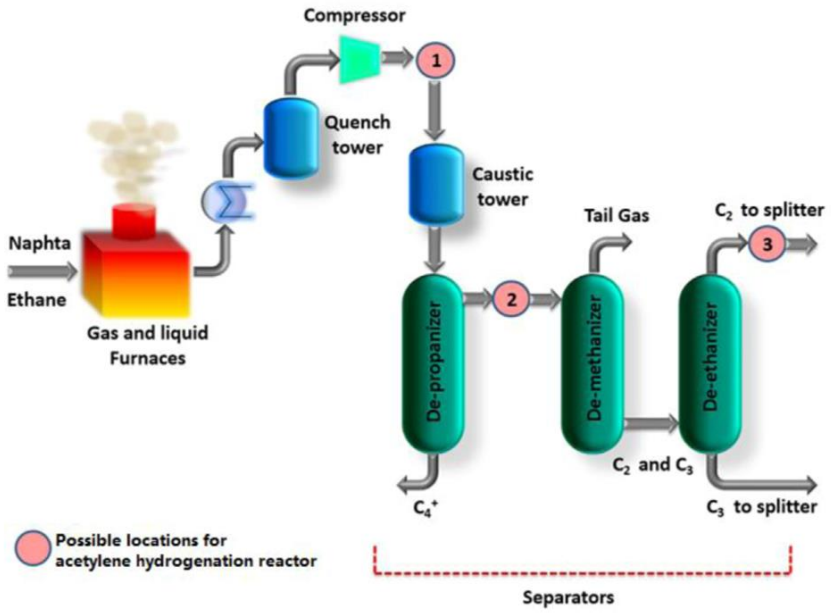

Figure 7: Schema of a cracking plant representing the possible location of the acetylene hydrogenation unit operation [18, p. 9].

The most employed configuration in ethylene plant is the tail-end configuration, with the acetylene hydrogenation located at the top stream of the deethanizer column [18, p. 10]. Additionally, if C3-alkynes are present in the gas stream, a second hydrogenation reactor to remove these compounds has to be placed in the top stream of the depropanizer column (see C_3H_4 hydrogenation in Figure 5). If an acetylene product is desired, a solvent scrubbing unit can also be used as an alternative [11, p. 624].

There are several ways to sort the order of the distillation columns. The most employed orders in ethylene plants are three: demethanizer first with tail-end hydrogenation, deethanizer first with front-end hydrogenation and depropanizer first with front end hydrogenation [14, p. 503]. The process depicted in Figure 5 corresponds to the first alternative, while the configuration in Figure 7 (variant Nr. 3) represents the third option.

Finally, the obtained side products such as Ethane and propane can either be used as fuels for the plant or sent to a second cracking reactor to be further cracked to maximize olefin yield. The obtained cracked gas can be subsequently recycled into the main pyrolysis gas stream (see Figure 5).

In case of the C4 fraction, it can be either recycled or upgraded in order to be obtained as a product or undergo a hydrogenation process in order to be recycled back to the cracking unit. The recovered hydrogen obtained by chilling can be purified and either used in the hydrogenation processes occurring in the plant, as a fuel or sold. Finally, the pyrolysis gasoline can be sold as a fuel after hydrotreatment or as a feedstock for aromatics production [14, p. 499].

2.2.2 Methanol to Olefins (MTO)

The MTO process offers the possibility to produce basic petrochemicals from non-crude oil feedstock. The process is a variant of the methanol to gasoline process (MTG), in which light olefins are intermediates in the reaction. By selecting a suitable catalyst and operation conditions, the process can be altered to maximize olefin yields. [19, p. 159].

This technology has become popular in China, which employs coal as a main resource to produce methanol and subsequently olefins. There are mainly four technologies available for the MTO process [20, p. 561 ff.]:

- UOP/Hydro MTO Process
- DMTO/DMTO II (dimethylether/methanol to olefins)
- Methanol to Olefins-Sinopec
- Lurgi Methanol to Propylene (MTP)

The UPO/Hydro-MTO was the first process to be industrially applied and nowadays remains to be the most popular technology for the MTO process. In case of China, the DMTO/DMTO II has the biggest market share (about 64-70% in 2019) [20, p. 561 ff.].

The conversion of methanol to olefins is an exothermic catalytic reaction, which employs zeolite catalysts (e.g., SAPO-34). The reaction is carried out at temperatures around 330-500 °C and pressures at approximately 1.1 to 1.5 bar [13, p. 73]. A simplified flowsheet of the MTO process is shown in Figure 8.

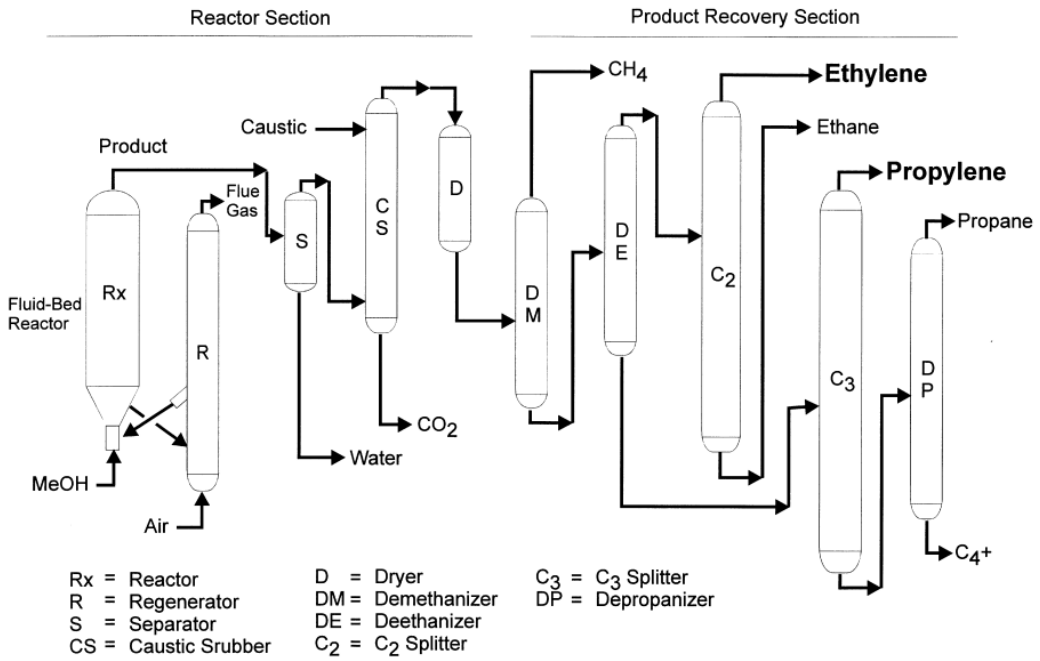

Figure 8: Simplified flowsheet of the UOP/Hydro MTO-Process for polymer-grade products [21, p. 64].

As shown in Figure 8, the process can be divided into the reaction and the product recovery section. The principal component in the MTO process is the fluidized bed reactor, in which methanol is converted to olefins with dimethylether as an intermediate [13, p. 72]. Ethylene, propylene, and byproducts such as water, methane, C4-C6 hydrocarbons, and coke are produced with nearly 100% methanol conversion [22, p. 328].

Coke is an undesired product which deposits on the catalyst, leading to catalyst deactivation. Therefore, the catalyst is continuously regenerated through combustion with air in a regenerator placed beside the reactor (see Figure 8). However, the presence of small amounts of coke in the catalyst favors light olefins selectivity. Therefore, the coke content in the catalyst is maintained on an average of approx. 8 wt.%. This is achieved by adjusting the catalyst residence time in the reactor [12, p. 1932].

The heat produced in the regeneration is used to produce steam, which can be further used to control the temperature and to remove the heat of the reactor [13, p. 74]. The further processing of the gaseous reactor effluent is similar to the processing of the pyrolysis gas in steam cracking, especially in the product recovery section. Key differences appear in the quenching section. A detailed overview of the reactor set up is shown in Figure 9.

In contrast to steam cracking, no significant amounts of tar and high boiling components, such as pyrolysis oils, are present in the gas. Therefore, a water quench tower with steam stripping to recover the dissolved volatile compounds in the quench water are sufficient for the quenching section. Additionally, a few heat exchangers are placed for heat recovery and feed reactor preheating (see Figure 9).

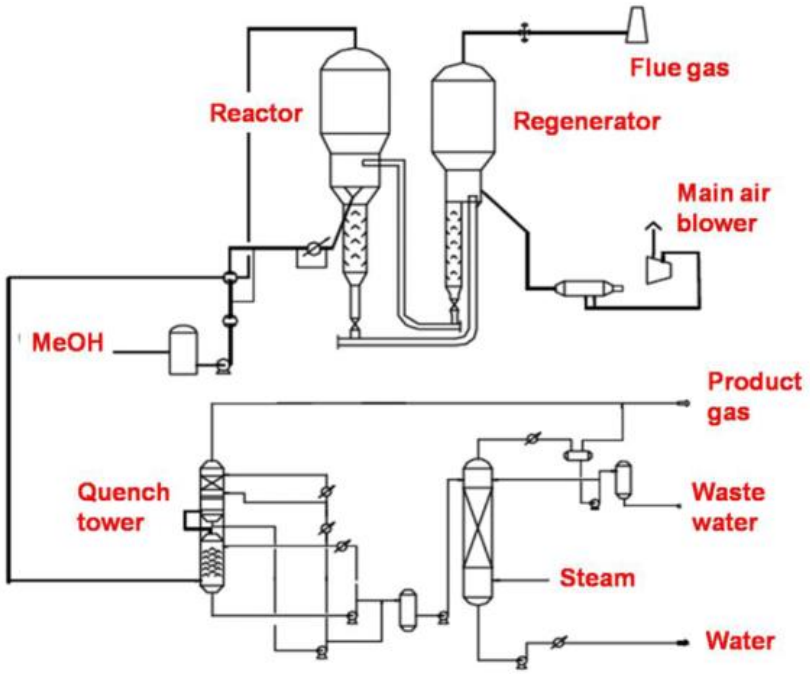

Figure 9: Overview on a DMTO unit with its quenching section [12, p. 1933].

In the next step, the gas is compressed and prepared for the cryogenic part of the product recovery section. The compression section and the caustic washer set-up are the same as in the steam cracking processes and have been previously described in chapter 2.2.1.

The product recovery section of the MTO process is very similar to the one in the steam cracking process. However, the MTO product fractionation is much simpler. As no diolefins or acetylenic compounds are present in the MTO product, acetylene hydrogenation units are not required [23, p. 92]. Furthermore, the amounts of C5+ hydrocarbons (hydrocarbons with more than 4 carbon atoms) in the stream are very low. Hence, no debutanizer is necessary (see Figure 8).

Additionally, there are some cases in which the propane amount in the stream is so low, that chemical-grade propylene can be produced without a C3-Splitter [23, p. 94]. However, this may not apply for polymer-grade requirements, as these are higher than chemical grades (see Figure 8).

Another difference between the steam cracking and the MTO product recovery section is that C3-Splitter and the depropanizer have switched positions (see Figure 5 and Figure 8). Furthermore, in some process set ups, a DME recovery unit could be placed to convert the unreacted methanol into DME and recycle it back to the reactor. Optionally, it is possible to recycle the C4+ products by adding a cracking unit to increase light olefin yields [13, p. 74 ff.].

2.2.3 Other Processes

There are alternative technologies for the industrial production of light olefins (ethylene and propylene). However, these technologies have small share in the market compared to the leading commercial processes (e.g., steam cracking). Therefore, these technologies will be described shortly in this chapter. The main alternative production pathways for ethylene and propylene can be summed up as follows:

- Ethanol dehydration: Ethylene is obtained through catalytic dehydration of ethanol, producing water as a byproduct. Selectivities of over 99% can be achieved. Bioethanol can be used as a feedstock [14, p. 515 ff.], which would make this technology a potential environmentally friendly alternative.
- Fluid Catalytic Cracking (FCC): Ethylene and propylene can be recovered from the off gas of a FFC unit in petroleum refineries [14, p. 521].
- Heavy oil feedstocks: Ethylene and propylene are obtained as a byproduct through cracking of unprocessed hydrocarbon feedstocks (e.g., vacuum gas oil) [14, p. 521].
- Fisher-Tropsch process: Olefins are obtained as a byproduct from the production of gasoline, diesel fuel and other compounds from syngas [14, p. 521].
- Ethane and propane dehydrogenation: Ethylene and propylene are produced from the catalytic dehydrogenation of ethane and propane (e.g., catofin process, olefex process, Linde process) [24, p. 286 ff.], respectively.

2.3 Classification of Polymers

Although the words "plastic" and "polymer" are often treated as synonyms, strictly speaking this is not always the case. The concept of polymer refers to large molecules, also known as macromolecules, composed by a large number of repeating units. The basic feedstock for producing polymers, also known as "building blocks" are called monomers. Monomers undergo a process called polymerization, in which the monomers are combined to form many polymer chains or sometimes a network structure [1, p. 9].

Under this definition, some compounds produced in nature are included, for example polysaccharides like cellulose, proteins such as silk or casein and Polynucleotides (DNA and RNA) [1, p. 9]. However, most of the polymers with commercial application are not natural but synthetic materials. Usually, this kind of compounds are referred as plastics. Although it is not very easy to strictly define the term "plastic", it can be said that all plastics are polymers, but not all polymers are plastics. Furthermore, plastics are usually not exclusively composed of polymers, but they do incorporate other compounds such as additives and fillers to improve their properties [2, p. 4].

Under the previously mentioned definition of polymers, a huge number of possible materials with different properties arise. For this reason, various categories have been created to classify the variety of polymers (see Figure 10).

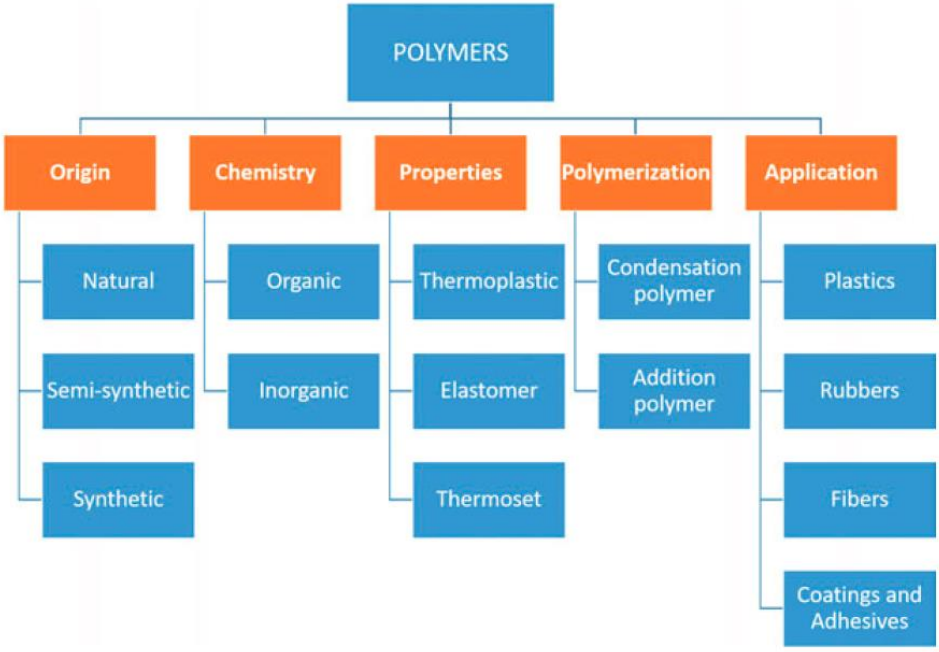

Figure 10: Different ways to classify Polymers based on origin, chemistry, physical/thermal properties, polymerization route and application [1, p. 10].

Regarding the presented categories in Figure 10, it may be noted that plastics are mostly of synthetic origin and carbon-based compounds(organic). Respecting the other categories of polymers, except for the application category, plastics can be found mostly in each of them. However, two of these categories are essential from the polymer recycling point of view: the physical/thermal properties and the polymerization mechanism, then the most suitable method for the degradation of a polymer is strongly linked with the two previous mentioned characterization criteria [2, p. 4].

2.3.1 Polymerization Mechanism

According to the polymerization mechanism, polymers are classified into two different groups:

- Addition polymers: Polymerization occurs by chemical combination of a large number of monomer molecules into the growing polymer chain. The process develops without the separation of any compounds during the reaction. Consequently, the resulting polymers have the same chemical composition as the used monomers [2, pp. 7-8]. Most addition polymerizations occur through continuous addition of double carbon bounds, such as the polymerization of ethylene to polyethylene (PE) or propylene to polypropylene (PP) [1, p. 11].
- Condensation polymers: In contrast to addition polymers, byproducts are produced during the polymerization process (mostly water or hydrochloric acid). Common examples for condensation polymers are polyamides and polyesters [1, p. 11].

2.3.2 Physical and Thermal Properties

According to their physical and thermal properties, polymers can be classified into three groups (see Figure 11):

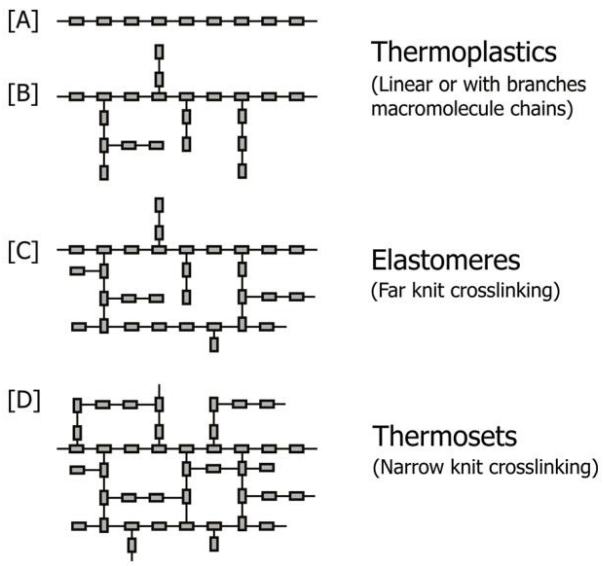

Figure 11:Macromolecular structure of thermoplastics ([A] linear structure, [B] side chains), elastomers [C] and thermosets [D]. Polymer classification according to physical/thermal properties [25, p. 8]

- Thermoplastics: About 90% of the produced plastics belong to this category. This type of polymers is composed of separate linear [A] or branched [B] polymer chains (see Figure 11). Due to the absence of covalent bounds between the polymer chains, thermoplastics can be easily melted by heating and solidified by cooling. This behavior facilitates the reprocessing of thermoplastics waste, which makes then a very suitable material for the recycling process. Examples of this category are Polyethylene (PE), polypropylene (PP) and polyethylene terephthalate (PET) [1, p. 11].
- Thermosets: Contrary to thermoplastics, the polymer chains in thermosets are linked by strong covalent bonds, forming three-dimensional network structures (see Figure 11). Consequently, once a thermoset has been processed into a particular shape, the reprocessing or remodeling by heating is not possible. An example for this category is polyurethane (PU) [2, pp. 5-6].
- Elastomers: This type of polymer has, like thermosets, a network macromolecular structure formed by covalent bounds between the polymer chains. However, the quantity of these bounds is less than in the case of thermosets. This new structure provides the polymer with elastic properties. An example for this kind of polymer are rubbers [2, pp. 6-7].

2.3.3 Polyolefins

Polyolefins are not a plastic category per se. They are a group of thermoplastics that are produced from the polymerization of olefins (see chapter 2.1.2), concisely from ethylene and propylene, producing polyethylene and polypropylene respectively [26]. Among the major synthetic polymers, polyethylene costs the least. The overall chemical equation for the polymerization of polyethylene is depicted as follows [27, p. 4]:

$$n(C_2H_4) \xrightarrow{\text{catalyst}} \sim(CH_2CH_2)_n\sim \quad (1)$$

In equation (1) n is defined as the degree of polymerization. For commercial polyethylene, this value is generally greater than 1000 [27, p. 4]. As stated in the presented chemical equation, the polymerization of PE is triggered by a catalyst.

Polymers have a huge field of application. Nevertheless, plastic packaging is, with approximately 40% share of the total amount, the major field of consumption [2, p. 2]. The most used polymers for the production of plastic packaging are polyolefins [28, p. 10].

In Europe, Polyolefins represent almost 50% of the plastic consumption. Polyolefins can be classified into four different plastics [26]:

- Low-density polyethylene (LDPE): LDPE is a flexible and though material with a density range between 0.91 and 0.94 g/cm³. Is mostly used to produce carrier bags, agricultural film, and electrical cable coatings.
- Linear low-density polyethylene (LLDPE): LLDPE is similar to LDPE but has higher resistance to mechanical stress. Additionally, it is a very flexible material with good chemical resistance. Some examples of application are industrial packaging film and thin-walled containers.
- High density Polyethylene (HDPE): HDPE is a harder and more opaque material that LDPE and LLDPE. Furthermore, compare to LDPE and LLDPE, HDPE has higher resistance to mechanical stress and can withstand higher temperatures. It has a density range between 0.93 and 0.97 g/cm³. Mostly, is used to produce crates, boxes, bottles, food containers, toys petrol tanks, pipes, and houseware.
- Polypropylene (PP): PP is a though and flexible material with higher resistance to mechanical stress but lower chemical resistance that the other types of polyethylene. With a density range between 0.895 and 0.92 g/cm³ is the polyolefin with the lowest density. Polypropylene is commonly used to produce food packaging, carpet fibres, medical packaging, luggage, and pipes.

In summary, polymers can be classified into distinct categories according to different criteria. Due to the thermal properties, chemical structure, polymerization mechanism, and important share in the plastic production, thermoplastics and additive polymers are very suitable for reprocessing. As most of these plastics belong to the family of polyolefins, this group of plastics becomes relevant when addressing the topic of feedstock plastic recycling.

2.4 Plastic Recycling

As stated before, plastics play an important role in the present global economy. Moreover, their relevance seems to be increasing drastically with the passage of time. In 2021, the worldwide plastic production amounted to 390.7 million tones (see Figure 12). Compared to the last century, only 1.5 million tons of plastic were produced in 1950 [1, p. 3]. The evolution of the worldwide plastic production is depicted in Figure 12. Additionally, the amount of produced fossil based, recycled, and bio-based plastics in the recent years is presented in Figure 13.

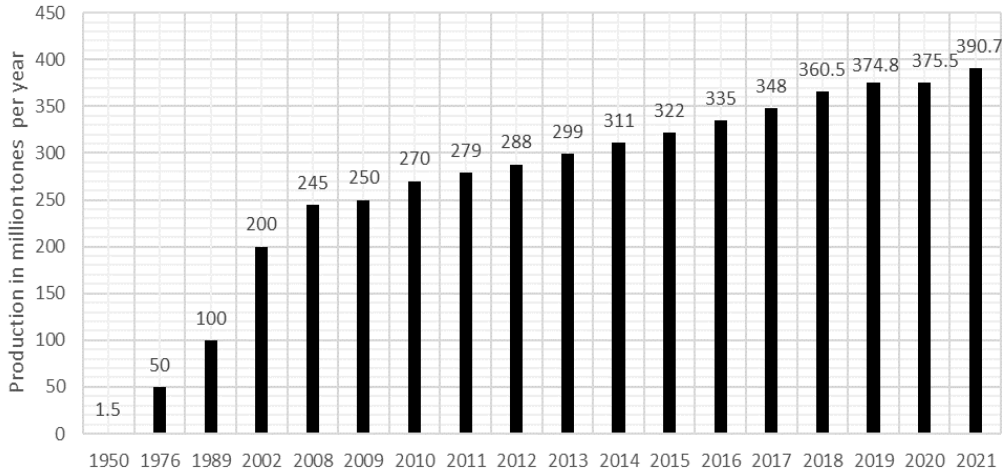

Figure 12: Evolution of the global plastic production [29, p. 2] [30, p. 16].

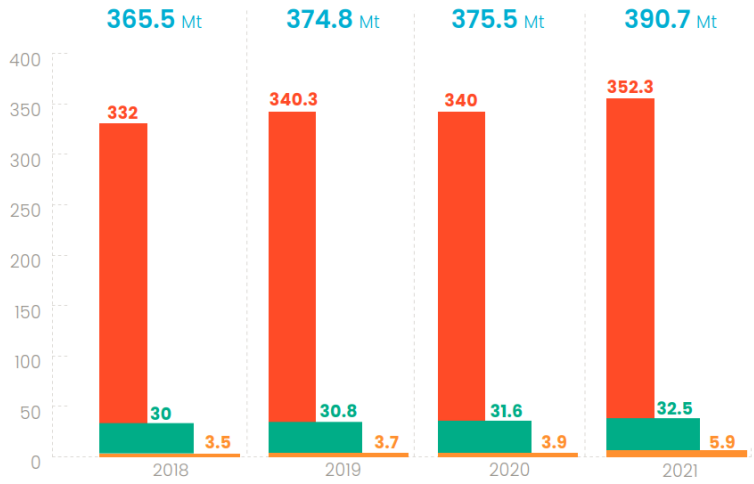

Figure 13: Plastic production in million tons between 2018-2021 for fossil-based plastics (red), post-consumer recycled plastics (green) and bio-based plastics (orange) [30, p. 16].

As presented in Figure 12, the plastic production is constantly increasing since 1950. Furthermore, most of the plastics worldwide are produced from fossil-based feedstock (e.g., Petroleum), while recycled plastics represent only a small amount of the total produced plastics (see Figure 13). Consequently, an increasing production leads to a continuous increase in the generation of plastic waste. Alongside all the benefits that plastics provide, the consequences of the increasing plastic waste represent a serious environmental issue.

Plastic industry is nowadays still dominated by a linear model of production and consumption. This means plastic is mostly manufactured from raw materials to be later sold, used and disposed. However, this model has been dominating not only the plastic industry, but most of the overall production of goods as well. Nevertheless, as the increasing consumption leads to the overexploitation of natural resources, resulting into environmental issues, a new economic model has been proposed to address these emerging problems: The circular economy model [31]. According to Plastics Europe, 9.8% of the produced plastics worldwide in 2021 were circular plastics (see Figure 14).

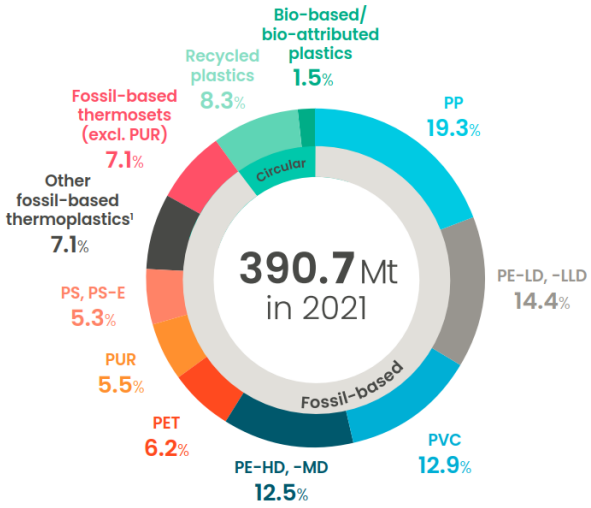

Figure 14: Produced plastics worldwide by feedstock (fossil-based/circular plastics) and type (PP, PE, PVC, etc.) [30, p. 21].

In contrast to the predominating linear economy model, the circular economy model is basically a restorative and regenerative closed loop economy. In this model, waste is not generated. This means, materials are not disposed but kept circulating in and contributing to the economy. This model was proposed by the Ellen McArthur Foundation and has the aim to decouple global economic development from finite resource consumption [32].

The circular economy model of the Ellen McArthur Foundation comprises of two paths: a biological cycle, in which products are made from renewable materials (e.g., Bioplastics), and the technical cycle, which involves the management of stocks of finite materials [32]. The presented recycling loops in this work belong to the technical cycle.

In the case of plastics, which are mostly made of a non-renewable feedstock, the 3R model is proposed by the Ellen McArthur Foundation. The 3R model promotes to reduce, reuse, and recycle plastic products. This translates into reducing the consumption of raw materials, for example by not purchasing unnecessary products (reduce), extending the lifespan of the products as long as possible and using then in many purposes as possible (reuse) and waste collecting at the end of the product lifespan for reprocessing into new raw materials for new products (recycling) [1, p. 205].

Regarding plastic recycling, four different types of recycling can be implemented depending on the stage in the production chain. An overview about the production and recycling process of plastic is presented in Figure 15.

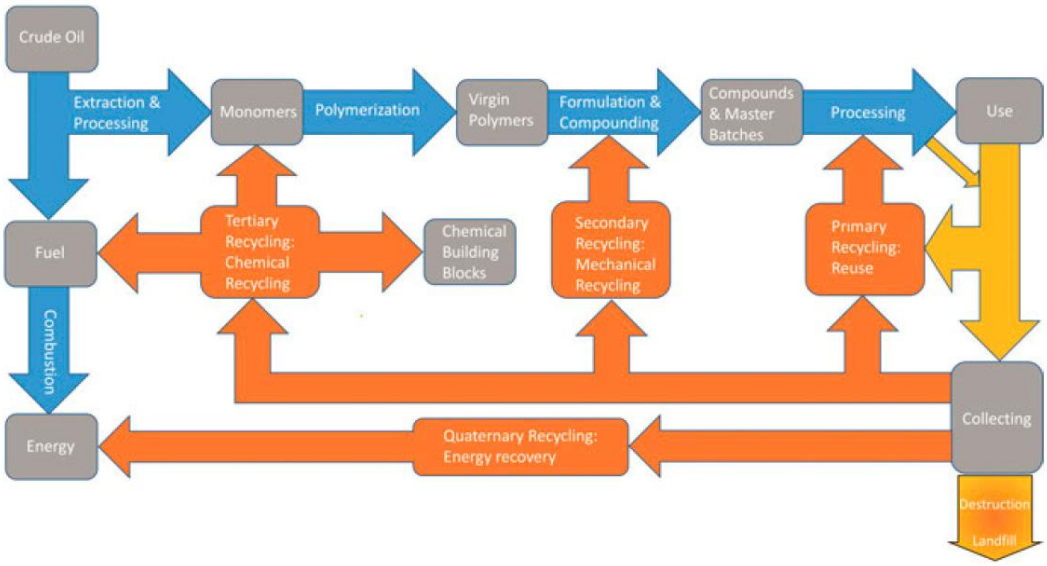

Figure 15: Schematic representation of the different types of recycling (primary, secondary, tertiary and quaternary recycling) and their implementation in the plastic production chain [1, p. 206].

The four types of plastic recycling are primary recycling (reuse), secondary recycling (mechanical recycling), tertiary recycling (chemical recycling) and quaternary recycling (energy recovery). The suitable method for the plastic waste is chosen depending on the degree of contamination with organic or inorganic material, such as other polymers or impurities [28, p. 14]. Additionally, the molecular structure of the plastic type also serves as a determining factor to choose a suitable recycling process (see chapter 2.2).

2.4.1 Primary Recycling/Reuse

Primary recycling consists of collecting uniform and not contaminated plastic waste to be later used for the same purpose as the original product. This process can be implemented with or without the help of auxiliary products. In practice, however this type of recycling is mostly carried out by reusing in-plant scrap to manufacture plastic products by reprocessing. When applied to collected plastic waste, this type of recycling is used for packaging products, for example bottles, bags, etc. [1, p. 206] [2, pp. 16-17].

2.4.2 Secondary Recycling/Mechanical Recycling

Mechanical recycling comprises several processes for reprocessing plastic waste into new products leaving the macromolecular structure of the polymer intact. In contrast to primary recycling, which is mostly used for pre-consumer waste (in-plant scrap), secondary recycling is applied to post-consumer plastic waste. Post-consumer waste is highly contaminated and requires further preparation before reprocessing [28, p. 14].

Firstly, the plastic waste has to be collected, sorted, and cleaned. Afterwards, the material is regrinded and remelted into new plastic products [28, p. 14]. However, the recycled polymers often show lower properties and performance as virgin materials. Therefore, the recycled plastic is used for products that require less performance than the original material. As secondary recycling requires the processed material to be melted by heating, this type of recycling is restricted to thermoplastics [2, pp. 19-20].

2.4.3 Tertiary Recycling/Chemical Recycling

Chemical recycling, also known as feedstock recycling, is usually applied when the quality of the recycled material produced by mechanical recycling is not sufficient [28, p. 15]. Contrary to secondary recycling, in chemical recycling the macromolecular structure of the polymer is degraded to produce a variety of products, which can vary from the starting monomers to diverse hydrocarbon mixtures [2, p. 20].

The produced feedstock from chemical recycling has comparable properties and quality to the feedstock produced by non-renewable sources and can be applied to produce several chemicals and fuels. Examples of feasible processes for feedstock recycling are chemical depolymerization, gasification, thermal degradation (pyrolysis), catalytic cracking and reforming, and hydrogenation [2, p. 20].

Chemical recycling is currently limited by the economic viability of the process. Feedstock recycling is at the present day only feasible for a minority of polymers, such as polymethylmethacrylate (PMMA) and polyether ether ketone (PEEK). However, the chemical process has been technically proven for other polymers, such as polyolefins [28, p. 15].

In the past, many projects for feedstock recycling were not successful due to relative low prices of the obtained products. For the process to be economically feasible, three main factors have to be considered: the pre-processing expenditure to meet the required purity of the raw wastes, the value of the obtained products and the investment for the process facilities [2, pp. 20-21].

The main problems of chemical recycling can be summarized into high capital expenditure, lack of regional plastic waste supply to realize continuous operation of large-scale plants, and the wide range of compounds obtained in the product mixture in some feedstock recycling process, such as Pyrolysis and hydrogenation, then the obtained mixture requires further processing, mostly a refining process, to obtain the desired final products [2, pp. 20-21].

2.4.4 Quaternary Recycling/Energy Recovery

The energy recovery path is the last resort for plastic waste that is so highly contaminated that it cannot be reprocessed through the other three previously mentioned recycling types [33, p. 273]. Quaternary recycling means the incineration of plastic waste in Waste to Energy facilities (WTE) to produce heat. This process is also known as combustion. The combustion heat is used to produce steam, which can be further used to produce electricity [28, p. 5].

Quaternary recycling is only feasible for very heterogenous waste. Consequently, plastic is generally not incinerated pure, but mixed with other waste [33, p. 5]. The principal goal of waste incineration is to reduce the volume and mass of the solid waste that ends in the landfills [28, p. 5]. Although the energy value of plastic waste is recovered, solid waste (ash) and flue gas remain after the combustion process and have to be disposed. This means, the full value of the plastic waste is not being obtained. For this reason, this type of recycling does not fulfill the requirements of the circular economy model.

The biggest problem of waste incineration is the generation of carbon dioxide (CO_2) emissions, which nowadays is a dangerous pollutant in the context of global warming [28, p. 70]. Although energy recovery represents the least circular path in terms of plastic recycling, most of the plastic ends in waste to energy facilities. According to

Plastics Europe, 42 % of a total of 29.5 million tones waste plastic produced by the European Union plus Norway, Switzerland, and the United Kingdom in 2020 was used for energy recovery. In comparison, only 35% plastic waste was processed in recycling facilities (see Figure 16).

Figure 16: Post-consumer plastic waste management in the European Union plus Norway, Switzerland, and the United Kingdom in 2020 [30, p. 48].

Nevertheless, new efforts are being done by the plastic industry regarding the transition to a circular economy. Among such efforts is the inclusion of feedstock produced by carbon capture and storage technologies (CCU) into plastic production [3, pp. 7-11], making possible to use the CO_2 produced in incineration facilities to produce new plastics.

2.5 Plastic Recycling Loops

There are several methods to target the production of circular plastics. For this work, the focus will rely on the chemical recycling and the energy recovery path. Two approaches will be presented in this chapter: the chemical recycling loop and the combustion loop. An overview of these paths and their connection with the plastic production process is presented on Figure 17.

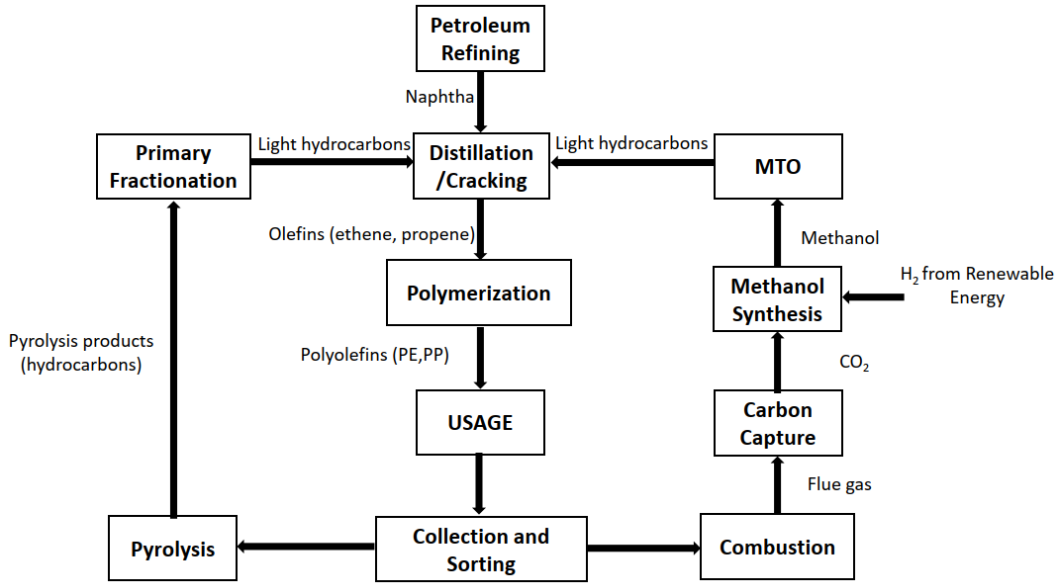

Figure 17: Overview of the chemical recycling loop (left), combustion loop (right) and plastic production path (center).

The chemical recycling loop involves the thermal degradation of plastic and subsequently a refining process. The combustion loop combines plastic waste incineration with carbon capture technologies (CCU), methanol synthesis with hydrogen supply from renewable energies, and finally the conversion of methanol to olefins (MTO). The two methods aim to gain valuable feedstock at the end of the process path. This feedstock consists of ethylene, propylene and other side products that can be use either as a chemical feedstock for other processes or as a fuel.

2.5.1 Chemical Recycling Loop

The chemical recycling loop explained in this work consists of the treatment of plastic waste with pyrolysis. In plastic pyrolysis, the feedstock is heated and cracked in an inert atmosphere to avoid undesired reactions (e.g. combustion). The process takes place generally at atmospheric pressures. The obtained pyrolysis gas is then cooled down and treated to obtain different product fractions (liquid and gaseous products) and a solid residue (char) [4, p. 6].

There exist mainly two possibilities for plastic pyrolysis [34, p. 76]: low temperature pyrolysis to produce pyrolysis oil and waxes, which can be further processed to monomers in a steam cracking plant, or high temperature pyrolysis to obtain the valuable gaseous feedstock directly from the plastic waste in one step.

2.5.1.1 Low Temperature Pyrolysis

Low temperature pyrolysis favors the yield of liquid products. In this variant, the cracking is carried out at temperatures of approximately 300 to 600°C, depending on the feedstock [4, p. 6 ff.]. The pyrolysis process can be carried out thermally (thermal cracking) or with the help of a catalyst (catalytic cracking).

For the production of liquid fractions (e.g., gasoline, kerosine and diesel), catalytic cracking has several advantages over thermal cracking: it lowers the activation energy and cracking temperature, increases the reaction rate, and improves the selectivity and quality of the desired products, which improves the process efficiency and lowers the energy consumption [35, p. 386]. An example of a commercial process for catalytic cracking of plastic waste is the Thermofuel process. The process flow diagram of this technology is depicted in Figure 18.

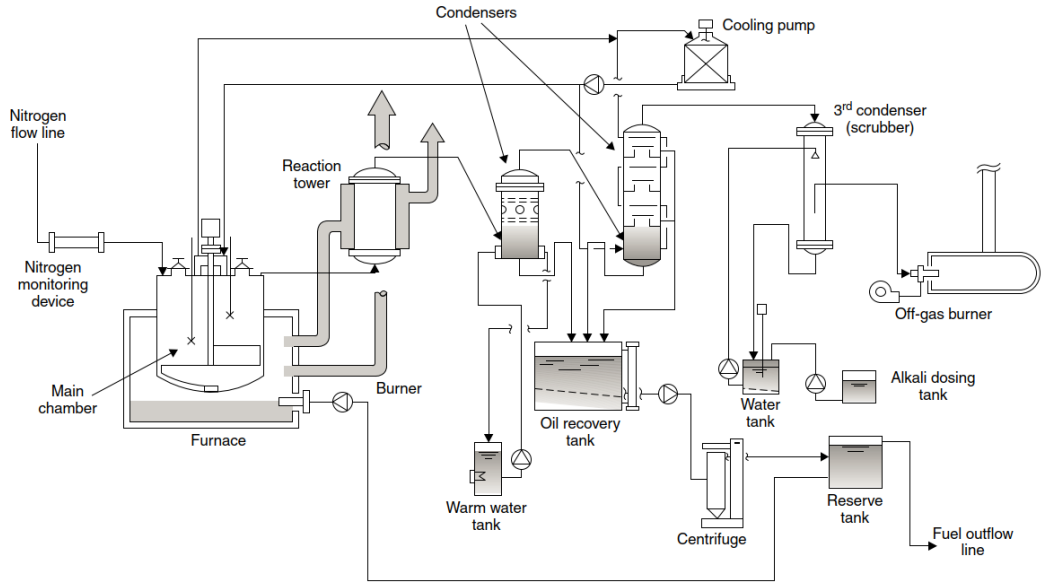

Figure 18: Overview on the Thermofuel process (catalytic cracking) [35, p. 409].

The Thermofuel process is designed to yield diesel from plastic waste. Plastic waste is melted and cracked in the main chamber at temperatures about 350-425°C. The main chamber is heated by burning a part of the fuel product. The exhaust gases exiting the main chamber are used to heat the reaction tower, in which the pyrolysis gas from the main chamber is catalytically upgraded at 220 °C to increase the quality and yield of the desired products [35, p. 407 ff.].

Afterwards, the upgraded pyrolysis gas is separated into a liquid and gaseous fraction. The liquid products are obtained in a two-step condensation process. The gaseous fraction is first purified in a scrubber with alkali to be further burned in the off-gas burner. The solid carbonous char accumulates in the walls of the main chamber and has to be continuously removed [35, p. 407].

Although the catalyst is not consumed or poisoned in the process, some char residues also accumulate in the metal plates of the reaction tower, which results in fouling. Therefore, the reaction tower needs to be treated periodically. The produced fuel in the Thermofuel process is equivalent to regular diesel [35, p. 407 ff.].

2.5.1.2 High Temperature Pyrolysis

High temperature pyrolysis occurs at temperatures above 600°C and is usually performed without a catalyst (thermal cracking). A high reaction temperature promotes higher yields of low boiling components and less coking tendency [4, p. 8 ff.]. However, more energy input is needed to achieve the required high temperatures. An example for thermal cracking of plastic waste is the Hamburg process, which was carried out at the University of Hamburg. An overview of a pilot plant for this technology is presented in Figure 19.

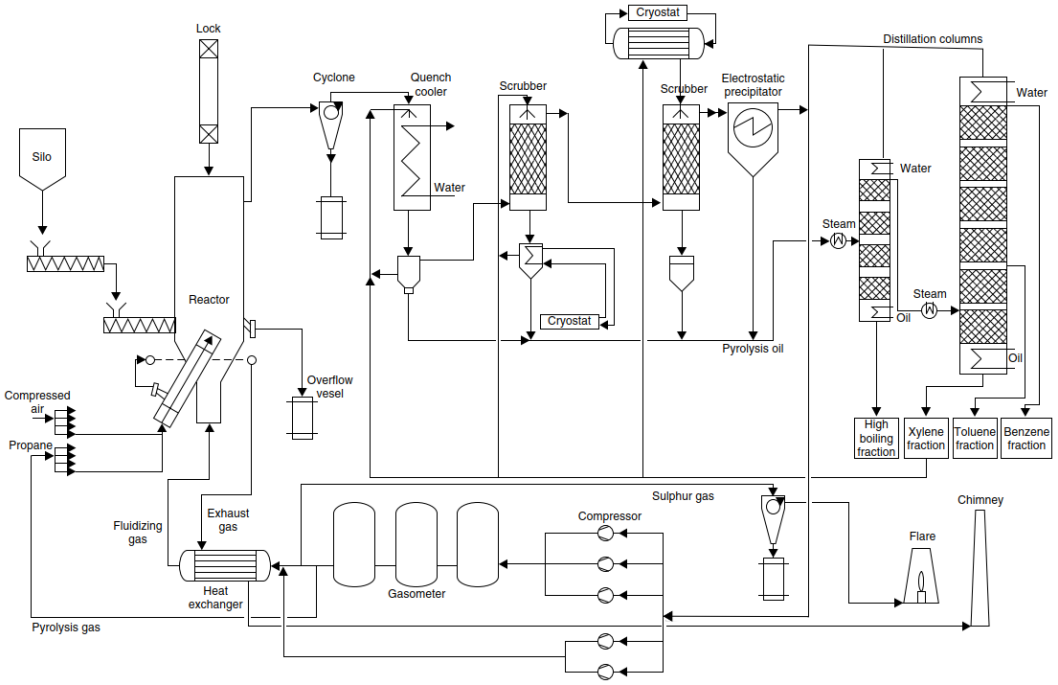

Figure 19: Process flow diagram of a pilot plant for the Hamburg process for plastic waste pyrolysis [36, p. 477].

The core of the Hamburg process is the fluidized bed reactor. The solid feedstock is feed into the sand-bed through two screw conveyors connected in series. The required heat for the reactor is provided through indirect gas heating with fire tubes, which are located diagonally in the reactor bed. Propane gas is burned at plant start-up for the reactor heating. When continuous operation is achieved, a part of the gaseous products is use as fuel for the reactor heat [36, p. 475 f.].

The hot pyrolysis gas leaves the reactor at the top and enters the cyclone, in which solid particles such as soot or fillers are separated from the stream. Afterwards, the gas enters a series of quenching units, in which the gas is cooled down to ambient temperature and a liquid fraction is recovered [37, p. 173]. The recovered liquids are further processed in two absorption towers, in which a second liquid fraction is recovered. Finally, the obtained liquid fractions are separated into 4 fractions in two distillation columns. The xylene fraction is recycled and used a quenching medium in the quenching units (see Figure 19).

The original set-up for the Hamburg process is design to recover BTX-Aromatics from mixed plastic waste or old tires. Additionally, a gaseous side product is obtained, which mainly severs as a fuel for the reactor. In this case, pyrolysis takes place at temperatures about 600-900 °C using pyrolysis gas as a fluidizing medium [37, p. 166 ff.]. Approximately 40-70% of the produced gas fraction is needed for the reactor heating [37, p. 178]. The rest can be used as fluidizing gas for the reactor. If no gaseous products are desired, the excess gases can be burned in a flare (see Figure 19).

However, the production of a rich olefin gaseous fraction can be achieved by using steam instead of pyrolysis gas at temperatures about 690-700 °C with short residence times [36, p. 483]. Experiments using a light fraction of household waste separation as feedstock, mainly consisting of polyolefins (95.8% PE and PP), polystyrene (3%) and PVC (0.2 %) [36, p. 483], show that gaseous product yields equivalent to naphtha

crackers are possible with this alternative. A detailed comparison of the main gaseous products is shown in Table 1.

Table 1: Comparison of the product yields of plastic waste pyrolysis with steam as fluidizing gas with conventional steam cracking yields [34, p. 86].

Products (wt. %)	Polyolefin Pyrolysis (Steam)	Steam Cracking (LPG)	Steam Cracking (Naphtha)
Ethylene	31	31	29
Propylene	14	22	16
Butene, butadiene	8	13	10
Pyrolysis gasoline	23	8	24
Other gaseous products	24	26	21
Ethylene and propylene	45	53	45

As shown in Table 1, the yield of ethylene and propylene is similar to that of the steam cracking process. However, the steam cracking of gaseous feedstock (in this case LPG) produces the highest yield of light olefins. Nevertheless, it shows a potential alternative to produce petrochemical feedstock from recycled material.

To avoid undesired chlorine compounds in the products, especially in the gaseous fraction, HCl compounds coming from the PVC are absorbed by adding calcium oxide in the reactor feed. The produced $CaCl_2$ can later be separated in the cyclone at the outlet of the reactor. Results for a mixed plastic feed containing 4% PVC show that, by adding CaO in a 5 wt.% fraction to the feed, no chlorine compounds are later present in the gas fraction, but small impurities of about 15 ppm can be found in the oil product [36, p. 482].

If the presence of large PVC fractions cannot be avoided, it is safer to produce first a waxy-oil product that can be analyzed and, if free of chlorine compounds, then fed in a steam cracker mixed with naphtha [36, p. 486]. On the other hand, if only olefins such as PE and PP are used as feedstock, monomer recovery (ethylene and propylene) through distillation, e.g. in a steam cracking purification facility, becomes a potential path for chemical plastic recycling.

2.5.2 Combustion Loop

The combustion loop presented in this work combines chemical recycling with energy recovery (tertiary and quaternary recycling). The process consists of burning plastic waste, following several unit operations to clean the exhaust gas from impurities and subsequently produce monomers feedstock for polyolefins (PE und PP). The process can be divided into following unit operations: Combustion, exhaust gas cleaning, carbon capture unit (CCU), electrolysis unit, methanol synthesis loop, and methanol to olefins (MTO) unit.

2.5.2.1 Combustion Process

Combustion is an exothermal chemical reaction in which a burnable substance (fuel), which is usually rich in carbon and hydrogen, is oxidized to produce mainly carbon dioxide and water, and other impurities such as sulfur dioxide (SO_2), hydrogen chloride (HCl), NO_x-compounds and Carbon monoxide (CO) [38, p. 9 ff.]. The resulting

composition of the exhaust gas from the combustion process depends mainly on the combustion temperature and the composition of the feed.

The oxygen required for the process can be provided from ambient air or with pure oxygen (Oxyfuel-Combustion), although combustion with air is the most commonly used technology [39, p. 18]. To ensure a complete oxidation of the fuel, combustion is carried out with over stoichiometrically dosed air [39, p. 19]. The amount of dosed air is represented with the Air-fuel ratio λ, which is defined as follows:

$$\lambda = \frac{l}{l_{\min}} \tag{2}$$

With l as the actual amount of used air and $l_{\min}$ as the minimum required air amount for stoichiometrically combustion. The value of λ is normally higher than 1 and varies depending on the feedstock [39, p. 20]. As l and $l_{\min}$ have the same composition, it is possible to represent λ as mass, volume or mol based ratio.

Several technologies exist for carrying out the combustion process according to the physical state of the fuel (solid, liquid, or gaseous). Regarding solid fuel, combustion in a fluidized bed, grate firing, and dust firing are the usually employed technologies [38, p. 519]. In the particular case of waste incineration, grate firing is the most employed technology on an industrial scale [40, p. 298]. An overview of a process of a grate firing waste incineration plant is presented in Figure 20.

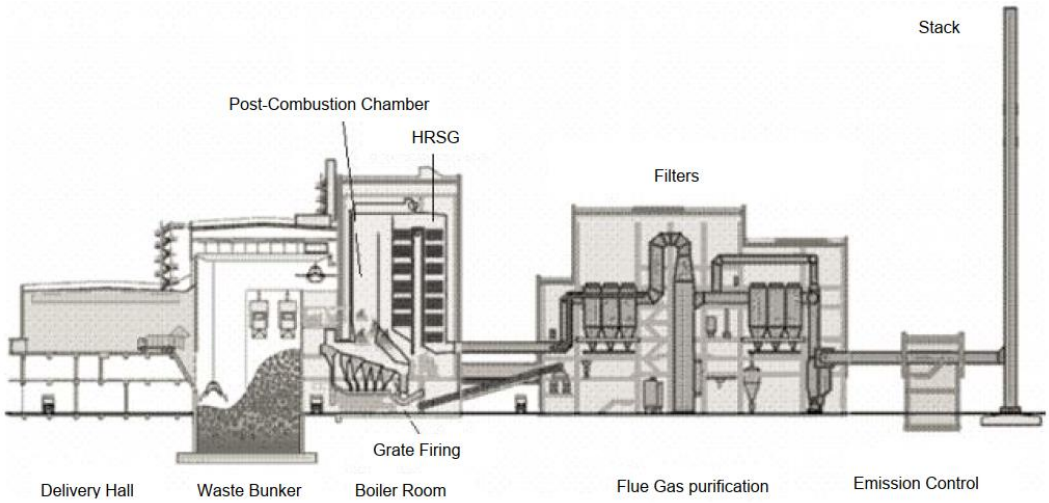

Figure 20: Overview on the waste incineration process [40, p. 298].

The waste incineration process can be described as follows: waste is delivered per truck (delivery hall) and brought into the waste bunker. From here, the waste is transported with a crane into the boiler room and subsequently the combustion chamber. The grate firing consists of inclined moving grates which transport the waste from the entry to the slag discharge, while combustion air flows from the bottom of the air through the waste [40, p. 298].

Afterwards, unburned compounds that could not be combusted in the grate are burned with secondary air in the post combustion chamber. Next, the flue gases exiting the post-combustion chamber enter the heat recovery steam generator (HRSG). The steam produce in this unit can be used to generate electrical power in a turbine or for other heating purposes in the plant.

Finally, the cooled flue gas enters the purification section. This part of the plant consists of multiple unit operations (e.g., filters, absorption units) in which the flue gas is cleaned from undesired pollutants. Before the flue gas is sent to the environment in the stack, the remaining pollutants concentration has to be measured to ensure that the local emission regulations are fulfilled.

2.5.2.2 Flue Gas Purification

Flue gas purification is a multistep process, in which different pollutants are separated from the main gas stream to meet the local emission regulations. In case of waste incineration, pollutants such as ash, acid gases (SO_2, HCl), NH_3 and NO_x compounds can be present in the flue gas stream [40, p. 312 ff.]. The emission limits for waste incineration facilities according to the European regulation (best available techniques - BAT) from 2019 for the previous named pollutants are shown in Table 2.

Table 2: Emissions regulation for waste incineration plants according to the BAT [41].

Compound	New plant	Existent plant	Unit
Dust/ash	2-5	2-5	$\frac{mg}{Nm^3}$
HCl	2-6	2-8	$\frac{mg}{Nm^3}$
SO_2	5-30	5-40	$\frac{mg}{Nm^3}$
NO_X	50-120	50-150	$\frac{mg}{Nm^3}$
NH_3	2-10	2-10	$\frac{mg}{Nm^3}$

The concentrations for the emission limits are given in a dry basis and based in an oxygen content of 11 vol%. For the removing of ash, fabric and/or electro filters are employed. In case of the acid gases, absorption units with a liquid solvent (wet variant) or adsorption units with solid compounds (dry variant) are the commonly used technologies. Combinations of both technologies (partial-wet or partial dry) are also possible [40, p. 312 ff.]. An example of a wet acid gas removal is depicted in Figure 21.

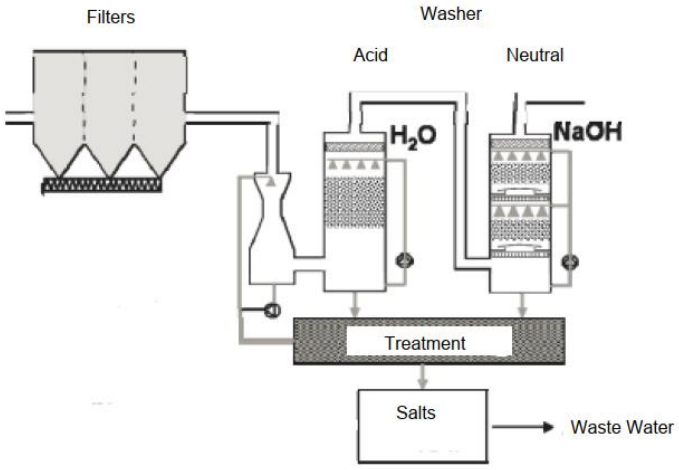

Figure 21: Overview on wet acid gas removal of in the waste gas purification of a waste incineration plant [40, p. 314].

In the presented example in Figure 21, the acid gas removal occurs in two steps (acid and neutral washer). In the first washer, acid gases such as HCl, HBr, HF and mercury compounds are absorbed with a recirculating liquid solvent. In the second step, SO_2 is

separated with an alkaline solution (NaOH or $Ca(OH)_2$ solution). The remaining rich solvent from the absorption process undergoes a treatment before being recirculated in the system. Wastewater containing dissolved salts is produced in the process. Alternatively, a wastewater free variant can be employed with the help of additional components (spray absorber, additional filters). Moreover, valuable compounds such as NaCl, HCl or plaster can be recovered from the rich solvent [40, p. 314 ff.].

In the case of NOx compounds, precautions can be taken in the combustion process to avoid the formation of these pollutants. The NOx compounds are formed from the oxidation of nitrogen compounds present during combustion. There are mainly three known sources for NOx formation in the combustion process: thermal NOx, fuel NOx and prompt NOx [42, pp. 117-118]. The formation of NOx depends strongly on the combustion temperature. The temperature dependence of the NOx formation mechanism is depicted in Figure 22.

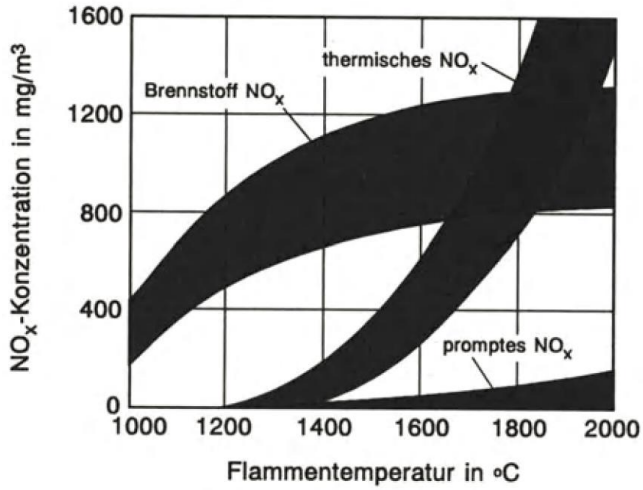

Figure 22: Exhaust gas NOX concentration (NOx-Konzentration) in dependence of the flame temperature (Flammentemperatur)for thermal NOx (thermisches NOx), Fuel NOx (Brennstoff Nox) and prompt NOx (promptes NOx) [42, p. 118].

As it can be seen in Figure 22, NOx formation is mainly determined by thermal and fuel NOx. If temperatures are kept below 1200 °C, thermal NOx is negligible and fuel NOx becomes a determinant for NOx formation. Prompt NOx plays a secondary role and forms first at temperatures above 1300 °C. In case that no nitrogen compounds are present in the fuel, NOx formation can be avoided by keeping the combustion temperature in a suitable range. Otherwise, additional purification processes such as selective catalytic reduction (SCR) and selective non-catalytic reduction (SCNR) have to be implemented [42, p. 318 ff.].

2.5.2.3 Carbon Capture

Nowadays, this technology has become more relevant in the context of climate change mitigation, then the use of a carbon capture unit (CCU) enables the reduction of carbon emissions from industrial exhaust gases. Moreover, such units can be used to capture CO_2 directly from the environment. There exist several technologies for a CCU, such as membrane, cryogenic, absorption and adsorption processes. Chemical absorption with monoethanolamine (MEA) is currently the industrial standard [43, p. 1413 ff.]. An overview on an amine scrubbing CCU is shown in Figure 23.

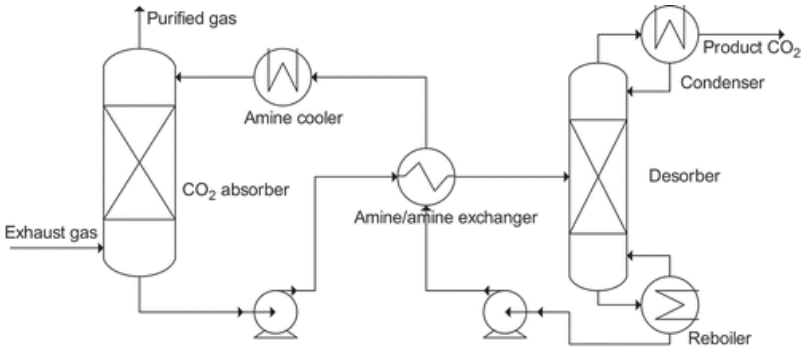

Figure 23:Process flow sheet of a CCU with an amine solution [44, p. 512].

As described in chapter 2.5.2.1 and 2.5.2.2, the fuel is burned in a combustion chamber to produce steam; to be subsequently purified of pollutants. An efficient removal of NO_x and SO_x compounds has to be carried out before the CCU, as they may cause undesired reactions in the absorption process [45, p. 1901]. Afterwards, the cleaned flue gas enters the CCU (absorber).

Optionally, it is possible to reduce the water content in the flue gas before entering the CCU. This can be achieved through partial condensation and has the aim to increase the partial pressure of CO_2 in the flue gas to facilitate CO_2 absorption [46, p. 486]. The CCU operates at atmospheric pressures. Absorption temperature is usually set between 40-60°C [47, p. 16], while the regeneration takes place at 100-120 °C [48, p. 4466].

The CCU consists basically of an absorption and a regeneration stage. The flue gas enters at the bottom of the absorption column, and it is stripped by a recirculating amine solution (lean solution), which enters at the top of the column. The rich solution, loaded with CO_2, exits at the bottom of the column, while the purified gas exits at the top of the absorber. The CO_2-rich amine solution enters the amine heat exchanger, in which it is preheated in counter current flow with the hot lean solution exiting the desorber.

The rich amine solution enters the regeneration column (desorber). The solution is partially evaporated in a reboiler which is heated with low-pressure steam. The low-pressure steam is extracted from the power generation cycle at temperatures of about 100-140 °C [47, p. 16]. The solvent vapors are partially condensed and returned to the desorber, while the absorbed CO_2 product leaves the desorber at the top of the column.

The hot regenerated amine solution leaves the desorber and bottom and is cooled down in the amine exchanger and a secondary amine cooler to the absorption temperature before entering the absorber, closing the solvent loop. In case of absorption with MEA, an aqueous solution containing 30 wt.% MEA is commonly used as a solvent. The concentration is limited to this value to avoid corrosion in the system, which can occur at higher concentrations [45, p. 1901].

Although amine scrubbing is a well proven and established technology in the industry, it requires large amounts of energy, with the regeneration process being the most energy consuming part of the CCU [46, p. 490]. Furthermore, the absorption process is exothermal, which requires the use of expensive cooling systems. Additionally, large volumes for the absorber with expensive packings and high recirculation rates of the solvent are needed. These factors result in high capital and operational cost for CO_2 scrubbing with amine solutions [49, p. 1450].

2.5.2.4 Methanol Synthesis and Methanol to Olefins

Methanol is valuable feedstock for the chemical industry. It can be used as a fuel or as intermediate for the production of other chemicals, such as formaldehyde, acetic acid, gasoline (MTG process) or olefins (MTO process) [50, p. 103]. Nowadays, methanol is produced by methanol synthesis using synthesis gas (syngas) as a feedstock. Syngas is a mixture of mainly CO, H_2 and lower amounts of other gases such as CO_2 [51, p. 346].

Syngas is produced by natural gas reforming or coal gasification. Afterwards the syngas is prepared and treated before entering the methanol synthesis loop. The process can be carried out either at high (250-300 bar) or low pressures (50-100 bar). Currently, the leading technologies for methanol synthesis are low pressure processes, from which the Imperial Chemical Industries (ICI) method and Lurgi process from Air Liquide are the most commonly used at industrial scale [50, p. 103 ff.]. A process flowsheet diagram of the ICI-process is presented in Figure 24.

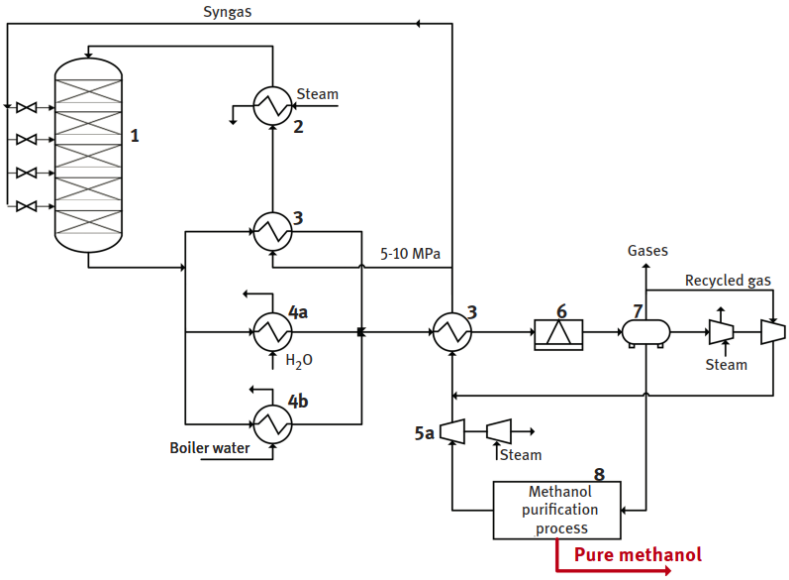

Figure 24: Overview on the ICI methanol synthesis loop [50, p. 106].

The synthesis loop can be sum up as follows: fresh synthesis gas (5a) is compressed and mixed with recycled gas before entering the synthesis loop. The feed preheated in a heat recovery heat exchanger (3) with the hot outlet gases of the reactor. Afterwards a part of the main stream is further preheated (2) and fed at the top of the reactor (1).

The synthesis of methanol is an exothermal process. The reactor employs quenching with fresh feed at several reactor stages. After every quenching step the reaction temperature and the methanol concentration drop, preventing the reaction to reach equilibrium. This improves the methanol yield and keeps the temperature in a feasible range [52, p. 66 ff.]. Afterwards, the reactor outlet is cooled down in a series of heat exchangers (4a, 4b, 3, 6) and partially condensed to be further split into a phase of unreacted and inert gases and a crude methanol product (7).

The unreacted and inert gases are further recycled into the loop. To avoid high concentrations of inert gases in the loop, a small amount of the gaseous stream exiting the flash drum (7) is purged from the system. The crude methanol product is further separated from water and other impurities with the help of distillation columns (usually two columns) [50, p. 106] to yield pure methanol (8).

Both ICI and Lurgi processes are carried out with the help of $Cu/Zn/Al_2O_3$ catalyst. The main difference between the two processes relies on the reactor set up. While the ICI process uses an adiabatic reactor with intermediate quenching, the Lurgi process employs an isothermal reactor, in which the heat of reaction is continuously removed by steam generation. Moreover, the ICI process is carried out at temperatures about 200-300°C, while the Lurgi process is operated at 250-260°C [50, p. 105 ff.].

Recently, methanol synthesis using CO_2 and hydrogen as feedstock (CO_2 hydrogenation) has become a promising alternative to conventional methanol synthesis using fossil fuels. In this process, a mixture of captured CO_2 coming from a CCU of industrial facilities and H_2 from renewable energy is employed instead of syngas. This alternative helps to simultaneously reduce carbon emissions and the usage of fossil fuels as feedstock [50, pp. 111-112].

Although this technology is relatively new, several investigations have been made to determine optimal operation conditions. Methanol synthesis by CO_2 hydrogenation can be carried out at similar operation conditions as the conventional method (200-280°C, 50-75 bar) using a $Cu/Zn/Al_2O_3$ catalyst [53, p. 460] [54, p. 41 ff.]. The main difference relies on the use of an adiabatic reactor with one single injection point.

Subsequently, it is possible to use the methanol produced from the CO_2 obtained from flue gases as a feedstock for the MTO process. The MTO process was described in detail in chapter 2.2.2. By adding the MTO process after the methanol synthesis with CO_2 hydrogenation, the obtained methanol can be further processed into valuable chemical feedstock. An overview of the process is presented in Figure 25.

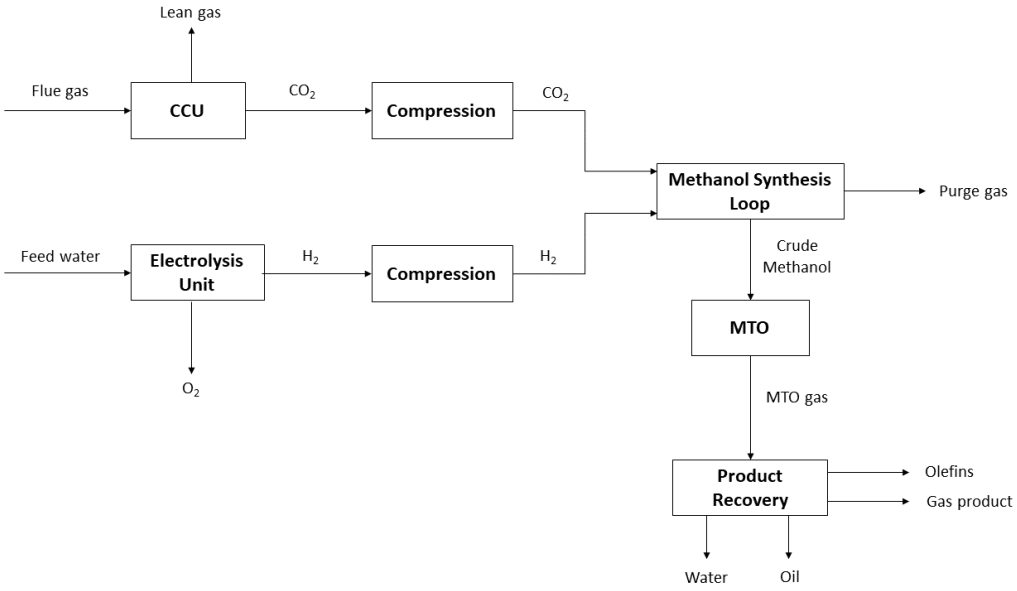

Figure 25: Overview on the coupled methanol synthesis with CO_2 hydrogenation and the MTO process.

The process presented in Figure 25 is described as follows: CO_2 coming from the CCU is compressed and mixed with H_2 coming from an electrolysis unit. In the electrolysis unit, water is separated into H_2 and O_2 with electrical power coming from renewable energy sources. The compressed H_2 and CO_2 enter the methanol synthesis loop, in which crude methanol is produced. A small amount of purge gases is produced as byproduct.

Afterwards, the produced crude methanol enters the MTO-Unit. Crude methanol consists mainly of a liquid methanol-water mixture with small amounts of dissolved gases [54, p. 41]. As the presence of water in the feed is not disadvantageous for the MTO process [55, p. 104], the methanol purification step can be omitted.

After the outlet gas mixture of the MTO reactor (MTO gas) undergoes a purification and separation process (product recovery section), the obtained polymer-grade olefins can be reinserted in the plastic production process, closing the plastic recycling loop. Water, oils, and other gaseous components are recovered as byproduct.

However, several problems arise if pure CO_2 and H_2 are employed. The first problem is to ensure a continuously H_2 supply from renewable energy sources. Currently, there is an industrial plant for methanol production by CO_2 hydrogenation in Iceland (George Olah plant). In this industrial facility, hydrogen is produced by electrolysis using geothermal energy. However, if other renewable energy sources are employed, problems with the continuously supply may arise [51, p. 356 ff.].

The second problem is the catalyst used in the synthesis loop. Although the methanol synthesis with CO_2 hydrogenation is possible with the current catalyst, the operation with pure CO_2 is not optimal, causing a loss on the methanol synthesis catalyst activity and therefore to a reduction of the methanol conversion [50, p. 112]. Therefore, improvements on the used catalyst have to be made to make the process more feasible.

3 Methodology

The aim of this work is to perform a technical and economical evaluation of two different recycling loops (chemical recycling and combustion loop) for polyolefins. In these loops, recycled polyolefins (PE and PP) undergo a recycling process consisting of multiple unit operations to yield ethylene and propylene, which can be reinserted in the conventional plastic production processes (linear economy), creating an alternative circular process for polyolefins production (circular economy).

In this chapter, the methodology used to perform the technical and economical evaluation of the two investigated plastic recycle loops is described. Furthermore, the mathematical background of the recycling loops technologies presented in the previous chapter, as well as the employed tools used for the calculations, together with assumptions and simplifications made during the evaluation are explained.

3.1 System Boundary

The boundary of the plastic recycling loops investigated in this work starts with the feed of the prepared, recycled plastic waste into the first loop unit operation. Plastic waste preparation and collection processes (e.g., shredding, washing, etc.) are not considered in the further calculations. The system boundary ends at the product recovery section, in which polymer-grade ethylene and propylene are obtained. An overview on the system Boundaries for the pyrolysis and combustion recycling loops is depicted in Figure 26.

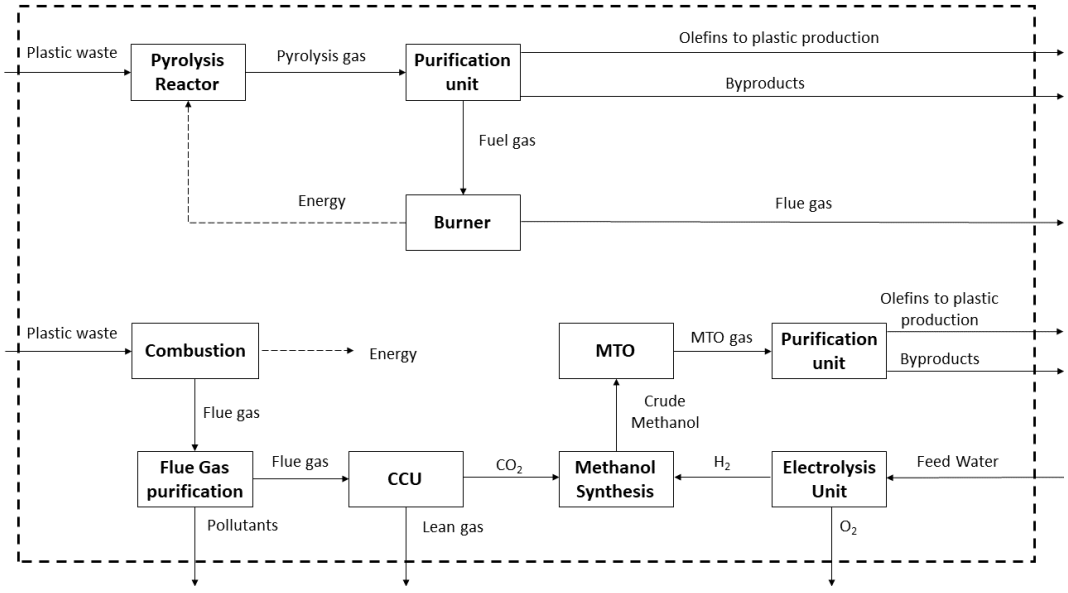

Figure 26: System boundary (dashed line) of the chemical recycling loop (upper side) and combustion loop (lower side).

An overall process flow diagram for both loops (chemical recycling and pyrolysis loop) with the corresponding unit operations (white boxes) is presented in the previous figure. The material flows are presented as solid lines, while the energy flows are thin dashed lines. As the aim of the diagram is mainly to depict the system boundary, some energy and material streams, as well as intermediate unit operations are omitted in the diagram.

The chemical recycling loop consist mainly of three unit operations: the pyrolysis reactor, the purification unit, and the gas burner. The supplied and prepared plastic waste enters the pyrolysis reactor, in which is converted into pyrolysis gas. Afterwards, the pyrolysis gas undergoes a purification process, consisting of multiple unit operations, from which the main olefin product is obtained. Fuel gas is obtained as byproduct and is used to provide the heat required for the reactor.

The combustion loop involves more individual unit operations and is more complex than the chemical recycling loop. In this loop, the plastic waste is burned to produce energy, to be further treated in a flue gas purification process and a CCU to obtain CO_2. The captured CO_2 is mixed with H_2 obtained from water electrolysis and fed into the methanol synthesis loop, from which crude methanol is obtained. Subsequently, crude methanol is further processed in the MTO unit to obtain an olefin rich gas mixture, which is later purified to yield the main olefin products.

Polymer-grade light olefins (Ethylene and propylene) are obtained at the end of the system boundaries of the two recycling loops. Other byproducts, that can be further sold or used as feedstock for other processes beyond the system boundary are obtained as well. The further processing of the olefin feedstock (e.g., polymerization processes) and the byproducts are not considered in this work.

3.2 Technical Evaluation

The technical evaluation implemented in this work consists of the process simulation of the chemical recycling and the combustion loop. The Simulation is performed with the help of EBSILON Professional (version 15.04) and DWSIM (version 8.0.4). EBSILON is a commercial process simulation software for power plants. The license used in this work was provided by AFRY. DWSIM is an open-source chemical simulation software which is available for free.

Furthermore, excel spreadsheets and python scripts are used for side calculations (e.g., for interpolation and curve fitting functions). The aims of the evaluation can be summed up as follows:

- Elaboration of a process flow diagram of the loops, with the corresponding mass and energy balances for the overall process and the corresponding unit operations within the system boundary.
- Comparison of product yields and energy demand for the loops based on the same input amount.
- Evaluation of the process energetical self-sustainability, which is performed with the simulation of simplified energy recovery loops and networks (e.g., Rankine cycle).
- Calculation of the produced/ absorbed CO2 streams to determine the carbon footprint of the processes.
- Evaluation of the technology readiness level (TRL) of the unit operations within the system boundary, which has the aim to compare which of the loops is more likely to be applied in the future.

Moreover, the results of the technical evaluation, such as the required capacities (volume flows, mass flows, etc.) and sizing of the equipment are employed as a basis for the economical evaluation. In the following subchapters, the methods, assumptions, and parameters for the simulation of the different unit operations involded in the loops will be explained in detail.

3.2.1 Feed Characterization

The feed employed for the recycling loops simulation consist of a light fraction extracted from household plastic waste (e.g. plastic packaging, bags, bottles, etc.). This fraction was previously treated and later use to perform pyrolysis experiments to yield olefins. The fraction was previously mentioned in chapter 2.5.1.2 and consists mainly of polyethylene and polypropylene (95.8 %), with some traces of polystyrene (3%) and PVC (0.2 %). A detailed elementary analysis of the plastic feed is presented in Table 3.

Table 3: Elementary analysis of plastic waste feed employed for the process simulation [34, p. 78].

Compound	wt.%
C	84,70
H	14,00
N	-
Cl	0,08
S	-
O	-
Ash	1,23
Sum	100

For comparison purposes, the same plastic waste feed was used as input for both plastic recycling loops. Furthermore, other secondary feeds such as feed water and ambient air are required in the process, the boundary conditions for the feeds are presented in Table 4.

Table 4: Boundary conditions for the used feeds in the process simulation.

	Plastic feed	Feed water	Ambient Air
Mass flow (t/h)	4.1	-	-
Pressure (bara)	1.013	1.013	1.013
Temperature (°C)	25	25	25
Rel. Humidity (%)	-	-	81

The mass flow used for the plastic waste feed was taken from the average value for the feed capacity (approx. 100 t/d) of a production line in waste incineration facilities [56, p. 41]. The pressure and temperature for the feeds correspond the assumed ambient conditions in the simulation. The relative air humidity is an average value from winter and summer data of the city of Hamburg, Germany [57].

3.2.2 Chemical Recycling Loop

The chemical recycling loop consists of the pyrolysis of the recycled plastic waste to yield a valuable hydrocarbons gas mixture to yield light olefins (ethylene and propylene). The main process consists of a fluidized bed reactor, in which a high temperature pyrolysis is performed. Afterwards, the obtained gas mixture is treated in a conventional steam cracking product recovery section, which was explained in chapter 2.2.1. A schematic representation of the adapted process used for the process simulation is presented in Figure 27.

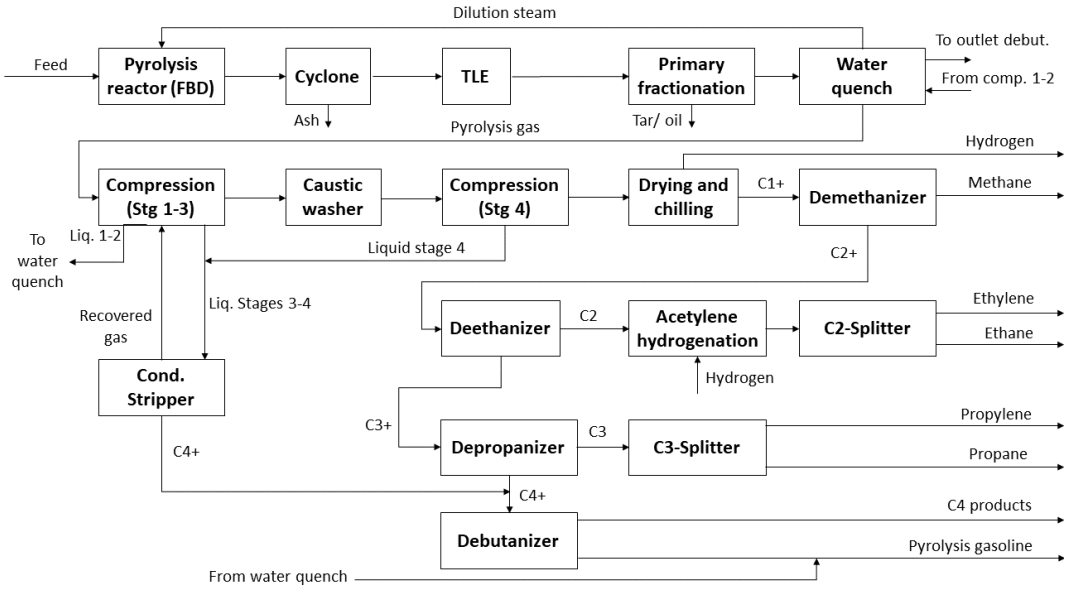

Figure 27: Process flow diagram of the chemical recycling loop.

The process flow diagram has been adapted from the process flow diagrams from Figure 5 and Annex 1. The chosen configuration for the plant was a font-end demethanizer with tail end acetylene hydrogenation. The process flow diagram from Annex 1 [58, p. 2] presents a more detailed description of the unit operations in the cracking plant. The condensate stripper has been added from this diagram. This unit is a product recovery unit located between the 3rd and 4th compression stages.

Furthermore, with the help of the detailed flow diagram in Annex 1, the connections of the liquid flows obtained from the flashing unit operations between the compression stages are improved. This results in the liquids from Stages 1 and 2, which have a high-water content, to be refed into the water quench for water and oil recovery. Moreover, the liquids from stages 3 and 4, with low water content, are sent to the condensate stripper for oil and gas recovery.

The simulation is split into three parts. The first part, consisting of the pyrolysis reactor, the cyclone, the dilution steam generator, and a small energy recovery cycle is simulated in EBSILON. The second part is simulated in DWSIM and contains all the unit operations from the TLE to the end of the product recovery section depicted in Figure 27. The third part, containing the power generation cycle (Rankine-cycle) from the TLE, is simulated separately in EBSILON. The process model in EBSILON containing the first part is depicted in Figure 28.

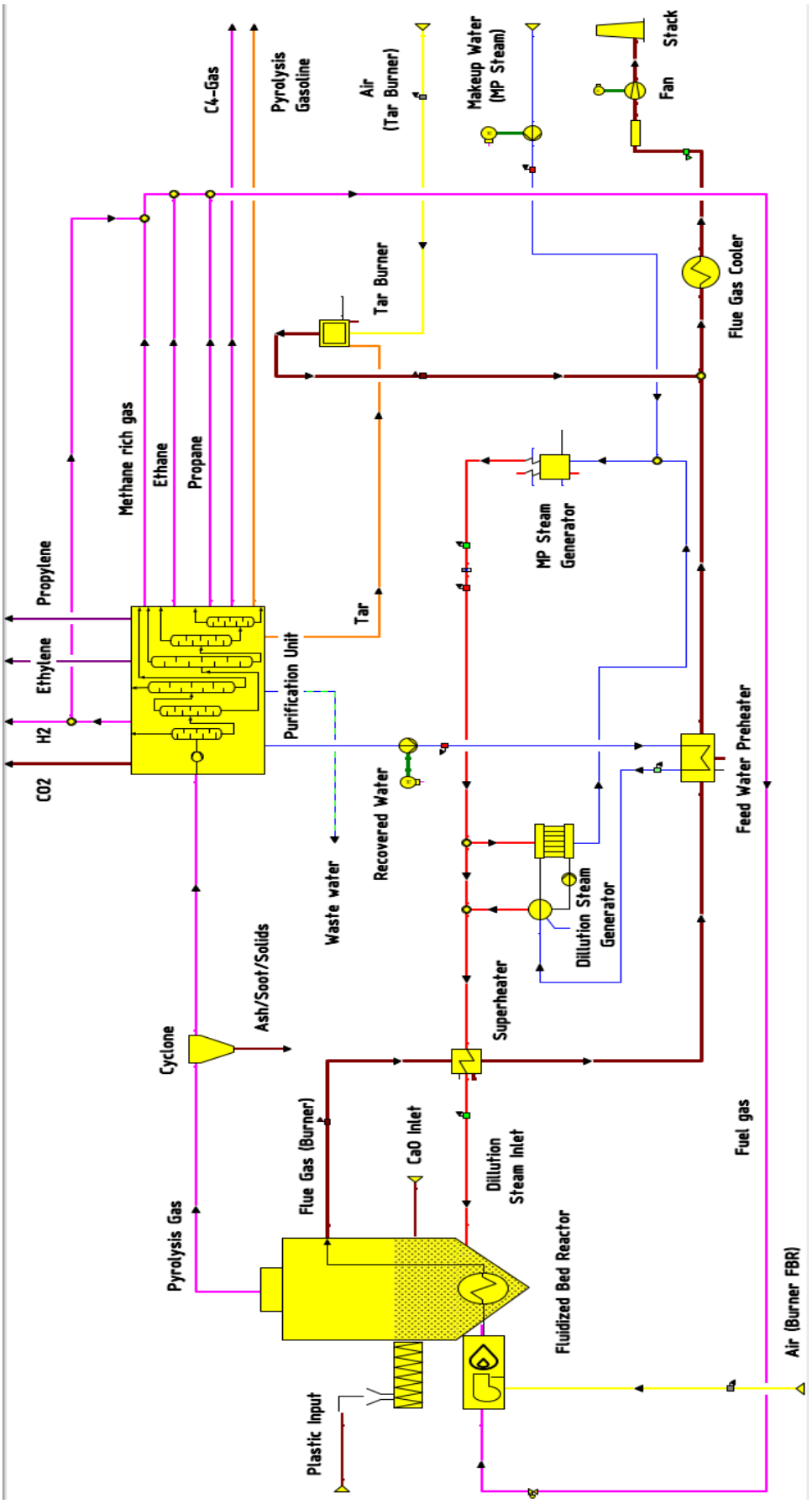

Figure 28: Process model in EBSILON for the chemical recycling loop.

The EBSILON (first part) and the DWSIM model (second part) described previously are nested simulations. The first part represents the "outer shell" (Figure 28), while the DWSIM simulation is represented as a "purification unit" in the EBSILON model. This unit is implemented as a black box into the EBSILON model. The results from the streamline after the cyclone are transferred to the DWSIM model. After the DWSIM simulation is completed, the results from the DWSIM model are transferred back to the EBSILON model as the output streams of the purification unit.

A part of the gaseous fraction exiting the purification unit is burned in a gas fired burner to provide the required heat for the pyrolysis reactor (fuel gas). This fraction is extracted from the methane, ethane, propane, and a part of the hydrogen byproducts obtained from the product recovery section.

The energy recovery cycle implemented in the EBSILON model consists mainly of the extraction of the rest heat of the reactor flue gases through a dilution steam superheater and a feed water preheater. The remaining heat is extracted with a flue gas cooler. An extra amount of heat is gained through the combustion of the recovered tar/ fuel oil from the primary fractionation. The cool exhaust gases from the tar burner are mixed with the cool reactor flue gases before going to the stack.

Furthermore, a medium pressure (MP) steam generator is implemented in the energy recovery cycle. This steam is used as a heating medium for the dilution steam generator. A part of this steam is used as makeup steam for the dilution steam. The makeup water is dosed into the cycle before entering the MP steam generator (see right side in Figure 28).

The DWSIM simulation (purification unit) is performed using the non-random two-liquid model (NRTL) for the thermodynamics. Regarding the EBSILON simulation, different thermodynamic models available in the software are used, which are automatically assigned depending on the stream type (e.g., steam table for water streams, flue gas tables for gaseous streams, solid tables for solid streams, etc.). The equipment pressure drop is not considered in the simulation.

3.2.2.1 Pyrolysis Reactor

The technology chosen for the pyrolysis reactor is the fluidized bed reactor for the hamburger process (high temperature pyrolysis) described in chapter 2.5.1.2, using steam as a fluidizing medium. This technology was chosen to increase the yield of olefins from the plastic pyrolysis, avoiding intermediate steps which lead to product loss. The reactor set up in the EBSILON simulation is shown in Figure 29. The fluidized bed reactor is a self-programmed component, and it was build using different available units and tools in EBSILON.

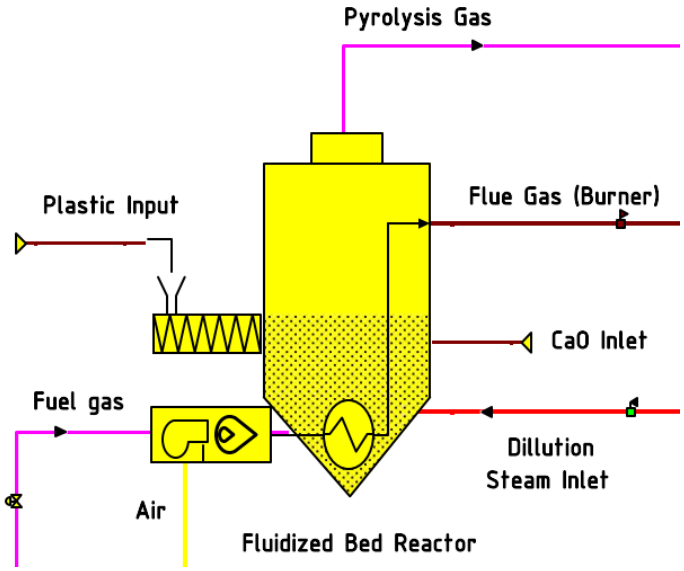

Figure 29: EBSILON model for the pyrolysis fluidized bed reactor with steam as fluidizing gas.

The reactor model consists of 5 inlets and 2 outlets, and it can be divided into the reactor chamber and the gas burner. The plastic waste feed (plastic input), CaO and the dilution steam are fed directly into the reactor chamber, while the combustion air and the fuel gas are fed into the gas burner. The two sections are separated from each other, so that there is no mixing of the streams coming into the different sections.

The fuel gas is burned and used to heat the reactor through indirect heat exchange. The hot flue gas exits the reactor at the upper right side. The plastic input, the dilution steam and the CaO feeds are converted into the pyrolysis gas, which leaves the reactor at the top. An overview of the design parameters for the reactor and the dilution steam inlet is depicted in Table 5.

Table 5: Overview of the design parameters for the simulation of the pyrolysis reactor.

Conditions	Reactor	Source	Dilution steam	Source
Pressure (bara)	1	[4, p. 6]	9	[17, p. 4]
Temperature (°C)	700	[34, p. 78]	500	[34, p. 77]
Steam to feed ratio (kg/kg)	1.9	[34, p. 78]	-	-
Residence time (s)	2.3	[34, p. 78]	-	-

The residence time in the reactor is used to estimate the reactor volume for the cost estimation. The plastic feed, the CaO and the combustion air enter at ambient conditions (25°C, 1.01325 bar). A detailed description of the plastic feed is given in chapter 3.2.1. The CaO is added in a 0.25 wt.% basis of the plastic feed. This value is based on the PVC content of the feed and was estimated through cross multiplication using the results of the pilot plant experiments described in chapter 2.5.1.2 (4% PVC -> 5% CaO, 0.2 % PVC -> 0.25 % CaO).

Regarding the absorption of the Cl compounds with calcium oxide (CaO), the chemical reaction for the Cl absorption (see chapter 2.5.1.2) is neglected, principally due to the absence of the $CaCl_2$ compound in EBSILON. Instead, the added CaO in a 0.25 wt.% feed basis is considered as a solid residue together with the Cl present in the feed. As

just a very small amount of Cl is present in the feed, the impact of the side products from the Cl absorption is neglected.

The reactor is modeled as a simple conversion reactor. The product composition based on the dry plastic input is adapted from literature data. The reactor converts the plastic input to the product and mixes it with the dilution steam. As described before, the Cl absorption with CaO is modeled separately. The products (pyrolysis products, CaO and Cl) are heated to the reaction temperature (700 °C) and exit the reactor at the top as pyrolysis gas. The conversion rates (dry product composition based on carbon and hydrogen content from the elementary analysis) used for the plastic pyrolysis are shown in Table 6.

Table 6: Conversion rates for the net dry plastic feed (based on C and H of the elementary analysis) implemented in the EBSILON reactor model, adapted from [34, p. 80].

Compound	wt. %	wt (-)
Hydrogen	0.6	0.006
Carbon monoxide	1.0	0.010
Carbon dioxide	1.4	0.014
Methane	11.0	0.110
Ethylene	31.0	0.310
Ethyne (acetylene)	0.3	0.003
Ethane	3.4	0.034
Propene	14.0	0.140
Propane	0.5	0.005
1-Butene	2.2	0.022
Trans-2- Butene	0.6	0.006
1,2-Butadiene	6.0	0.060
TOTAL GAS	**72.0**	**0.720**
n-Pentane	3.1	0.031
n-Hexane	0.6	0.006
TOTAL ALIPHATICS	**3.7**	**0.037**
Benzene	14.2	0.142
Toluene	4.8	0.048
TOTAL Aromatics	**19.0**	**0.190**
TOTAL OIL	**22.7**	**0.227**
DR as Fluorene	4.7	0.047
Soot	0.6	0.006
TOTAL (ash and water free)	100.0	1.000

The pyrolysis product consists mainly of a gaseous fraction (72 wt.%), a liquid phase (22.7 wt.% oil and 4.7 wt.% distillation residue) and a solid residue (soot, 0.6 wt.%). The distillation residue (DR) is a mixture of substances with a boiling point above 295°C and atmospheric pressure, containing mainly fluorene, other high boiling hydrocarbons and a small ash residue. For the simulation, this fraction was simplified as fluorene.

Afterwards, the pyrolysis gas (pyrolysis products, solid residues, CaO, Cl and dilution steam) are heated to the reactor temperature. The reactor is programed to calculate the required heat for the pyrolysis process, which is defined as [14, p. 475]:

$$Q_{\mathrm{R}} = Q_{\mathrm{py.}} + Q_{\mathrm{R,heat}} \quad (3)$$

With Q_{R} as the total required reactor heat in kW, which is the sum of the pyrolysis heat $Q_{\mathrm{py.}}$ and the required thermal duty to heat the products to the reactor temperature $Q_{\mathrm{R,heat}}$. The pyrolysis heat $Q_{\mathrm{py.}}$ is obtained from following equation:

$$Q_{\mathrm{py.}} = \dot{m}_{\mathrm{pl.}} \cdot \Delta H_{\mathrm{py.}} \quad (4)$$

With $\dot{m}_{\mathrm{pl.}}$ as the plastic feed mass flow in kg/s and $\Delta H_{\mathrm{py.}}$ as the specific heat for the pyrolysis of plastic in kJ/kg. The value for $\Delta H_{\mathrm{py.}}$ is equal to 2476.4 kJ/kg. This value is obtained from the energy balance of the pyrolysis reactor in the Hamburger process [37, p. 191], and considers the melting enthalpy, the heat of vaporization of the melted plastic and the endothermic heat of reaction of pyrolysis. The value is slightly higher that the specific heat of pyrolysis of biomass (2016.8 kJ/kg) [59, p. 3072].

After the reactor heat requirement is calculated, the needed amount of gaseous fuel to cover the heat demand is calculated. This is implemented with the help of a combustion chamber model, which is already available in EBSILON. The model is configured to perform a complete combustion with 10 % excess air (λ= 1.1). This is sufficient to keep the temperature in the fired tubes in the reactor below 1200 °C, avoiding the formation of significant amounts of NO_x in the flue gas [37, p. 189]. The outlet temperature of the flue gas at the top of the reactor is assumed to be 20 K over the reactor temperature (720°C).

3.2.2.2 Cyclone

The cyclone is placed between the pyrolysis reactor and the TLE, which is the first unit operation of the purification unit (see Figure 28). This unit is implemented to separate the solids residues containing in the pyrolysis gas exiting the reactor. This unit is not present in the conventional steam cracking process but was added in the model as it was necessary to separate the solid residue from the pyrolysis gas (ash, soot, CaO and absorbed Cl) in the Hamburger process.

The cyclone is modeled as a simple separator with a specified compound separator rate. Its assumed, that all solid components are removed in this unit (100 % separation rate). In reality, small traces of solid components remain in the gas stream and are later removed in the quench section of the purification unit. This simplification is taken principally to avoid the simulation of solids in DWSIM, which is more suitable for gaseous and liquid compounds.

3.2.2.3 Purification Unit

The purification unit comprises the product recovery section of the steam cracking plant. This unit is modeled as a black box in EBSILON. The detailed process simulation is performed separately in DWSIM. The thermodynamics are simulated with the NRTL property package available in DWSIM. The purification unit implemented in EBSILON is shown in Figure 30.

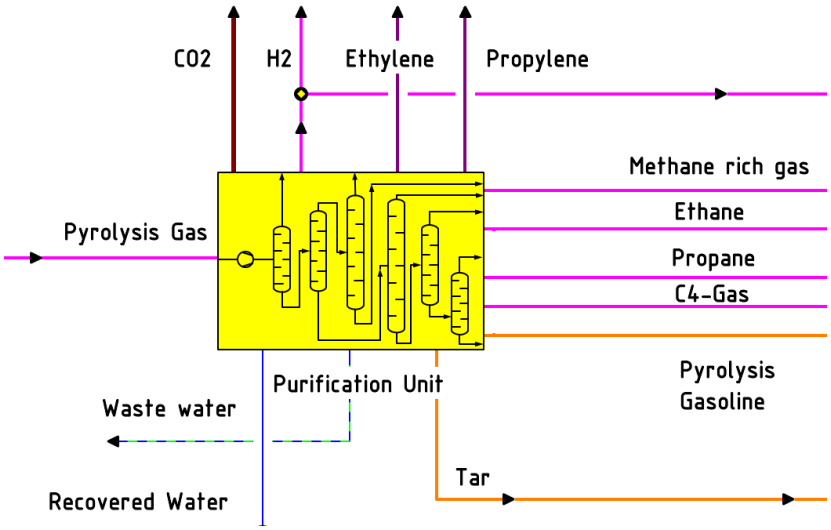

Figure 30: Implementation of the product recovery section (purification unit) in EBSILON.

The purification unit consist of 1 input and 12 outputs. The pyrolysis gas exiting the cyclone enters the unit at the left side. The light olefin products (ethylene and propylene) exit the unit at the top, together with the recovered hydrogen fraction and the absorbed CO_2 from the caustic washer.

Other gaseous side products such as methane, ethane, propane, and C4-gases exit the unit at the right side. The methane, ethane, propane, and a part of the hydrogen fraction are used as a fuel for the pyrolysis reactor. Pyrolysis gasoline is also recovered from the process and exits the unit at the lower right side. A part of the dilution steam present in the pyrolysis gas is recovered as water and exits the unit at the bottom, together with a wastewater and a tar/oil fraction.

For the recovery of water from oil, it is assumed that water from "oil in water" fractions can be fully recovered, while water streams from "water in oil" fractions are treated as wastewater (no recovery possible). The detailed modelling of the unit operations present in the product recovery section will be explained in the following.

Transfer Line Exchanger (TLE)

The transfer line exchanger is modeled as a simple cooler with a specified outlet temperature. This process step is the first in the purification unit. In a steam cracking plant, the TLE is followed by a series of heat exchangers, in which the temperature drops down to approx. 300 °C (see chapter 2.2.1). For this model, the TLE and the other heat exchangers before the primary fractionation are simplified as single unit with an outlet temperature of 300 °C.

The pyrolysis gas enters the TLE and is cooled down by extracting a certain heat amount. The outlet of the TLE goes to the primary fractionation. Furthermore, a simple Rankine-cycle was implemented to estimate the mechanical power generated from the recovered heat from the pyrolysis gas. An overview of the Rankine cycle is presented in Figure 31.

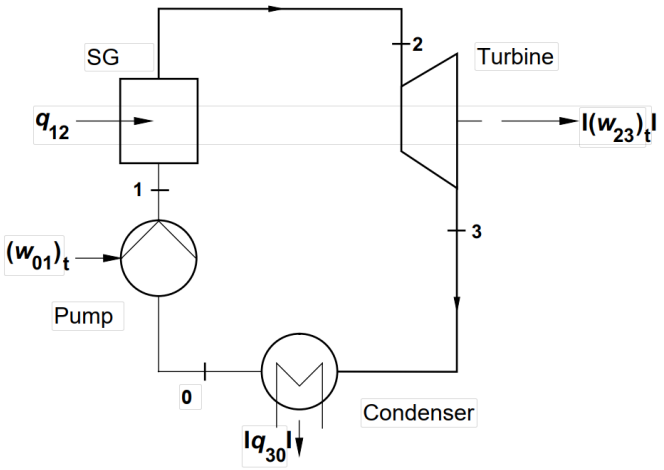

Figure 31: Process diagram of a simple Rankine-cycle [60, p. 350].

The Rankine cycle can be described as follows: feed water (0) is compressed with a pump (1), for which mechanical power (w_{01}) is needed. The compressed water enters the steam generator (SG). Steam is produced with the thermal heat q_{12} introduced into the cycle, to later enter the turbine (2). The gas is expanded in the turbine, generating mechanical power (w_{23}). The low-pressure steam exiting the turbine (3) is further condensed, generating thermal heat that has to be extracted from the cycle (q_{30}). The exiting condensed water enters the pump again, closing the cycle.

The model for the power generation for the TLE is modeled separately in EBSILON. The implementation of the Rankine-cycle is presented in Figure 32.

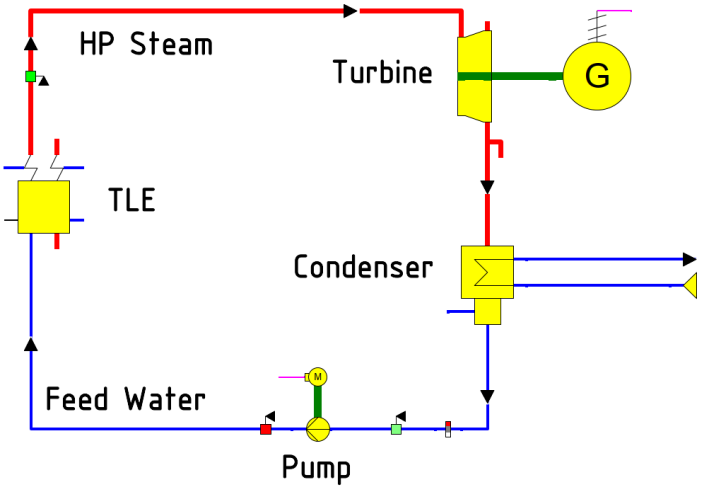

Figure 32: Implementation of the Rankine-cycle for the TLE in EBSILON.

In the EBSILON implementation, the TLE represents the steam generator in the Rankine-cycle. The temperature of the high-pressure steam (HP steam) is set to 500 °C [61]. The pressure of the cycle is set to 120 bara (see chapter 2.2.1). The outlet pressure is assumed to be 0.1 bara. The steam exiting the turbine is cooled in the condenser with cooling water. The condenser is designed with an upper temperature difference ($\vartheta_{steam} - \vartheta_{water,\ hot}$) of 10 K. The generator (G) is added just for visualization purposes. In reality, the power consumers (e.g., pumps, compressors) are connected directly to the turbine.

Primary Fractionation

The primary fractionation is located between the TLE and the water quench. In this unit, the tar/ oil fraction is separated from the pyrolysis gas. A simplified process flow sheet of the implementation of this unit in DWSIM is presented in Figure 33.

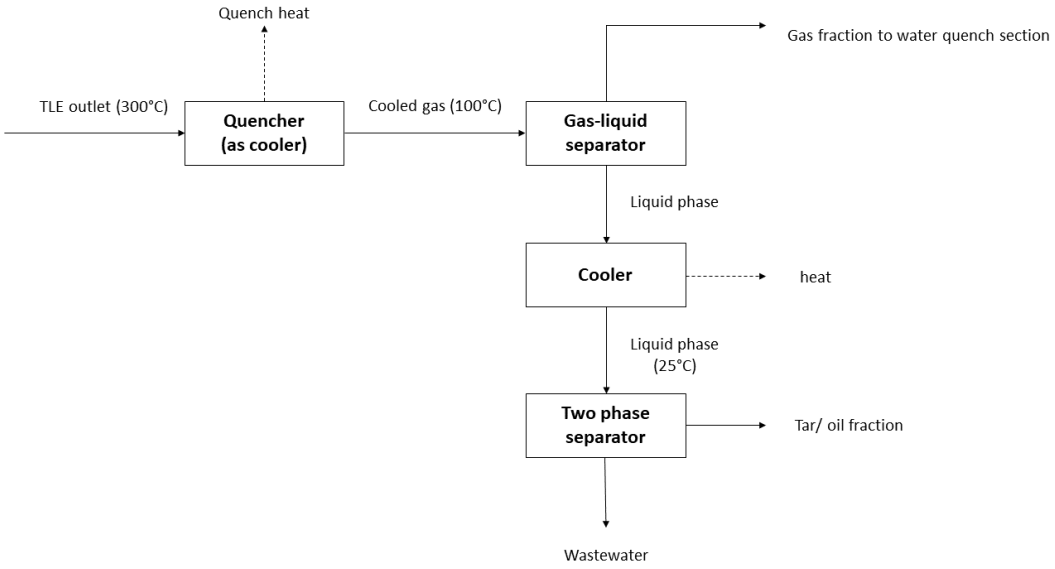

Figure 33: Implementation of the primary fractionation in DWSIM.

The primary fractionation with recirculating oil quench is simplified and simulated as an indirect cooling quench with partial condensation of the high boiling components. The simulation is composed of a cooler, in which the pyrolysis gas is cooled and partially condensed. Afterwards, the pyrolysis gas enters a gas liquid separator, in which the condensed tar fraction is recovered. The outlet temperature of the unit is set to 100°C (see chapter 2.2.1).

The raw tar liquid fraction is further processed and cooled down to ambient temperature. This part of the unit operation consists of a simple cooler and a 2-phase separator. The hot tar fraction is first cooled down to 25 °C and afterwards separated into a high boiling hydrocarbon fraction and a water fraction. The 2-phase-separator is modeled as a simple separator with a given separation rate. It is assumed that the water is fully recovered from the oil. However, as the raw tar is a "water in oil" mixture, the recovered water fraction is labeled as wastewater.

Water Quench

As described in chapter 2.2.1, the water quench tower forms a closed loop with the dilution steam generator. In this unit, most of the dilution steam present in the pyrolysis gas is recovered. Additionally, an oil fraction is obtained, which is sent to the debutanizer downstream of the process for pyrolysis gasoline recovery. The implementation of this unit in DWSIM is based on the process flow diagram presented in Figure 6. A part of the loop is implemented in DWSIM, while the part outside the purification (DSG and MP-steam generator) is implemented in the EBSILON model shown in Figure 28.

The adapted process flow diagram from Figure 6, showing the boundary of the DWSIM implementation (dashed line) is presented in Figure 34.

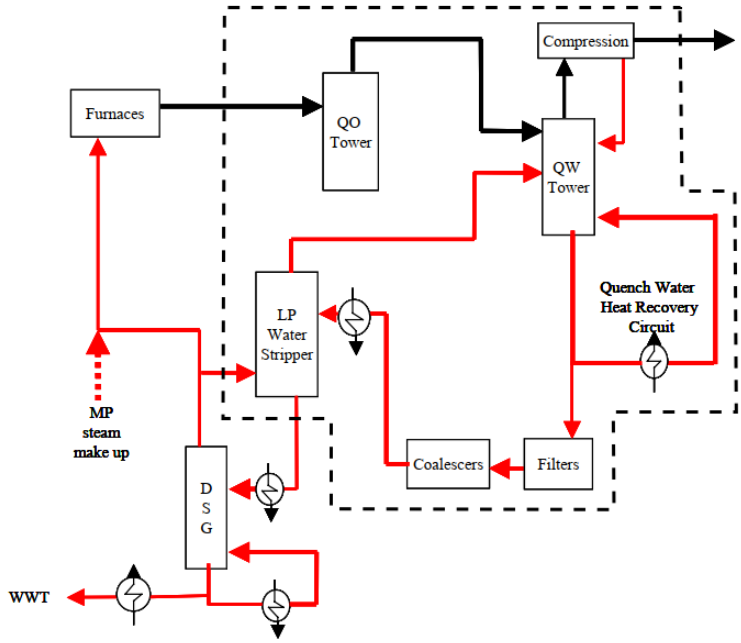

Figure 34: System boundary (dashed line) of the implementation in DWSIM for the quench water tower- dilution steam generator (DSG) loop.

As shown in Figure 34, the quench water tower (QW Tower), the quench water heat recovery, filters, coalescers and the low-pressure water stripper (steam stripper) are implemented in DWSIM. The rest of the loop is presented in the EBSILON model outside the purification unit. Analogous to the primary fractionation, the water quench tower and the steam stripper are simplified in the simulation as indirect quenching units. The implementation of the units in DWSIM is shown in Figure 35.

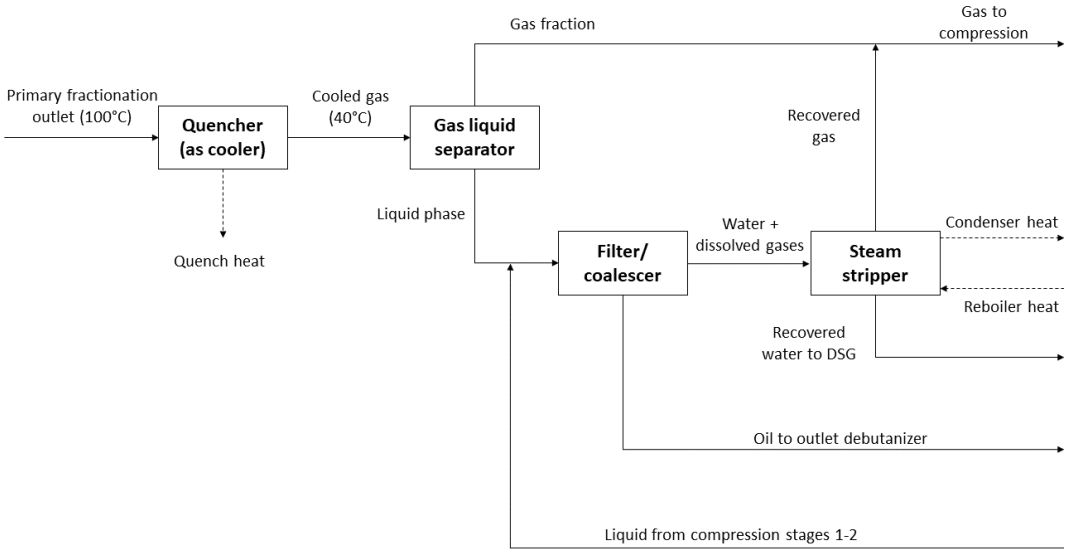

Figure 35: Process model for the water quench tower and the steam stripper.

The water quench tower is simulated as a simple cooler and a gas-liquid-separator. The pyrolysis gas exiting the primary fractionation is cooled down in the cooler and partially condensed. According to design examples for ethylene quench water towers, the outlet temperature is in the range of 37-48°C [16, p. 16]. For the simulation, the temperature

is set to 40°C. Afterwards, the mixture of condensed dilution steam and pyrolysis gas is separated in a gas-liquid separator.

The condensed dilution steam is mixed with the recovered liquids from the flashing in the compressor stages 1 and 2 downstream of the quench water section. The mixture of condensed dilution steam and recovered flash liquid is sent through filters and coalescers, in which the condensed oils are separated. It is assumed, the oils can be completely separated from the water fraction.

The water fraction containing dissolved gases enters the steam stripper. The steam stripper is simulated as a simplified distillation column. In reality, the heat required for the column reboiler is provided through direct contact with medium pressure steam. The pressure in the column is nearly atmospheric [62, p. 550]. For the simulation, the column pressure is kept constant and set to 1.01325 bara. The design parameters for the Steam stripper are presented in Table 7.

Table 7: Design values for the simulation of the water quench tower and the steam stripper.

Parameter	Value	Source
Pressure (atm)	1	[62, p. 550]
Top specification	5 mol% water	Assumption
bottom specification	<0.1 mol% 1,2-butadiene	Assumption
Tray efficiency	0.7	[63, p. 261]
Tray spacing (m)	0.5	[64, p. 310]
Diameter (m)	2.5	[65]

The column top and bottom specifications in Table 7 are adjusted manually in a way that a significant amount of disolved gases are recovered, while the condenser temperature lies close to the pyrolysis gas temperature (40 °C). The outlet temperature of the steam stripper is calculated in the simulation. The parameters for the column sizing (tray parameters and diamerter) are average values from literature data. The height and the diamerter of the column are used for the later economic evaluation. The height of the column is calculated as follows:

$$H = n_{\mathrm{th}} \cdot \frac{H_{\mathrm{Tray}}}{\eta_{\mathrm{Tray}}} \tag{5}$$

With H as the height of the column, n_{th} as the theorical number of stages (simulation result), H_{Tray} as the tray spacing and η_{Tray} as the tray efficiency.

The recovered gas in the steam stripper leaves at the top of the column and is mixed back to the pyrolysis gas stream. The gaseous mixture leaving the quench water section is led to the first compression stage. The water fraction recovered at the bottom of the column is send to the dilution steam generator outside of the purification unit. The recovered oil fraction from the coalescer is sent to the outlet of the debutanizer.

Compression

The compression section consists of 4 compression stages with intermediate cooling and flash units to separate condensed liquid before entering the next compression stage. According to the literature, the compressed gas is cooled down to 38°C after each compressor [58, p. 23], excepting for the last compression stage. After this compression stage, the gas stream is cooled to approx. 15 °C. This temperature is chosen to

condense as much water as possible before entering the drying unit, which helps to reduce the load on the dryer [14, p. 503].

The intermediate cooling is performed with cooling water in stages 1-3. After stage 4, the compressed gas is cooled in two steps, first with cooling water and afterwards with a refrigerant to the desired inlet temperature for the dryer [14, p. 503]. The pressure after the final compression stage is usually between 33-39 bara [14, p. 502]. For simplification reasons and to compensate possible pressure loses not considered in the simulation, the outlet pressure of the compression section is set to 40 bara. The pressure ratio Π for the compression is calculated with following formula [66, p. 777]:

$$\Pi = \sqrt[n]{\frac{p_\mathrm{n}}{p_0}} \tag{6}$$

With n as the number of stages (in this case 4), p_0 as the pressure before the first compression stage (1 bara) and p_n as the outlet pressure after stage n (in this case 40 bara). Equation (6) yields the optimum pressure ratio for a multistage compression. The outlet pressure for the corresponding compression stage is obtained by multiplying the inlet pressure of the compressor by Π. For this simulation, a value of approx. 3 was obtained for Π.

For the compression section, the heat exchangers used for intermediate cooling are simulated as simple coolers with a given outlet temperature (38 °C). Furthermore, an adiabatic efficiency of 75 % was assumed for all compressors in the DWSIM simulation. The process flow diagram for the compression section is shown in Figure 36.

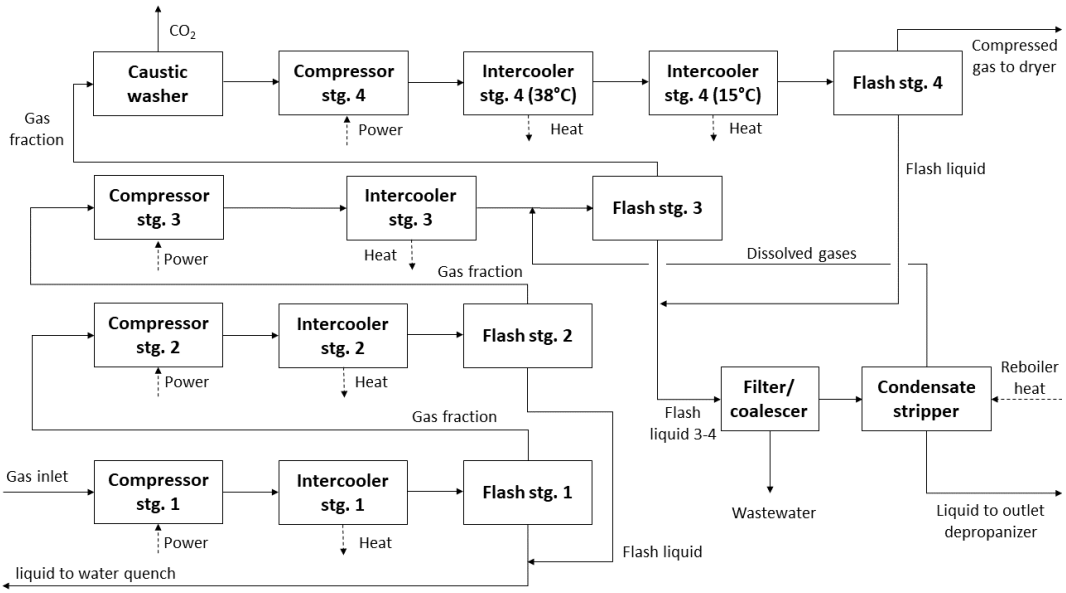

Figure 36: Process flow diagram of the compression section.

In this part of the purification unit, compression with intermediate cooling and flashing takes place. The liquids of the flash drums from stages 1 and 2 are mixed and recycled back to the quench water section (see Figure 35) to be fed into the coalescer before the steam stripper. The flash drums are simulated as gas-liquid separators. The gas fraction exiting the flash drum of stage 2 enters the stage 3 of the compression.

The outlet of the intermediate cooler is mixed with the recovered gases from the condensate stripper before entering the flash drum of stage 3. The liquids from the flash drums of stages 3 and 4 are mixed and fed to the coalescer, in which a water fraction is separated from the liquid. This coalescer is modeled in the same way as the coalescer of the water quench section (see Water quench). Afterwards, the water-free liquid is fed into the condensate stripper.

The condensate stripper is modeled as a reboiled stripper in ChemSep, which is possible in DWSIM with the help of Cape Open components. The ChemSep model of the reboiled stripper is presented in Figure 37.

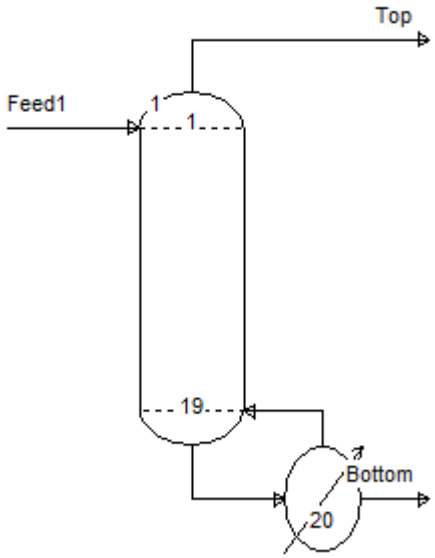

Figure 37: Process model of the condensate stripper in ChemSep.

The reboiled stripper consist of a liquid feed, which enters the column at the top stage, a liquid bottom product and a gaseous top product. The set-up is very similar to the one of a distillation column, but with no reflux at the top. Twenty theoretical stages are assumed for the design of the column. Furthermore, a propylene content of 0.1 mol% is assumed for the bottom's liquid product.

The bottom product of the condensate stripper is sent to the outlet of the depropanizer, while the top product is feed back to the flash drum of stage 3. The gas exiting the flash drum enters the caustic washer. This unit is implemented to lower the CO2 content in the gaseous stream, as this affects the purity of the ethylene product. As no sulfur compounds are present in the pyrolysis gas, the H_2S removal is omitted in the simulation. The unit is modeled as a simple separator with a given separation rate. A separation rate of 95 % for CO2 was assumed for the design. The Absorbed CO2 leaves the caustic washer at the top of the unit, while the lean gas enters the last compression stage.

The compressed gas at stage 4 is cooled down in two steps first to 38 °C and subsequently to 15 °C before entering the flash drum of stage 4. The liquid product is sent to the condensate stripper, while the gaseous fraction is ready to enter the drying unit.

Drying and Chilling

This section of the simulation covers the drying of the gas stream and the refrigeration system with hydrogen fractionation. In the dryer, the moisture remaining in the gas stream after the compression section is removed. This is required to avoid the formation of ice in the cryogenic processes downstream of the plant.

Afterwards, the dried gas enters the refrigeration system, in which temperatures drop down in a range of -140 to -160 °C [14, p. 506]. At this temperature, most of the C2+are condenses, which allows the separation of the hydrogen fraction through chilling in a flash drum. The hydrogen rich gaseous phase is then feed into a pressure-swing absorption unit (PSA), in which pure hydrogen can be recovered [14, pp. 512-513].

A part of this hydrogen is used for the acetylene hydrogenation process, while the other part is either used as a fuel or recovered as a side product. The liquid exiting the chilling is first preheated before entering the first unit of the hydrocarbon fractionation (demethanizer). The flowsheet of the DSWIM simulation is presented in Figure 38.

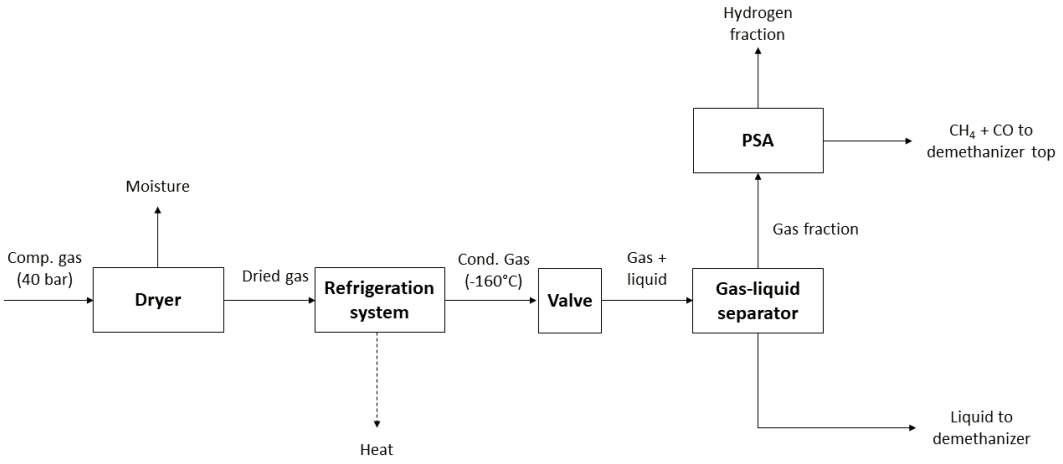

Figure 38: Process model for the drying and chilling section.

The dryer is simulated as simple separator with a given separation rate. It is assumed that the whole moisture contained in the gas is removed. The dried gas enters the refrigeration system. This unit is simulated as simple cooler with a given outlet temperature.

To allow a high removal of a hydrogen fraction with low content of C2+ hydrocarbons, the outlet temperature of the refrigeration system is set to -160 °C. In reality, the refrigeration system is a complex unit with several refrigeration cycles, that is connected to all cryogenic processes in the plant. For the simulation, a simple vapor-compression refrigeration system is assumed. The power requirement for the refrigeration system is estimated with following equation [67, pp. 2-3]:

$$P_{\mathrm{el.}} = \frac{Q_{\mathrm{cool}}}{\eta_{\mathrm{RS}} \cdot \varepsilon_{\mathrm{th}}} \tag{7}$$

With $P_{\mathrm{el.}}$ as the required electric power in kW for the vapor-compression refrigeration, $\varepsilon_{\mathrm{th}}$ as the theoretical coefficient of performance of the refrigeration system, η_{RS} as the efficiency of the refrigeration system and Q_{cool} as the required thermal heat in kW for

the cooling process. The theoretical coefficient of performance is calculated with following formula [67, p. 2]:

$$\varepsilon_{\mathrm{th}} = \frac{\mathrm{T_{cool}}}{T_{\mathrm{amb.}} - T_{\mathrm{cool}}} \tag{8}$$

With $\mathrm{T_{cool}}$ as the lower temperature of the refrigerant in K and $T_{\mathrm{amb.}}$ as the ambient temperature in K. The value for Q_{cool} is obtained for the simulation. The calculation of the required power is carried out separately in Excel. The value for T_{cool} is assumed to be 10 K below the desired temperature of the gas stream (-160°C). The efficiency is set to 60%, which is a reference value from the literature [67, p. 2].

After the main gas stream exits the refrigeration system, it is chilled by using a valve to the inlet pressure of the demethanizer and then fed into a flash drum (gas-liquid separator), in which the gaseous hydrogen rich fraction is obtained at the top of the unit. This fraction is then feed into the PSA unit, in which pure hydrogen is obtained. This unit is simplified as a simple separator, in which pure hydrogen is recovered. The remaining impurities are later mixed with the top product of the demethanizer. The liquid fraction enters the hydrocarbon fractionation section.

Hydrocarbon Fractionation

The hydrocarbon fractionation consists of a set of 6 distillation columns and an acetylene hydrogenation reactor. The configuration chosen for this simulation is a front-end demethanizer with tail-end acetylene hydrogenation. The distillation columns are simulated as shortcut columns in DWSIM. This type of column requires a given pressure and a mol fraction input for the top and bottom products of a chosen component. The design parameters for the simulation are given in Table 8.

Table 8: Design specifications for the distillation columns of the hydrocarbon fractionation in DWSIM.

Column	Pressure (bara)	Source	Bottom specification	Top specification
Demethanizer	31.0	[68, p. 1689]	< 0.1 mol% Methane	< 0.1 mol% Propylene
Deethanizer	27.0	[69, p. 1226]	< 0.1 mol% Ethane	< 0.1 mol% Propane
C2-Splitter	19.0	[69, p. 1226]	0.1 mol % Ethylene	< 0.1 mol% Ethane
Depropanizer	7.8	[69, p. 1226]	< 0.1 mol% Propane	< 0.1 mol% 1,2-Butadiene
C3-Splitter	19.0	[14, p. 512]	0.3 mol% Propylene	0.1 mol% Propane
Debutanizer	3.4	[69, p. 1226]	0.1 mol% 1,2-Butadiene	<0.1 mol% N-pentane

The procedure for the column sizing was previously described in the water quench chapter. As the columns in this section are higher than the steam stripper, the column diameter for columns higher than 15 m was adjusted to 6 m, which is an average value for larger columns [65]. According to literature, the C2 and C3-splitter are the largest columns of the plant, with approximately 150-230 stages for the C3-Splitter [14, p. 512].

The operating pressures for the calculation are obtained from design examples from the literature (see sources in Table 8). A constant pressure in the columns was assumed, excepting the C3-splitter. For the C3-splitter, a pressure difference of 1 bar between top and bottom of the column was assumed. This assumption was taken to reach a

temperature difference between top and bottom of at least 10 K, which was necessary in this column due to the close boiling points of propane and propylene.

The bottom and top product specifications were adjusted manually to reach the polymer grade quality of the olefin products (>99.9 wt.% ethylene and > 99.5 wt.% propylene) [14, pp. 510, 512], but without exceeding the number of stages given in the literature (see given literature in Table 8). The only exception to this assumption was the propane splitter, from which the top and bottom specification were taken directly from design data of a C3-splitter simulation [70, p. 118].

Regarding the inlet temperature of the column feeds, it was assumed that the bottom products enter the next column without being preheated or precooled (nearly as saturated liquid). For the top products, it was assumed that they enter the next column as saturated liquids. For the demethanizer (first column), an inlet temperature of -68 °C was set for the feed (design specification from [68, p. 1689]).

For visual purposes, the layout of this section is depicted in two process flow diagrams. The process flow sheet for the first part of the simulation is presented in Figure 39.

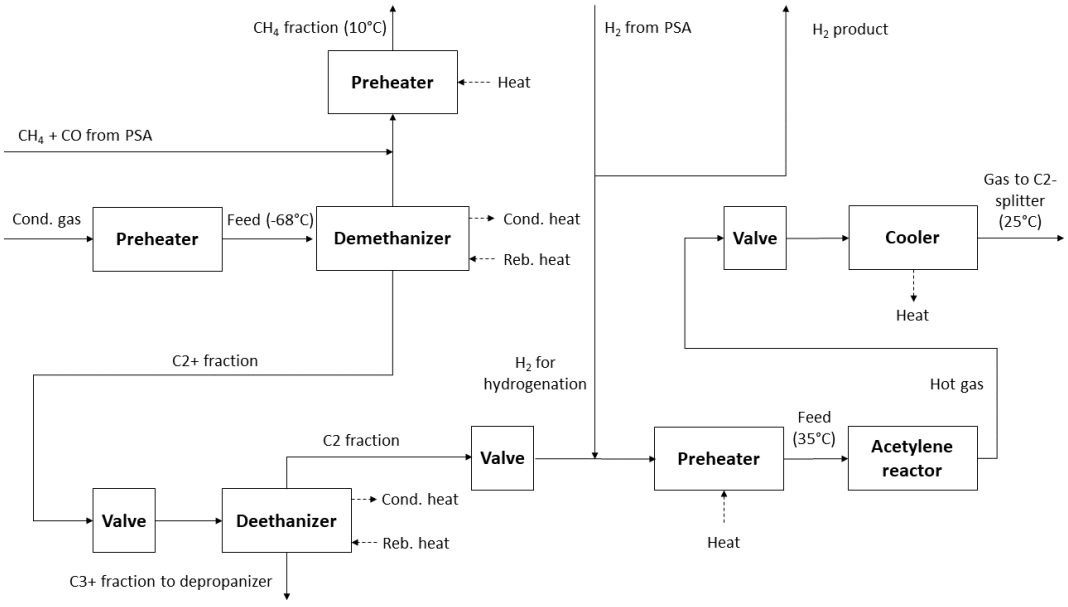

Figure 39: First part of the hydrocarbon fractionation.

The liquid outlet of the feed chilling section (cond. gas) is preheated to -68°C before entering the demethanizer column. The Top product is mixed with the impurities of the hydrogen fraction exiting the PSA unit. These impurities consist mainly of methane and carbon monoxide. It is assumed that the methane fraction, which represents the main part of gas fuel for the pyrolysis reactor, leaves the purification unit at 10 °C. Therefore, the methane fraction is heated to this temperature in a simple heater after exiting the demethanizer column.

The bottom product of the demethanizer is first brought to the operation pressure of the deethanizer through a valve before entering the column. The top product leaves the column and moves to the acetylene hydrogenation section, while the bottom product goes to the depropanizer. The next section contains the acetylene hydrogenation reactor. The reactor is set to operate at 35 °C and 25 bar [18, p. 5]. In reality, this section comprises two parallel process lines, consisting of two fixed-bed reactors set in

series. The process consists of a reaction-regeneration cycle, in which one line is operated while the other fixed bed reactors undergo regeneration.

Acetylene concentrations below 1 ppm are achievable at the outlet of the operation line [18, p. 4]. For the simulation, this set-up is simplified as a single adiabatic conversion reactor with a conversion rate of 99.9% acetylene to ethylene. The simulation of the acetylene hydrogenation is described as follows: The top product of the deethanizer is brought to the acetylene hydrogenation pressure in a valve. The hydrogen fraction coming from the PSA unit is split into two streams. The first stream goes to the acetylene convertor, while the other stream leaves the purification unit as a side product.

For the economical evaluation, the reactor volume is approximated with the residence time. The residence time is calculated using operational data from the literature [18, p. 5]. The acetylene hydrogenation costs are calculated assuming 4 reactor vessels. The acetylene hydrogenation is carried out with stoichiometrically dosed hydrogen. The hydrogen feed is mixed with the top product of the deethanizer and heated to the reaction temperature before entering the acetylene convertor. Afterwards, the reactor outlet is cooled down to ambient temperature before entering the second section of the hydrocarbon fractionation. The process flow diagram of this section is shown in Figure 40.

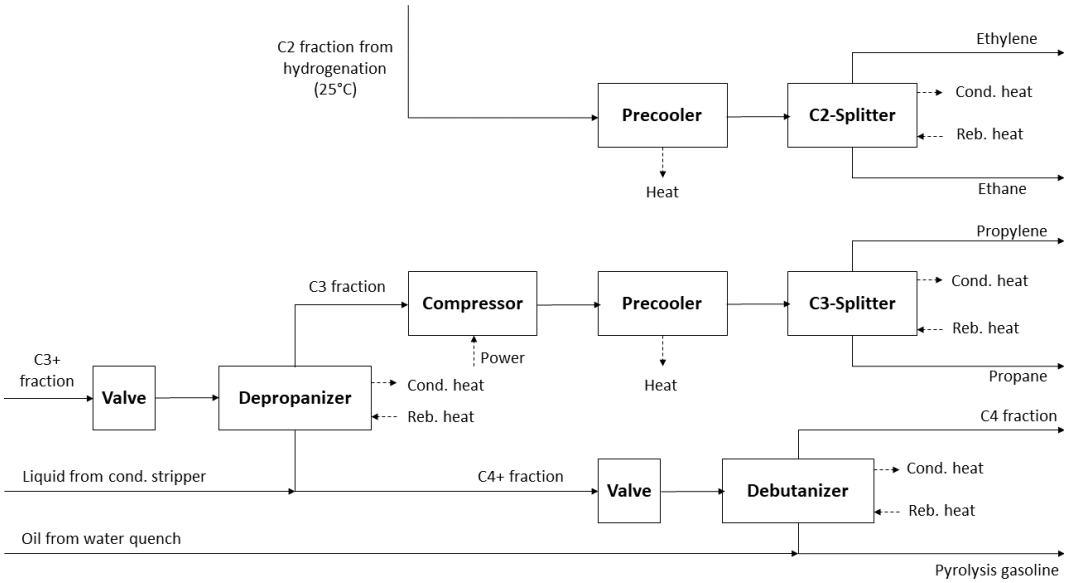

Figure 40: Process flow diagram of the second part of the hydrocarbon fractionation.

After the outlet of the acetylene reactor is cool down to ambient temperature, the gaseous stream is further cooled down in a second cooler to the inlet temperature of the C2-splitter. The polymer-grade ethylene fraction is obtained at the top of the column, while the ethane fraction is gained as a side product from the column bottoms. The bottom product of the deethanizer (C3+ fraction) goes into the depropanizer section. This stream is first brought into the depropanizer operating pressure through a valve before being feed into the depropanizer column.

The top product of the depropanizer is compressed to the operation pressure of the C3-splitter and subsequently cooled down to the column feed temperature, to be subsequently fed into the C3-splitter column. Polymer grade propylene is obtained at

the top, while propane is gained at the bottom as a side product. The bottom product of the depropanizer goes to the debutanizer.

The bottom product of the condensate stripper coming from the compression section is mixed with the column bottoms of the depropanizer before entering the debutanizer section. The mixture is first brought to the debutanizer operation pressure through a valve and then fed to the debutanizer column. A C4 fraction is gained at the top as a side product. The bottom product of the debutanizer is mixed with the recovered oil fraction from the water quench section coalescer and exits the purification unit as a side product.

3.2.2.4 Energy Recovery

After the products fraction in the purification unit (DWSIM) are calculated, the outlet streams data is transferred manually to the outputs of the black box model in EBSILON. The outlet streams of the purification unit and the flue gas stream of the reactor burner are used to simulate a simplified energy recovery section in EBSILON. This part of the simulation contains the second part of the water quench cycle and the energy recovery for the reactor exhaust gases.

The simulation of the whole energy recovery section and their integration in the whole process is presented in Figure 28. The first part of this section comprises the continuation of the water quench cycle. In this section, the recovered water from the steam stripper is used to produce a part of the dilution steam required for the pyrolysis reactor.

The process was adapted from a plant example from the literature, which can be found in [17, p. 4]. The parameters taken for this example are 15 bara and 260 °C for the medium pressure steam (MP-Steam). The parameters for the dilution steam are set to 9 bara and 175 °C (saturation temperature). The implementation in EBSILON is shown in Figure 41.

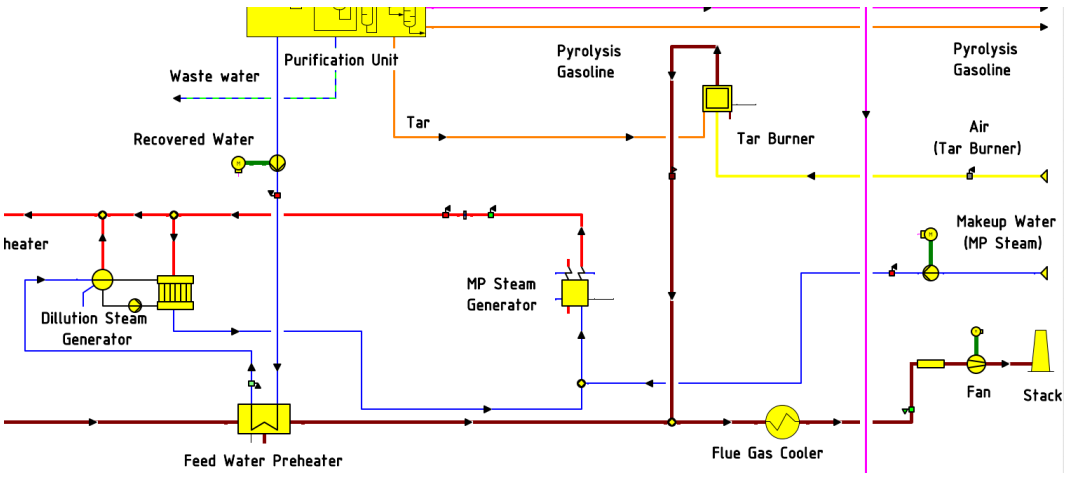

Figure 41: First part of the energy recovery section in EBSILON.

Two water fractions leave the purification unit after the EBSILON simulation: the first one contains the wastewater fraction, which comes from the primary fractionation, the condensate stripper, and the dryer. The second fraction comes from the steam stripper in the water quench section. This stream goes first into the feed water preheater, which uses the exhaust gases from the pyrolysis reactor as a heating medium, and then to the dilution steam generator (DSG).

After the recovered water has been evaporated, it is mixed with MP-steam makeup. The mixture leaves to the superheater before entering the pyrolysis fluidized bed reactor. MP-steam is used as a heating medium in the DSG. This steam is generated separately in another boiler (MP Steam Generator). The MP-steam is recirculated between the two boilers. Makeup water is mixed to the feed of the MP-Steam generator to replace the part of the water fraction than cannot be recovered (wastewater).

Additionally, the tar fraction coming from the primary fractionation is burned (Tar burner) to estimate the amount of heat that can be recovered from this stream. The outlet temperature of the burner is set to 170 °C [56, p. 41]. The exhaust gases are mixed with the cold flue gases from the reactor and send to a last heat exchanger, in which they are cooled down to 10 K above their dew point [61] to extract the remaining heat in the stream, to later exit the process at the stack.

The second and last part of the energy recovery section consist of the superheating of the dilution steam before entering the fluidized bed reactor. The implementation in EBSILON is depicted in Figure 42.

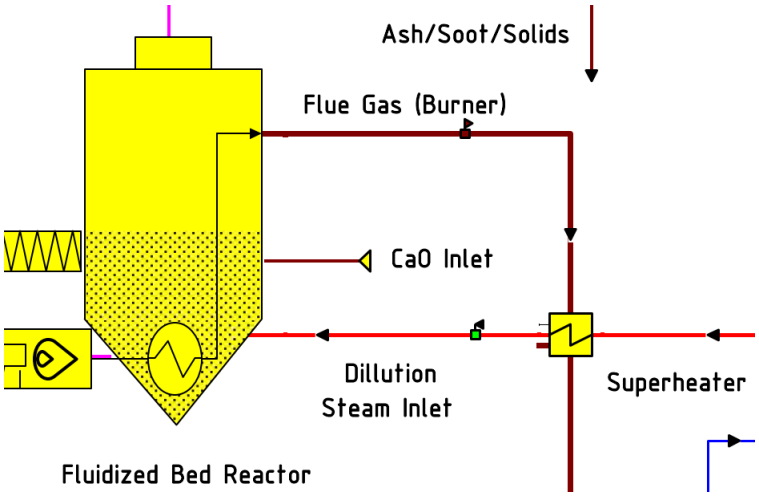

Figure 42: Implementation of the superheating of the dilution steam before entering the pyrolysis reactor in EBSILON.

The mixture of dilution steam coming from the DSG, and MP-steam makeup enters the superheater. The dilution steam is heated in counter current flow with the exhaust gases from the pyrolysis reactor. The inlet temperature of the dilution steam in the reactor is set to 500 °C (see Table 5). The cold exhaust gas exiting the superheater goes to the feed water preheater.

3.2.3 Combustion Loop

The combustion loop consists of the incineration of the plastic waste and further treatment of the flue gases from the combustion process to yield a light olefin product. The flue gas treatment involves basically a flue gas purification, a carbon capture and an electrolysis unit, a methanol synthesis loop, and a methanol to olefins process with a product recovery section. The process flow diagram of the loop is depicted in Figure 43.

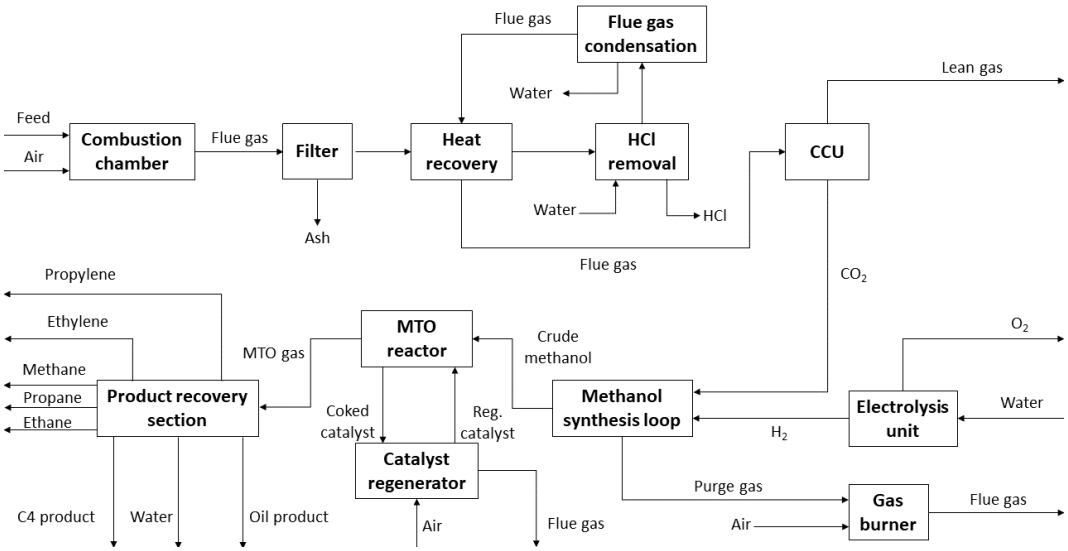

Figure 43: Overview on the process flow of the combustion loop.

The process overview presented in Figure 43 is a simplified process flow diagram of the combustion loop. Some material streams and intermediate steps are omitted for display purposes. The loop starts at the combustion chamber, in which the plastic waste feed is burned with combustion air to produce energy. The exhaust gases are led to a filter, in which the ash contained in the gas stream is separated.

The ash-free gas stream is led to the HCl removal section, which is composed by a heat recovery unit, a HCl washer (HCl removal) and a flue gas condensation section, which has the aim to improve the absorption in the CCU by increasing the CO_2 partial pressure in the flue gas (see chapter 2.5.2.3). First, the gas is cooled down in the heat recovery unit, to be purified afterwards from HCl compounds with the help of water. The cool and wet gas is further cooled down in the flue gas condensation section. The water contained in the gaseous stream is partially condensed and later removed from the gas.

The cooled gas is brought back to the heat recovery unit, in which it is used as a cooling medium for the hot inlet gas cooling. Afterwards, the flue gas goes to the carbon capture unit (CCU), in which most of the CO_2 contained in the gaseous stream is separated. The lean gas with a low CO_2 content exits the system boundary of the combustion loop, while the captured CO2 is led to the methanol synthesis loop.

The hydrogen stream required for the methanol synthesis with CO_2-hydrogenation is produced in an electrolysis unit from feed water, producing a O_2 stream as a side product. In the methanol synthesis loop, CO_2 and H_2 are used as feedstocks to produce methanol. A small purge stream containing gaseous components such as CO_2, CO and H_2 leaves the synthesis loop and is burned with combustion air to produce energy. The crude methanol product goes to the MTO section.

The MTO section consists mainly of a MTO reactor, a catalyst regenerator, and a product recovery section. The crude methanol exiting the methanol synthesis loop is led to the MTO reactor, in which it is converted into an olefin rich hydrocarbon mixture, producing coke as an undesired side product during the chemical reaction. The coke produced in the reactor deposits on the catalyst, which has to be continuously regenerated during

the process. This is performed through combustion with air in the catalyst regenerator, producing energy and a flue gas stream.

The gaseous products from the MTO reactor are led into the product recovery section, which consists of several unit operations. The product recovery section of the combustion loop is very similar to the purification unit of the chemical recycling loop, containing likewise a water quench and a hydrocarbon fractionation section. After the compounds of the MTO gas are separated into several fractions, ethylene and propylene can be obtained at the end of the process. Additionally, other gaseous products such as methane, ethane and propane can be obtained together with liquid products such as Oil, water, and a mixture of C4 hydrocarbons.

The simulation for the combustion loop is carried out in the same way as the chemical recycling loop (chapter 3.2.2) but with more unit operations. The EBSILON simulation (outer shell) contains the combustion chamber for the plastic feed, flue gas purification section, CCU and electrolysis unit, methanol synthesis loop, MTO section and the purification unit for the MTO products. The implementation in is shown in Figure 44.

The process flow set up is the same presented in Figure 43 but with more components and material streams. The plastic feed is burned in the grate firing producing a flue gas stream, which is led through a filter in which the solid ash is removed. Next, the gas enters a heat recovery heat exchanger, to be saturated latter with water before entering the HCl removal (HCl scrubbing) section and the flue gas condensation described previously. The flue gas condensation is composed of a cooler and an extra unit to remove the condensed water from the gas stream.

The gaseous stream exiting the heat recovery is cooled down and compressed before entering the CCU. The lean gas leaves the CCU to exit the system boundary at the stack. Analogous to the chemical recycling loop, the fans and stacks placed at the end of the flue gas streams are just for visualization purposes, as no pressure losses are considered in the model. The CCU is modeled as black box, but the calculations are performed in EBSILON directly.

The CO_2 captured in the CCU is further cooled down to ambient temperature before entering the methanol synthesis loop, together with the H_2 stream coming from the electrolysis unit. This unit is the first black box unit of the loop modeled separately in DWSIM (analogous to the purification unit of the chemical recycling loop). A crude methanol stream leaves at the left side of the unit, going to the MTO unit. A purge gas stream coming from the synthesis loop is combusted with air in a gas burner to further leave the system boundary at a second stack located in the middle of the process flow sheet.

The crude methanol product enters the MTO unit. This unit is a black box simulated separately in DWSIM as well. The unit consists basically of the MTO reactor, the catalyst regenerator, and the water quench section. The obtained gaseous mixture from the MTO reaction (MTO gas) is led to the purification unit for product recovery. A small fraction of the dissolved gases contained in the crude methanol is separated and mixed with the purge gas from the methanol synthesis loop, to be later burned in the gas burner.

A flue gas stream coming from the catalyst generator, in which the coke contained in the catalyst is burned with combustion air, exits the unit at the top to be mixed with the flue gases from the gas burner and leaves the system boundary at the second stack. A fraction of liquid products (water and oil) recovered from the quench water section (simulated in DWSIM) exit the unit at the bottom.

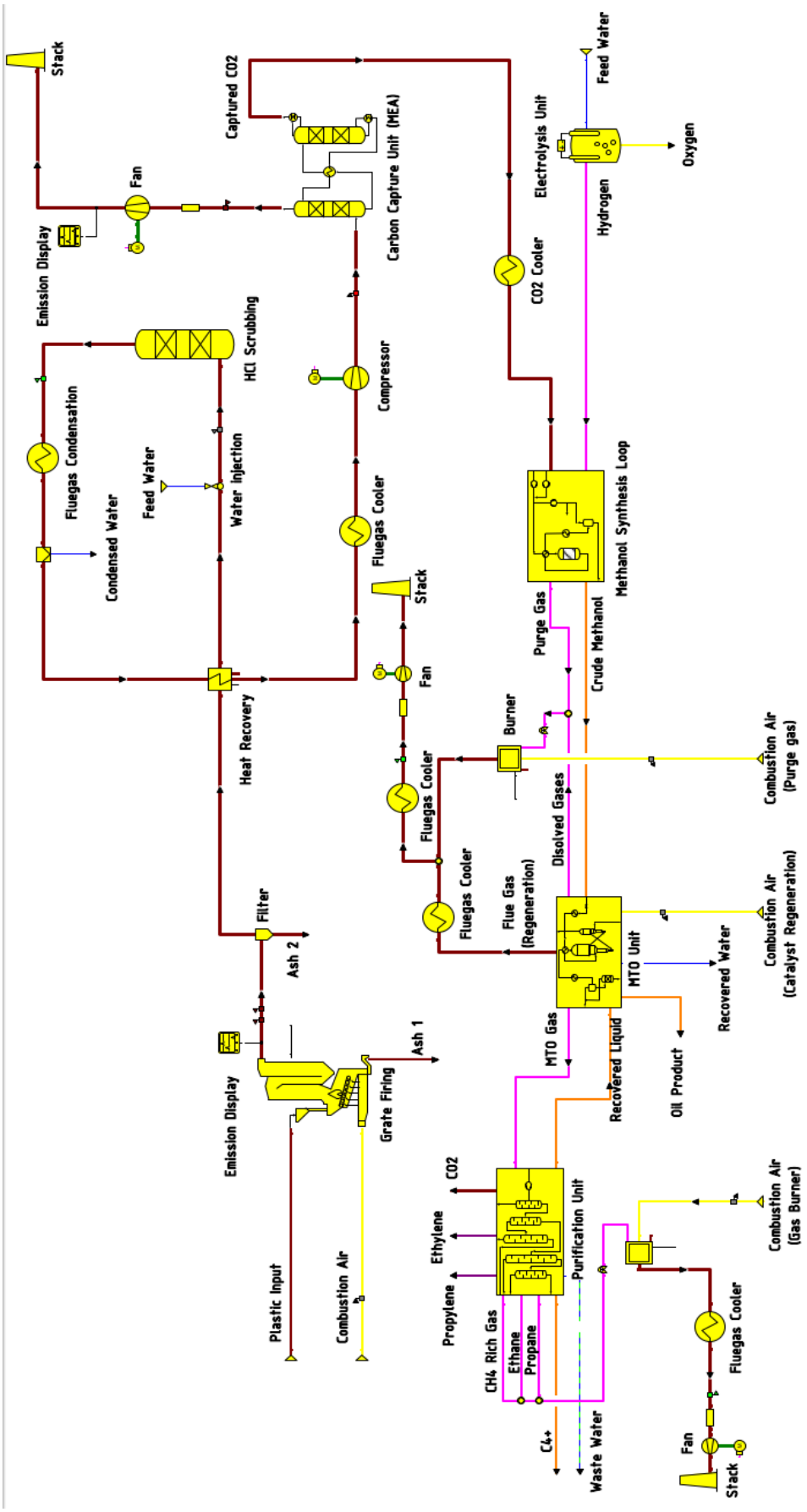

Figure 44: Process model of the combustion loop in EBSILON.

The MTO gas products are brought into the purification unit. This unit is a black box simulated separately in DWSIM as well. The set-up of this purification unit is very similar to the one in the chemical recycling loop with small differences (e.g., no primary fractionation, no debutanizer). The purification unit and the MTO unit are simulated in one single DWSIM simulation. However, they are split into two separated units in EBSILON for visualization purposes.

The ethylene and propylene fractions are obtained at the top of the purification unit, together with a CO_2 stream coming from the caustic washer inside the unit (DWSIM). The gaseous side products such as methane, ethane and propane exit the unit at the left side. These fractions are mixed and combusted with air in a second gas burner placed in the lower side of the unit. The combustion of these gases is not strictly necessary, but it is performed for comparison purposes, as the same fraction is burned in the chemical recycling loop to heat the pyrolysis reactor (see chapter 3.2.2.1.).

The flue gases coming from the second gas burner are first cooled down for heat recovery and later led to a third stack placed at the lower left side of the EBSILON model. A C4-hydrocarbons mixture is obtained in liquid state at the left side of the unit, while a wastewater fraction exits at the bottom of the unit. The liquid from the first two compression stages of the product recovery section inside the purification unit (recovered liquid) exits at the right side of the unit and is brought back to the water quench section inside the MTO unit for product recovery.

The EBSILON model for the combustion has 4 black box units in total, from which 3 are modeled in DWSIM. Additionally, two simulations for energy recovery using the Rankine cycle for power production are simulated separately in EBSILON. In the following, the system components used in the EBSILON and DWSIM simulations, as well as the process and calculations inside the black box models are described more detailed.

3.2.3.1 Combustion Chamber (Grate firing)

The chosen technology for this process is grate firing. To model the process, a simple combustion chamber unit already implemented in EBSILON is used. The combustion chamber for the incineration of the plastic feed is modeled as a complete combustion. The reactions considered in the combustion chamber model are represented as follows:

$$C + O_2 \rightarrow CO_2 \quad (9)$$

$$H_2 + \frac{1}{2}O_2 \rightarrow H_2O \quad (10)$$

$$S + O_2 \rightarrow SO_2 \quad (11)$$

$$H_2 + Cl_2 \rightarrow 2HCl \quad (12)$$

As no sulfur compounds are present in the feed, reaction (11) does not actually occur in the simulation. The amount of combustion air required for the combustion process is adjusted to obtain a O_2 content of 8 vol% in a dry basis in the flue gas [56, p. 41]. Moreover, the temperature at the outlet of the combustion chamber (after the HRSG) is set to 170 °C [56, p. 41]. This outlet temperature applies to almost every combustion process in both loops, except the catalyst regenerator of the MTO unit. Furthermore, no NO_x formation is considered in the model, as no nitrogen compounds are present in the plastic waste feed. The implementation in EBSILON is shown in Figure 45.

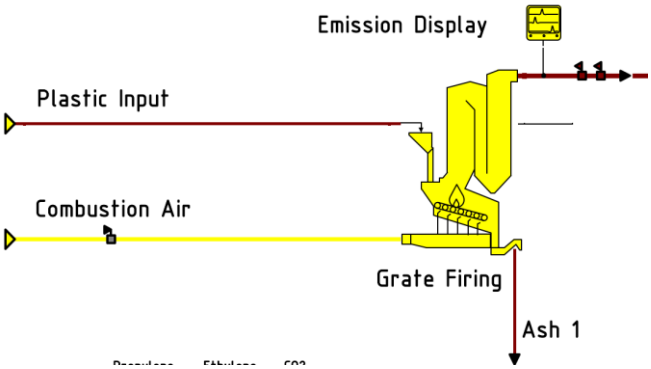

Figure 45: Implementation of the incineration of plastic waste in a grate firing in EBSILON.

The unit consists of two inlet and 2 outlet streams. The parameters for the inputs were already described in chapter 3.2.1. It is assumed that the whole ash content in the combustion exits with the flue gas (top right stream), so that the first ash stream is set to zero mass flow. The unit calculates the available heat in the HRSG at the defined outlet temperature (170 °C).

The emission display is a small unit that calculates the concentration of pollutants in the flue gas exiting the combustion chamber. For the model, the pollutants concentration was calculated to verify if a flue gas purification was necessary to meet the emission limits shown on Table 2 in chapter 2.5.2.1. As these limits are given in a 11 vol% O2 content, the concentration has to be converted to right values with following equation [41, p. 60]:

$$E_{\mathrm{B}} = \frac{21 - O_{\mathrm{B}}}{21 - O_{\mathrm{M}}} \cdot E_{\mathrm{M}} \tag{13}$$

With E_{B} as the pollutant concentration in a 11 vol% O_2 basis, E_{M} as the actual concentration in mg/Nm³, O_{B} as the base oxygen content (11 %) and O_{M} as the actual oxygen content in the flue gas. This conversion is already implemented in EBSILON.

Furthermore, a heat recovery section using the Rankine-cycle model described in chapter 3.2.2.3 is implemented to estimate the potential power and heat recovery from the HRSG. The implementation is presented in Figure 46.

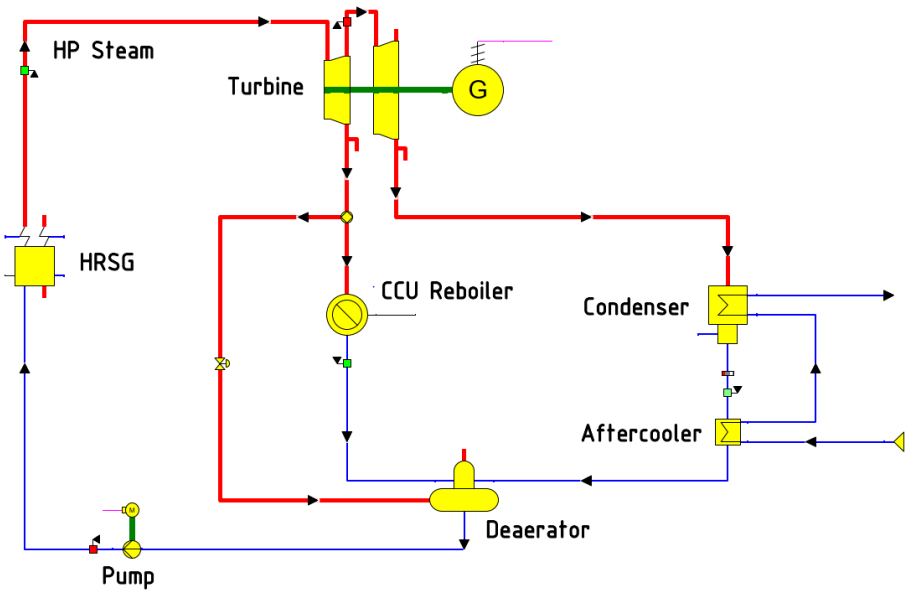

Figure 46: Implementation of the heat recovery cycle for the HRSG of the combustion chamber.

As the heat provided from the HRSG in the combustion loop is much higher and has more significance in the simulation, this cycle is modeled in more detail with additional components. The process can be described as follows: the feed water coming from the deaerator is compressed and fed to the HRSG, in which high pressure steam (HP Steam) is generated using the heat obtained from the plastic waste incineration. Analogous to the HP steam in the TLE, the steam parameters are set to 120 bara and 500 °C as well (see chapter 3.2.2.3).

The HP-steam is then expanded stepwise in two turbines. The additional turbine was added to obtain a hot steam stream to heat the reboiler from the solvent regeneration of the CCU, which operates at 120 °C. The pressure for the extraction at the first turbine is set to 4bara, which corresponds to a steam temperature of approx. 140 °C, which is usually the temperature of the heating steam for the CCU reboiler (see chapter 2.5.2.3).

The extracted steam is first split into two streams: one small part goes to the deaerator and serves as a stripping/heating medium for the feed water of the HRSG, while the other stream flows into the CCU reboiler, in which it is cooled and condensed to provide the required heat for the CCU. The CCU reboiler was modeled as a simple heat extraction unit with a given outlet temperature. The outlet temperature was assumed to be 130 °C, which corresponds to a 10 K temperature difference to the CCU reboiler temperature.

The condensed steam exiting the CCU reboiler is later led to the deaerator. The remaining steam at 4 bara (top-right of the first turbine) goes to the next expansion stage. In contrast to the Rankine cycle from the TLE, the pressure in this model is set to 1.3 bara [61]. This pressure is set at this value to elevate the temperature level of the cooling water used in the condenser and the aftercooler, which avoids high amounts of heat in the condenser at low temperature levels (35 °C).

The low-pressure steam exiting the second turbine goes then to the condenser and subsequently to an aftercooler. These two components are designed with a low temperature difference of 10 K (see chapter 2.5.2.3), which together with the new pressure level results in an increase of the temperature level of the low-pressure steam

condenser recovered heat to 97 °C. The condensed low-pressure steam is then led to the deaerator, which operates at 1.3 bara as well.

The deaerator is a standard component from EBSILON, which heats the feed to water until saturation using steam. The condensed LP-steam is mixed with condensate of the CCU reboiler, to be subsequently preheated/stripped with the rest of the steam from the first extraction stage of the turbine. The saturated feed water at 1.3 bara exits the deaerator to be compressed in the pump before entering the HRSG, closing the heat recovery cycle.

The turbines calculate the gained mechanical power in the cycle. Both turbines are connected in a generator (G). The generator is added in the model for visualization purposes. The potential power is estimated to verify if it is sufficient to cover the internal power demand of the loop.

3.2.3.2 Flue Gas Purification

The gas exiting the combustion chamber goes into the flue gas purification section. This section principally comprises removing of ash in a filter, followed by HCl removal and fuel gas condensation. The implementation in EBSILON is presented in Figure 47.

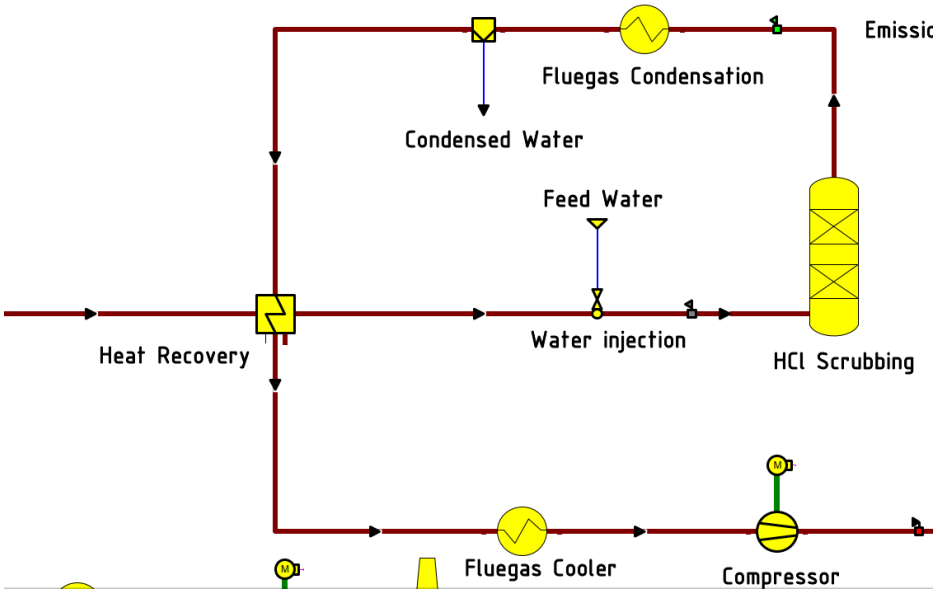

Figure 47: Simulation of the flue gas purification section in EBSILON.

As it can be seen in Figure 47, the flue gas passing the first emission display unit enters a filter unit, in which an ash fraction is separated (Ash 2). The filter is modeled as a simple separator with a separation rate of 99.98% for unburnable solid particles. This value is obtained from a reference value from the literature [61]. The ash-free flue gas enters then the heat recovery (HR) heat exchanger, in which the gas is cooled down before entering the HCl removal unit.

The HCl removal loop (HR-heat exchanger, HCl scrubbing and flue gas condensation) is adapted from an acid gas removal facility of an actual waste incineration plant. [61] The HR heat exchanger is designed with an upper temperature difference ($\vartheta_{hot,in} - \vartheta_{cold,out}$) of 20 K. The hot flue gas from the filter unit enters the heat exchanger at the left side, where it is cooled in counter current flow with the cold gases exiting the HCl removal

unit. The cooled flue gas exits the component at the right side, to be subsequently saturated through water injection before entering the HCl removal (HCl Scrubbing).

The relative humidity in the flue gas for the saturation is set to 94 %. The HCl removal unit design is simplified and modeled as a separator with a separation rate of 99% [61]. The flue gas cooler is designed to cool down the gas stream to 10 K below the dew point of the flue gas. The condensed liquid water is further removed in an additional unit. The cooled flue gas exiting the flue gas condensation is used as a cooling medium in the heat recovery heat exchanger.

The purified flue gas exits at the bottom side of the HR heat exchanger to be subsequently cooled down in an additional cooler (Flue Gas Cooler) before being compressed to the inlet pressure of the CCU. The flue gas cooler is modeled as a simple cooler with a given outlet temperature. The flue gas outlet temperature of the cooler is set to 40 °C.

3.2.3.3 Carbon Capture Unit (CCU)

The CCU is designed as a black box, in which the outlet gaseous stream of the absorber and the desorber are estimated in base of the flue gas stream entering the CCU. In contrast to other black box units explained in previous chapters, this unit is not designed separately in DSWIM, but the calculations are implemented in EBSILON directly. The calculations are implemented through a small self-written Pascal script (Kernel Script in EBSILON).

The chosen technology for the CCU is an anime absorption/ desorption cycle with a 30 wt.% aqueous MEA solution as solvent. The aim of this unit is to calculate the outlet gaseous material flows of a CCU and to estimate the reboiler heat duty of the desorption column for solvent regeneration, which is the most energy consuming part of the CCU. Other energy consumers within the CCU are neglected. The process model in EBSILON is presented in Figure 48.

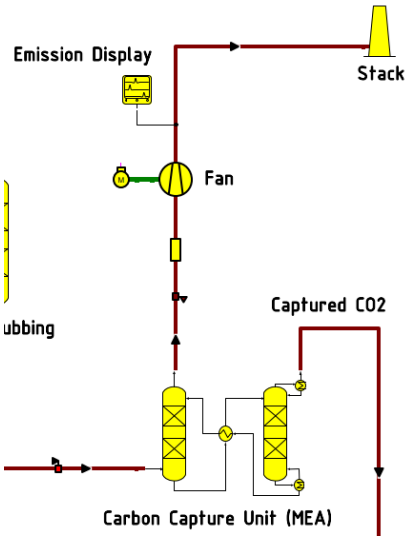

Figure 48: Simulation of the CCU in EBSILON.

The process is described as follows: the compressed flue gas enters the CCU at the left bottom side of the absorber. The lean gas exits the absorber at the top, to be further led into the stack through a fan. The stack and the fan are placed in the simulation just

for visualization purposes. Additionally, an emission display component is placed at the outlet of the desorber to verify if the emission limits presented in Table 2 are fulfilled in the lean gas stream.

The solvent stream flows are depicted as thin black lines in the CCU. However, these stream flows are not fully simulated in EBSILON. For the liquid solvent streams, just certain values that are needed for the calculation of the gaseous streams and the reboiler heat duty are calculated. The captured CO2 exits the CCU at the top of the desorption column condenser.

The temperature difference between the lean gas and the flue gas is set to 10 K. The operating pressure of the absorber is set to 1.2 bara, while atmospheric pressure is assumed for the desorber operation. The outlet temperature of the CO2 exiting the desorber condenser is set to 90 °C. These values were obtained from a plant design for a CCU in a coal fired power plant [45, p. 1903 ff.].

The CCU is simulated as a closed absorption/desorption solvent cycle. Water/solvent loses, e.g., through evaporation loses in the regeneration column, are neglected. It is assumed, that 86 % of the CO2 contained in the flue gas can be absorbed in the CCU [71, p. 74]. The reboiler heat duty is estimated as a function of the specific rich solvent loading, the specific lean solvent loading, and the amount of captured CO2 with following equation:

$$Q_{\text{Reb.}} = \dot{m}_{\text{CO}_2,\text{abs.}} \cdot \Delta H_{\text{Reb.}}(\alpha_{\text{rich}}\ ,\ \alpha_{\text{lean}}) \tag{14}$$

With $Q_{\text{Reb.}}$ as the reboiler heat duty in kW, $\dot{m}_{\text{CO}_2,\text{abs.}}$ as the amount of absorbed CO_2 in kg/s, $\Delta H_{\text{Reb.}}$ as the specific reboiler heat duty in kJ per kg CO_2, and α_{rich} and α_{lean} as the specific rich and lean loading of the solvent respectively, in kmol CO_2 per kmol MEA. $\Delta H_{\text{Reb.}}$ is a function of the rich and lean specific solvent loading of the MEA solution. For the simulation, the value of α_{rich} was set to 0.5 [71, p. 74] [48, p. 4467]. For this value for the rich solvent loading, the specific reboiler heat duty can be estimated with following equation:

$$\Delta H_{\text{Reb.}} = \Delta H_0 \cdot e^{-a_0 \cdot \alpha_{\text{lean}}} + b_0 \tag{15}$$

Equation (15) is obtained through curve fitting with the help of a python script. ΔH_0 , a_0 and b_0 are the curve fitting constants obtained with the curve_fit() function from the SciPy Python library. The values obtained are ΔH_0 = 142366.02, a_0 = 13.09 and b_0 = 163.13. The data used for the curve fitting is taken from the literature [48, p. 4469]. The implementation of the curve fitting function with the experimental data is shown in Figure 49.

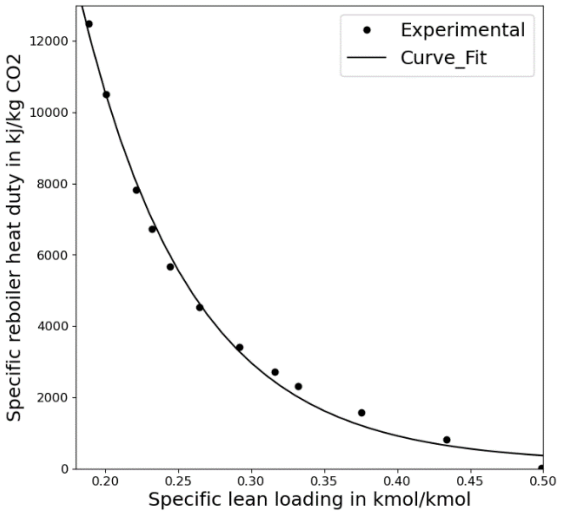

Figure 49: Curve fitting from literature data of the specific reboiler heat duty as a function of the lean solvent loading.

As it can be seen in Figure 49, the curve fitting function can estimate reasonable values for the specific reboiler heat duty as a function of the lean solvent loading (outlet of the desorption column). The accuracy of the function decreases as the lean solvent loading approaches 0.5 kmol/kmol. As this range of the curve does not rely in the operation window for the lean solvent loading (approx. 0.29 according to [71, p. 74]), and a value near 0.5 would mean almost no desorption takes place, these small deviations are neglected.

As the CCU is simulated as a closed loop, the specific lean solvent loading is obtained from the material balance of the absorber. To obtain an approximation of the material flows in the absorber, the standard equilibrium absorption model for a counter current absorber is used. Following equations are obtained from the material balance of an absorber [72, pp. 543, 547]:

$$LG_{\min} = \frac{L_{\min}}{G} = \frac{Y_{\text{in}} - Y_{\text{out}}}{X_{\text{out,max}} - X_{\min}} \tag{16}$$

$$LG = \frac{L}{G} = \frac{Y_{\text{in}} - Y_{\text{out}}}{X_{\text{out}} - X_{\min}} \tag{17}$$

With $LG_{\min}$ as the minimum solvent to gas ratio required for the absorption, LG as the actual solvent to gas ratio, $L_{\min}$ as the minimum unloaded solvent flow in kmol/h, G as the unloaded raw gas flow (without CO_2) in kmol/h, *Y* as the gas loading in kmol CO2 per kmol G, and *X* as the solvent loading in kmol CO2 per kmol unloaded solvent *L*.

The specific solvent loadings can be converted to solvent loadings with following formula:

$$X = \frac{\alpha}{1 + \frac{x_{H_2O}}{x_{MEA}}} \tag{18}$$

With x_{H_2O} and x_{MEA} as the unloaded solvent molar fraction of water and MEA respectively. The value for the maximum solvent loading $X_{out,max}$ is obtained with help of vapor-equilibrium data for a 30 wt.% MEA solution at 40 °C, which also considers the chemical equilibrium of the CO_2 absorption [73, p. 143]. The value for LG is assumed to be 1.3 times the value of LG_{min} [72, p. 547]. The other values required for the calculation of the reboiler heat duty are calculated from the material streams and design parameters previously described.

3.2.3.4 Electrolysis Unit

The electrolysis unit is implemented as a self programed component in EBSILON. The aim of this unit is to estimate the required electrical power for the production of the hydrogen stream for the CO_2 hydrogenation. The implementation in EBSILON is shown in Figure 50.

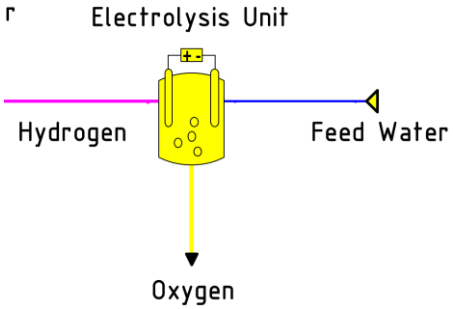

Figure 50: Implementation of the water electrolysis unit in EBSILON.

The feed water entering the electrolysis unit is split stoichiometrically into a hydrogen and an oxygen stream. It is assumed that the feed water enters the unit at ambient conditions. The amount of hydrogen is determined by the stoichiometrically required hydrogen for the methanol reaction. The pressure and temperature for the hydrogen and oxygen outlets are set to 30 bara and 25 °C [54, p. 40]. The required electrical power is calculated from the specific energy consumption of 4.8 kWh per Nm³ produced hydrogen, which is a reference value obtained from the literature [54, p. 40].

3.2.3.5 Methanol Synthesis Loop

In the same way as the purification unit of the chemical recycling loop, the methanol synthesis loop is designed as a black box and is simulated separately in DWSIM. The implementation in EBSILON is shown in Figure 51. The unit consist of 2 inlets at the right side of the unit (CO_2 and H_2 stream) and two outlets at the left side (purge gas and crude methanol stream). The Peng-Robinson property package is used for the thermodynamics in the DWSIM simulation.

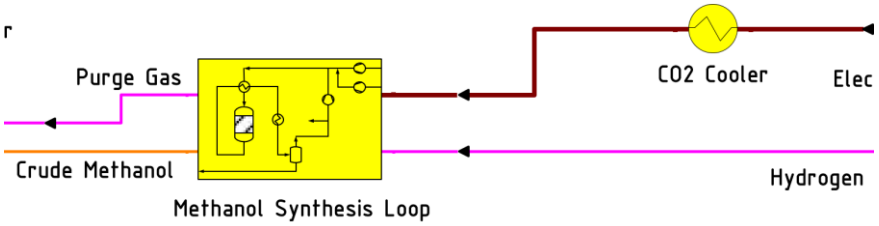

Figure 51: Methanol synthesis loop in the EBSILON graphical interface.

Before entering the methanol synthesis loop, the CO_2 stream coming from the CCU is cooled to ambient temperature in the CO2 cooler. This is done to avoid high temperatures at the first compression stage inside the unit. Afterwards, both streams enter the compression stage of the synthesis loop. The process flow diagram of the methanol synthesis loop implementation in DWSIM is shown in Figure 52.

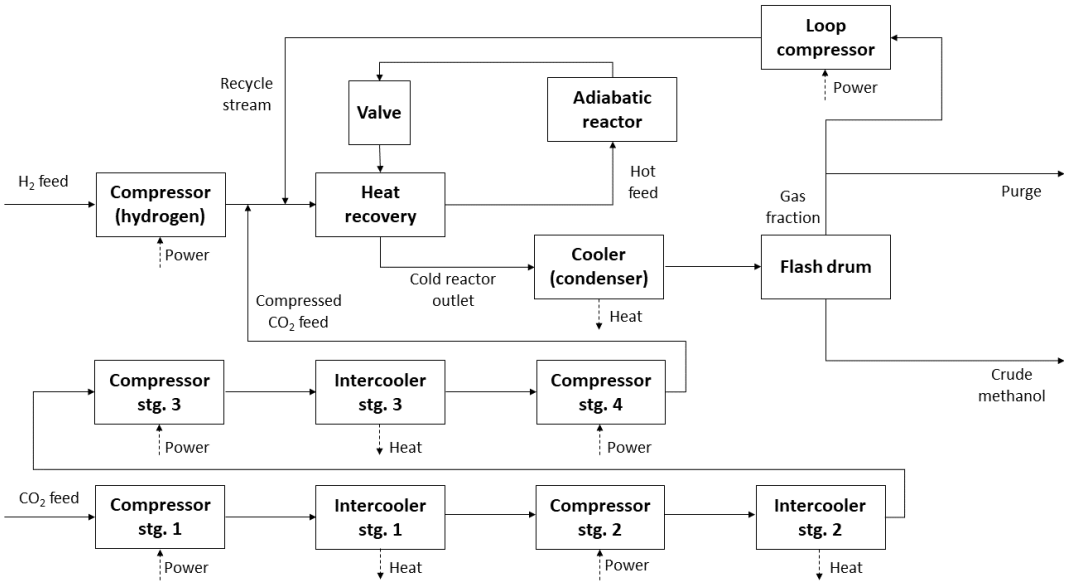

Figure 52: Process flow diagram of the methanol synthesis loop.

The synthesis loop starts with the CO_2 feed. This section consists of 4 compression stages with intermittent cooling. The outlet pressure of the compression section is set to 75 bara, which is a reference value from the literature [54, p. 41]. Although in this reference the outlet pressure is set higher (78 bara), the pressure at the inlet of the reactor is near 75 bara, because the model from the literature considers the pressure loses in the components. As these loses are not considered in this model, the pressure is set directly to 75 bara at the outlet of the compression section.

The outlet temperature of the intercoolers is set to 38°C [54, p. 41]. The pressures at the outlet of each compressor are calculated with the help of equation (6). The heat duty of the coolers and the required power for the compressor stages are calculated by DWSIM. The adiabatic efficiency of the compressors is assumed to be 75 %. As the hydrogen feed is delivered to the loop at a pressure of 30 bara, the compression section for this stream consists of one single stage. The compressed hydrogen feed is mixed with the outlet of the CO_2 compression section. As no other compression stage takes place, no intermittent cooling for the hydrogen feed is required.

The CO_2-H_2 mixture is mixed with the recycle stream coming from the loop compressor. The new mixture is then preheated in the heat recovery heat exchanger in counter current flow with the hot outlet gases coming from the reactor. The hot reactor feed enters the adiabatic reactor, in which a part of the CO_2-H_2 mixture is converted to methanol. Carbon monoxide is obtained as a side product from the Reverse Water-Gas-Shift (RWGS) reaction (equation (20)).

The hot outlet gas mixture exiting the reactor is brought into a valve. This valve is placed in the simulation to estimate the pressure drop in the synthesis reactor. Although no pressure losses are considered in the simulation, an exception is done with this component, as these losses are required to estimate the mechanical power for the loop compressor.

The hot outlet of the reactor is then cooled down in the heat recovery heat exchanger. The cold gases are further cooled and partially condensed in a simple cooler located after the heat recovery heat exchanger. The mixture is then separated into a gas fraction and a liquid product in a flash drum. The flash drum is modeled as a simple DWSIM gas-liquid separator.

The liquid fraction exists the methanol synthesis loop as a crude methanol product (see Figure 51). A small amount of the gaseous fraction separated from the loop and exits the unit a gaseous purge stream. The remining gas stream, which consists mainly of unreacted gases, is compressed to 75 bara in the loop compressor, before being mixed with the fresh CO_2-H_2 feed, closing the synthesis loop.

The reactor is simulated as a plug-flow-reactor model available in DWSIM, with a heterogeneous catalytic reaction setup. The reactions considered in the reactor are presented as follows:

$$\mathrm{CO_2} + 3\mathrm{H_2} \rightarrow \mathrm{CH_3OH} + \mathrm{H_2O} \tag{19}$$

$$\mathrm{CO_2} + \mathrm{H_2} \rightarrow \mathrm{CO} + \mathrm{H_2O} \tag{20}$$

Reaction (19) represents the methanol synthesis reaction, while reaction (20) depicts the RWGS reaction, which is a side reaction occurring during the synthesis. The kinetic equations for the reaction rates in the plug flow reactor is stated as follows [54, p. 42]:

$$r_{ME} = \frac{k_1 \cdot p_{\mathrm{CO_2}} \cdot P_{\mathrm{H_2}} \cdot \left(1 - \frac{p_{\mathrm{H_2O}} \cdot p_{\mathrm{ME}}}{K_{\mathrm{eq1}} \cdot {p_{\mathrm{H_2}}}^3 \cdot p_{\mathrm{CO_2}}}\right)}{\left(1 + k_2 \cdot \frac{p_{\mathrm{H_2O}}}{p_{\mathrm{H_2}}} + k_3 \cdot {p_{\mathrm{H_2}}}^{0.5} + k_4 \cdot p_{\mathrm{H_2O}}\right)^3} \tag{21}$$

$$r_{\mathrm{RWGS}} = \frac{k_5 \cdot p_{\mathrm{CO_2}} \cdot \left(1 - K_{\mathrm{eq2}} \cdot \frac{p_{\mathrm{H_2O}} \cdot p_{\mathrm{CO}}}{p_{\mathrm{CO_2}} \cdot p_{\mathrm{H_2}}}\right)}{\left(1 + k_2 \cdot \frac{p_{\mathrm{H_2O}}}{p_{\mathrm{H_2}}} + k_3 \cdot {p_{\mathrm{H_2}}}^{0.5} + k_4 \cdot p_{\mathrm{H_2O}}\right)} \tag{22}$$

With r_{ME} and r_{RWGS} as the reaction rates for the methanol synthesis and the RGWS reaction respectively, both in $\frac{\mathrm{mol}}{\mathrm{kg_{cat}s}}$. The Arrhenius parameters k_{i} are calculated with following equation [54, p. 42]:

$$k_\mathrm{i} = A_\mathrm{i} \cdot e^{\frac{B_\mathrm{i}}{R \cdot T}} \quad (23)$$

With R as the universal gas constant in j/mol K and T as the temperature in K. The values for A_i and B_i (B_i in J/mol) are given in Table 9.

Table 9: Values for the constants A and B for the calculation of the Arrhenius parameter k in the methanol synthesis plug flow reactor [54, p. 42].

k_i	A_i	B_i
k_1	1.07	40,000
k_2	3453.38	-
k_3	0.499	17.197
k_4	$6.62 \cdot 10^{-11}$	124.119
k_5	$1.22 \cdot 10^{10}$	-98.084

The equilibrium constants K_eq1 and K_eq2 are obtained with following formulas [54, p. 42]:

$$K_\mathrm{eq1} = 10^{\frac{3066}{T} - 10.592} \quad (24)$$

$$K_\mathrm{eq2} = 10^{-\frac{2073}{T} - 2.029} \quad (25)$$

Equations (21) - (25) can be implemented directly in the plug flow reactor model in DWSIM. The catalyst loading for the reactor is set to 1153.87 kg_{cat}/m^3. This value was calculated from the reactor data for the experimental setup [54, p. 44] for the developing of the kinetic model. The reactor volume was assumed to be 55 m^3. This value was manually adjusted to obtain a CO2 to methanol conversion of approx. 33% in the reactor, which is the conversion rate given in the literature for the reference design example [54, p. 42].

Furthermore, the pressure drop in the reactor bed is estimated with the Ergun equation (26). The calculation is performed separately in the spreadsheet of the DWSIM simulation and transferred to the valve. The Ergun equation stated as follows [74, p. 1275]:

$$\frac{\Delta p}{\Delta L} = 150 \cdot \frac{(1-\psi)^2}{\psi^3} \cdot \frac{\mu \cdot u}{{d_\mathrm{cat}}^2} + 1.75 \cdot \frac{1-\psi}{\psi^3} \cdot \frac{\rho \cdot u^2}{d_\mathrm{cat}} \quad (26)$$

With Δp as the pressure drop in the reactor bed in Pa, ΔL as the bed length in m, ψ as the porosity of the bed, u as the gas velocity of the fluid in the reactor in m/s, μ as the dynamic viscosity of the fluid in Pas, d_cat as the particle diameter of the catalyst pellets in m, and ρ as the fluid density in kg/m^3.

The reactor length is estimated from the reactor dimension. The reactor is dimensioned in DWSIM as a tube bundle with 2860 tubes, with a tube inner diameter of 40 mm [75, p. 819]. The bed void fraction is set to 0.4 and the particle diameter to 5.5 mm [54, p. 42]. The parameters of the catalyst bed and the tube dimensions are taken from reference methanol synthesis reactors from the literature. The fluid parameters are obtained from the simulation. The average values from the inlet and outlet streams of the reactor are used for the Ergun equation.

3.2.3.6 MTO Unit

The MTO unit is placed between the methanol synthesis loop and the product recovery section (purification unit) in EBSILON. The unit is simulated separately in DWSIM, excepting the coke combustion for the catalyst regeneration, which is simulated with a combustion chamber component in EBSILON located inside the black box of the MTO unit. The NRTL model is used for the thermodynamics of the DWSIM simulation. The implementation is shown in Figure 53.

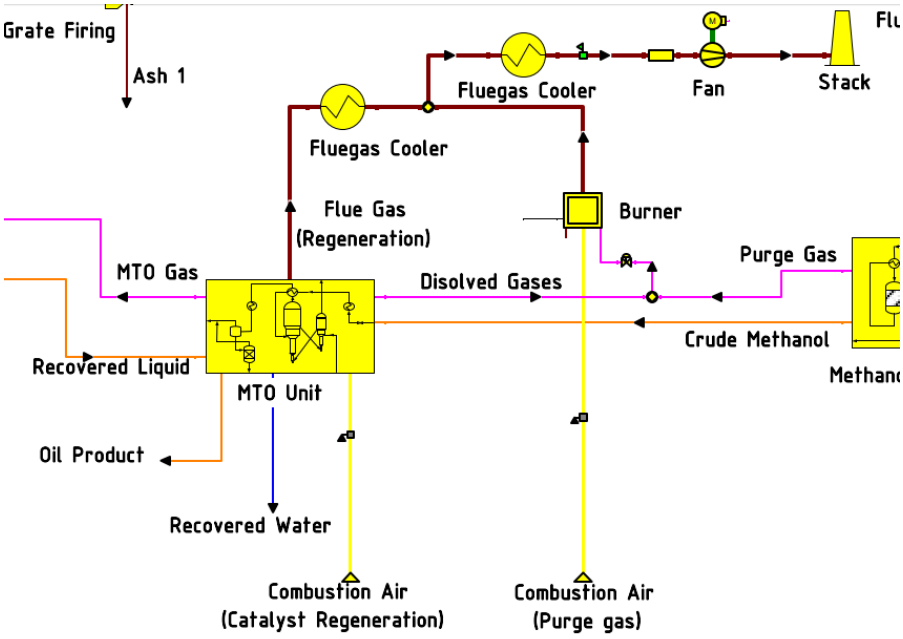

Figure 53: EBSILON simulation of the MTO unit.

The process is described as follows: the crude methanol product from the methanol synthesis loop enters the MTO unit at the right side. The dissolved gases contained in the crude methanol are separated inside the MTO unit (DWSIM) and mixed with purge gas stream coming from the synthesis loop. The mixture is burned in a gas burner with 10 % excess air (λ= 1.1). The hot flue gases are cooled down to produce heat and exit the combustion chamber at 170 °C.

The hot flue gases from the catalyst regeneration in the MTO reaction exit the unit at the top. These gases are cooled down first to 170°C and afterwards mixed with the flue gases from the gas burner. The flue gas mixture is further cooled down to 10 K above the dew point before exiting the system boundary at the stack. Three product streams exit the MTO unit (recovered water, oil product and MTO gas). The process flow for the inside of the MTO unit is presented in Figure 54.

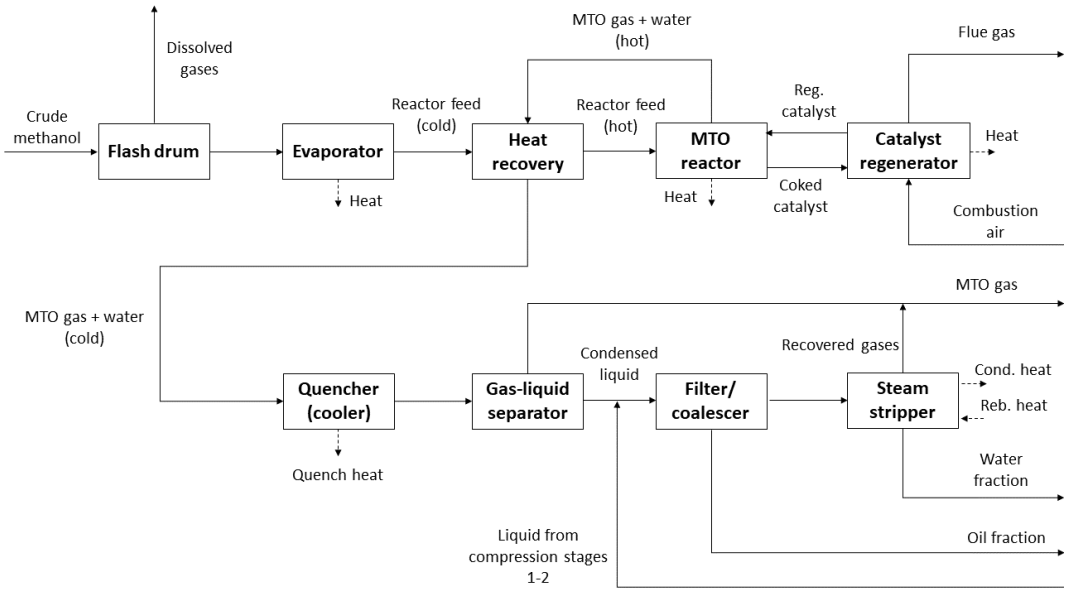

Figure 54: Process flow diagram of the MTO unit.

The process inside the MTO unit is described as follows: crude methanol enters the MTO unit and is flashed to remove the dissolved gases remaining from the methanol synthesis loop. The remaining liquid is the evaporated before entering a HR-heat exchanger, in which the cold reactor feed is heated in counter current flow with the hot outlet gases of the MTO reactor. The MTO reactor is modeled a conversion reactor with following conversion rates:

Table 10: Conversion rates for the MTO reactor (based on the carbon content in the methanol feed).

Compound	Conversion rate in % (C based)
CO	0.4
CO2	0.3
Methane	1.6
Ethane	1.2
Ethylene	45.4
Propane	2.3
Propylene	32.2
1-Butene	10.0
Cyclopentane	3.9
Cyclohexane	1.0
Coke	1.7

The conversion rates are adapted from reactor data from a MTO fluidized bed reactor given in the literature [22, p. 328]. A conversion of 100% for the methanol feed was assumed. The reaction temperature was assumed to be 450 °C and the outlet temperature to 500 °C. The reaction heat was calculated with the specific heat of reaction, which was set to -196 kcal per kg methanol feed [13, p. 73]. For the reactor sizing, a residence time of 2.5 s and a bed height of 3 m are assumed for this unit [12, p. 1932].

The coked catalyst from the MTO reactor is regenerated through combustion with air and feed back to the reactor. The regeneration temperature was set to 600 °C [22, p. 328]. The mixture of hydrocarbons and water goes then into the water quench section, which was simulated as an indirect quenching by cooling the gas to a given temperature. Analogous to the water quench section in the chemical recycling loop (see chapter 3.2.2.3), the temperature was set to 40 °C.

The condensed liquids separated in the water quench section are mixed with the flash liquids from the flash drums from the first two compression stages and then fed into filters and coalescers, in which an oil fraction is recovered. The oil free liquid enters the steam stripper, in which the dissolved gases are separated from the liquid stream. The dissolved gases are returned to the main gas stream (MTO gas). A water fraction is obtained at the bottom of the steam stripper. The steam stripper and the coalescers are modeled in the same way as in chapter 3.2.2.3.

Additionally, a simulation for the heat recovery of the MTO reactor and the catalyst regeneration is performed in EBSILON. The aim of this simulation is to estimate the potential electrical/mechanical power that can be produced with a Rankine cycle. The implementation in EBSILON is presented in Figure 55.

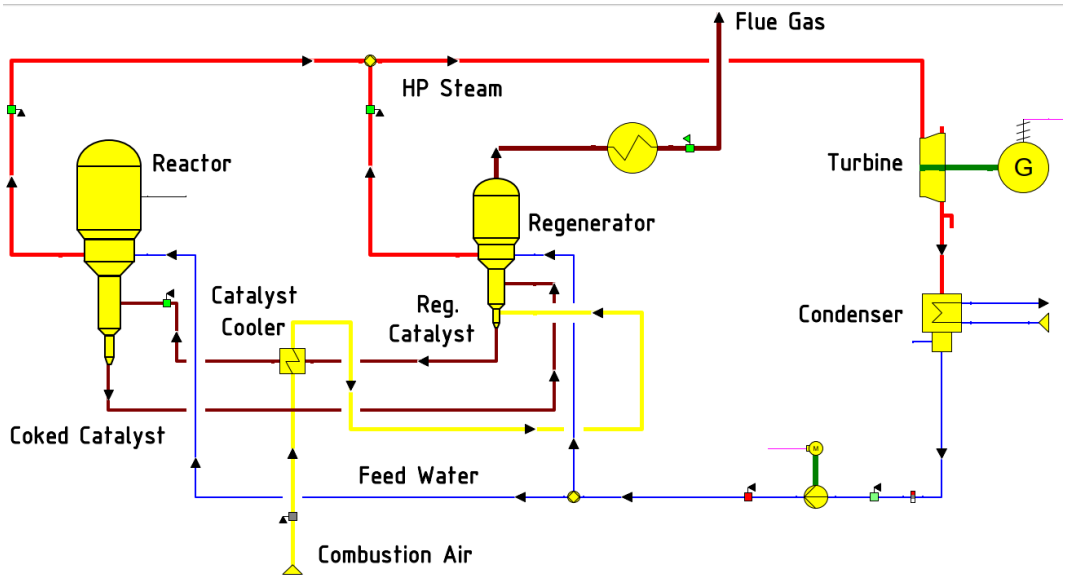

Figure 55: Simulation of the heat recovery cycle for the MTO reactor and the catalyst regenerator in EBSILON.

The heat recovery simulation consists of a simple Rankine cycle with two parallel steam generators (reactor and regenerator). The results obtained from DWSIM are used as basis for the calculation. The parameters for the heat recovery cycle are equal to the values used for the Rankine-cycle in chapter 3.2.2.3, with the difference that the steam temperature is assumed to be 450 °C, as the reaction temperature is limited to 500 °C.

For the coked catalyst stream, a coke content of 8 wt.% in the catalyst is assumed (see chapter 2.2.2). It is assumed that the coke is composed completely by pyrene [76, p. 1050]. The catalyst is simulated as an unburnable solid that is removed after the combustion process and cooled down in the catalyst cooler in counter current flow with the combustion air to the reactor inlet temperature (450 °C). A cooler is placed after the regenerator to estimate the heat recovery in the flue gas by cooling the stream to 10 K above the dew point.

3.2.3.7 Purification Unit

The purification unit is the last unit operation of the combustion loop simulation. The unit is simulated as a black box in EBSILON. The process inside the unit is simulated separately in DWSIM. The thermodynamics in the DWSIM simulation are modeled with the NRTL property package. The implementation in EBSILON is shown in Figure 56.

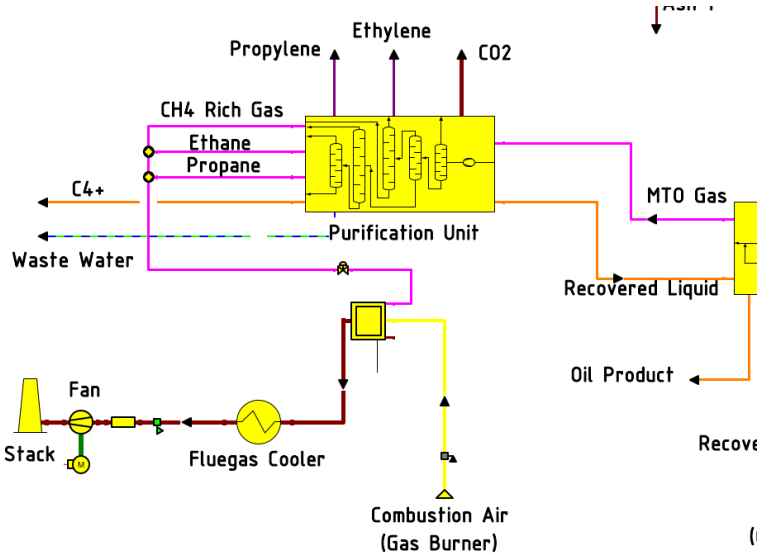

Figure 56: Purification unit of the combustion loop in the EBSILON graphical interface.

The MTO gas product coming from the MTO water quench enters the purification unit at the right side. Ethylene and propylene are obtained at the top of the unit, while the side gaseous (methane, ethane, and propane) and liquid (C4-hydrocarbons) side products exit at the left side of the unit. A wastewater fraction coming from the 3rd and 4th compression stages and the dryer exits the unit at the bottom side. The CO2 stream separated in the caustic washer exits at the top side of the unit.

Additionally, the gaseous product fraction is mixed and burned in a combustion chamber with air. This is performed to estimate the potential heat recovery from the gases for comparison with the chemical recycling loop, in which this fraction is used for the pyrolysis reactor heating. The outlet temperature is set to 170 °C. The flue gases are further cooled down to 10 K above the dew point before exiting the system boundary at the stack.

The process flow diagram of the simulation inside the purification unit is presented in Figure 57. The simulation follows almost the same path as that of the chemical recycling loop purification unit (see chapter 3.2.2.3), with the main difference that no feed chilling after demethanizer for hydrogen recovery is implemented, as no acetylene hydrogenation is required in this process. Furthermore, no debutanizer is implemented, as most of the C4+ hydrocarbons are separated in the water quench section upstream the plant.

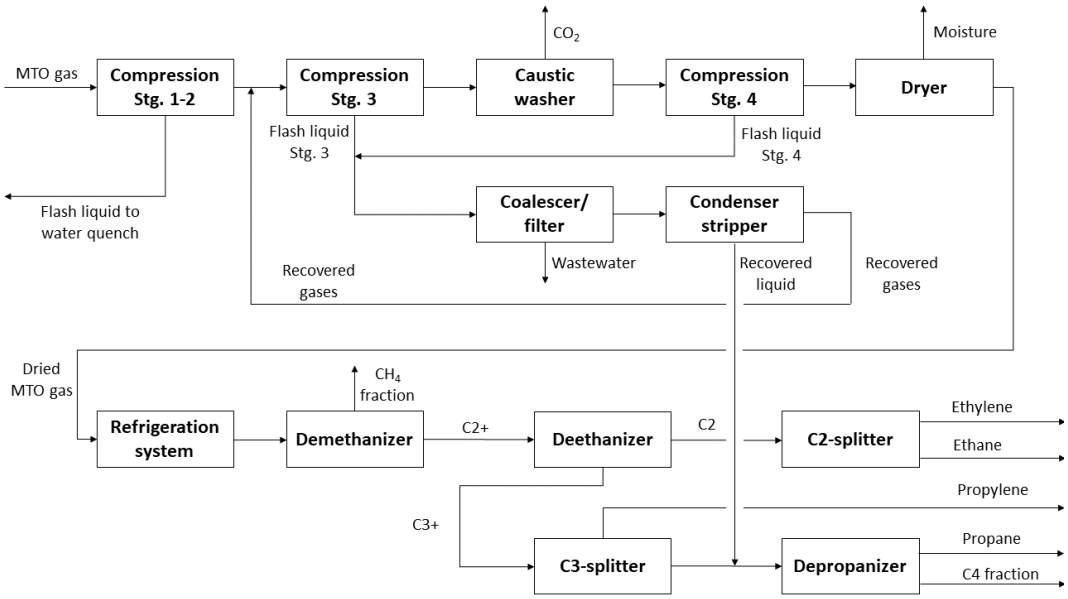

Figure 57: Process flow diagram of the combustion loop purification unit simulation in DWSIM.

The design parameters for the components are the same as the ones described in the chemical recycling loop, with the exception that the outlet temperature of the refrigeration system is set to -68 °C (inlet temperature of the demethanizer), as no hydrogen separation takes place. Furthermore, the bottom specification for the bottom liquid of the condenser stripper (recovered liquid) is assumed to be 1 mol% propylene, as the feed liquid mixture of the column has a 10 mol% higher content of propylene compared to the column liquid feed in the chemical recycling loop.

3.2.4 Technology Readiness level

The technology readiness levels (TRL) are a scale of 9 levels in which a specific technology can be classified according to its technological maturity. The original scale was developed by the NASA, and it was developed for space exploration technology. However, several approaches to adapt this scale for different branches have been created. In this work, the approach developed by Buchner et al. [77] is employed. This approach adapts the TRL for technologies in the chemical industry.

The aim of applying the TRL in this work is to rate and compare the technology maturity of the key unit operations present in the investigated recycling loops. First, the most important unit operations are selected and are rated independently from each other. Afterwards, the whole system is rated based on the TRL assigned to each unit operation. An overview of the TRL can be found in Table 11.

Table 11: TRL for the chemical industry according to [77, p. 6984].

TRL	Title
1	Idea
2	Concept
3	Proof of concept
4	Preliminary process development
5	Detailed process development
6	Pilot trials
7	Demonstration and full-scale engineering
8	Commissioning
9	Production

A detailed description and rating criteria for the TRL in the chemical industry can be found in [77, p. 6984]. The relevant criteria for each technology are chosen according to the available data in the literature.

According to the literature, there are three ways to choose a representative value for a composite technology: taking an average value, choosing the maximum value or choose the minimum value (critical technology element). In this work, the individual technologies are rated following the nine-step approach given in [77, p. 6987], choosing the minimum value of the criteria as individual representative number. Afterwards, the loops are rated and compared by the three representative values described previously (minimum, maximum, average), based on the individual TRL of the different technologies.

3.3 Economical Evaluation

To make a first estimation of the capital costs of the plant for both recycling loops, the investment costs of the main equipment (reactors, distillation columns, etc.) required for both loops are estimated. The costs for heat exchangers, flash drums, piping, pumps. induced draft fans and stacks for the flue gases are neglected, as these were not simulated in detail and play a minor role in the process. As the aim of the economical evaluation is a comparison between the loops, the cost for the caustic washer, the condenser stripper and the refrigeration system are neglected as well, as these units are set up almost identically in both loops.

Most of the reference costs are obtained from the book "chemical engineering economics" [78, p. 257 ff.], in which prices in dependency of the capacity of the equipment are given. Factors for the installation costs and the adjacent minor equipment are given as well. For some of the components, the reference costs are obtained directly by formulas given in the literature. In case of the distillation columns and the methanol synthesis adiabatic reactor, the cost is obtained from following equation adapted from the literature [79, p. 574]:

$$Purchased\ cost,\ \$ = 101.9 \cdot D^{1.066} \cdot H^{0.82} \cdot F_c \tag{27}$$

$$Installed\ cost,\ \$ = 101.9 \cdot D^{1.066} \cdot H^{0.802} \cdot (2.18 + F_c) \tag{28}$$

With D as the column/reactor diameter and H as the column height/ reactor length in feet. The factor F_c considers the influence of the pressure and construction material of

the equipment. Furthermore, the cost of the column trays was estimated with following equation:

$$Installed\ cost,\ \$ = 4.7 \cdot D^{1.55} \cdot H_{24} \cdot F_{\mathrm{c,tray}} \tag{29}$$

With H_{24} as the tray stack height assuming a 24-inch tray spacing and $F_{\mathrm{c,tray}}$ as the factor considering the tray material and the tray type. The columns were calculated as carbon steel columns with sieve trays. In the case of the electrolysis unit, the costs are estimated with following formula [53, p. 458]:

$$Capital\ cost,\ £ = 200 \cdot P_{\mathrm{elec.}} + 16 \cdot {P_{\mathrm{elec.}}}^{0.60625} \tag{30}$$

With $P_{\mathrm{elec.}}$ as the electrical power required for the electrolysis unit.

In case not enough data was available for the cost calculation, the costs are approximated with capacity method, taking reference prices from the literature. The formula for the cost estates as follows [80, p. 169]:

$$Capital\ cost\ of\ a\ = Capital\ cost\ of\ b \cdot \left(\frac{Capacity\ of\ a}{Capacity\ of\ b}\right)^{0.6} \tag{31}$$

With "a" as the investigated equipment and "b" as the reference equipment.

The units that were calculated using equation (31) are presented in Table 12, together with the literature source for the reference equipment price.

Table 12: Components in the recycling loops estimated with the capacity method.

Component	Capacity	Literature source
PSA unit	Molar flow	[81, p. 18]
CCU	Flue gas volume rate	[82, p. 3080]
MTO regenerator	Flue gas volume rate	Estimated from the MTO reactor

Furthermore, as the estimated capital costs are based on literature data at different times in the past, the values are adjusted to current prices. To calculate the adjusted capital costs, the chemical engineering plant cost index (CEPCI) is used to scale up the prices from the past. The adjustment is carried out with following formula [80, p. 164]:

$$Capital\ cost\ of\ year\ 1\ = Capital\ cost\ of\ year\ 0 \cdot \left(\frac{CEPIC_1}{CEPIC_0}\right) \tag{32}$$

With the index 1 representing the desired year and the index 0 for the reference year of the known price. The CEPCI for the past years can be found in the literature [80, p. 163] [83, p. 207]. For the current price, a CEPCI of 720.3 was used, as this represents the value for the equipment capital cost index in the year 2020 [84]. It is important to remark that this index corresponds to the last year before current global situations, like the war in Ukraine and the Covid-19 pandemic, which caused a global inflation and therefore resulted in a major price increase. However, as the loops cost are calculated using the same CEPCI, this doesn't affect the comparison of the costs.

4 Results and Discussion

In this chapter the results for the comparison of the two investigated recycling loops are presented. The results are divided in two sections: the technical evaluation, in which the simulations results regarding heat and material balance are shown, and the economical evaluation, in which the process economics are presented.

4.1 Technical Evaluation

The technical evaluation is divided mainly into two parts. In the first section, the product yields, the CO_2-foot print, and side product yields of both loops are presented and compared. The evaluation is performed based on the material balances of the loops. In the second part, the energy requirements (thermal heat and mechanical power) of each loop are compared. In an additional section, the technology readiness level for the main unit operations in each loop is compared and discussed. The detailed results for the EBSILON simulation can be found in Annex 2 to Annex 6.

4.1.1 Material Balance

The main purpose of the material balance is to compare the light olefin product yield (ethylene and propylene) of each recycling loop. Furthermore, the material flow for side products and waste streams are compared as well. For comparison purposes, the product yields are portrayed as tons or kg products per ton plastic waste feed. Furthermore, due to visualization purposes in the diagrams, the chemical recycling and the combustion loop are labelled as pyrolysis and MTO, respectively, as these are the key technologies for olefin conversion in each loop.

4.1.1.1 Product Yield

The results for the light olefin yield from the recycling loop simulation are shown in Figure 58.

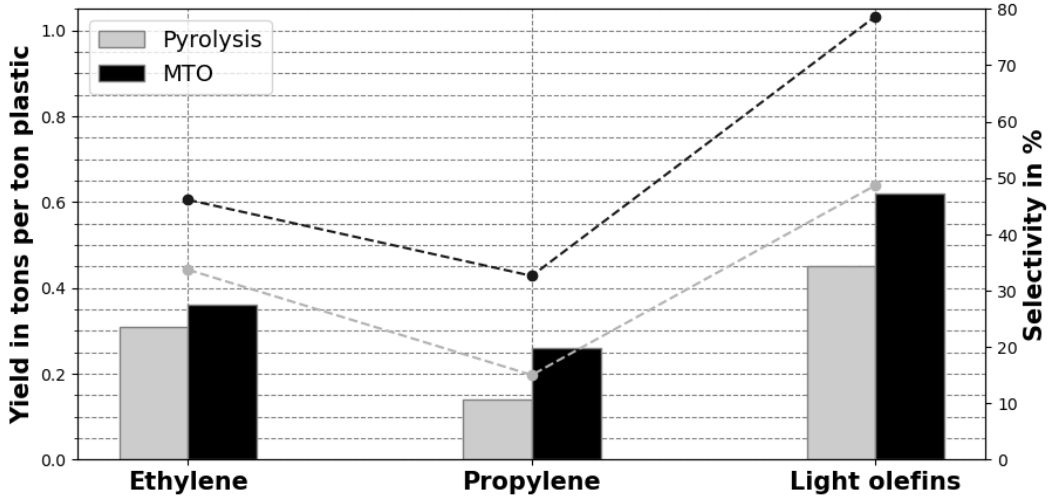

Figure 58: Comparison of the product yield (bars) and product selectivity (lines) of the recycling loops.

As shown in the presented diagram, the olefin yields in the combustion loop using the MTO process for olefin conversion are higher than in the plastic pyrolysis. The results shown that the ethylene and propylene yield in the combustion loop are 17 % and 83 %

higher than in the chemical recycling loop, respectively. Furthermore, the olefin selectivity in the MTO path, also the weight percentage of light olefins in the hydrocarbon products, is 30% higher than in the pyrolysis process.

It can be seen, that regarding product yields, the combustion loop is superior to chemical recycling loop, especially in the production of propylene. It is important to remark that only 86% of the carbon feed is captured on the CCU, while in the pyrolysis path, the whole carbon feed goes into the pyrolysis reactor. Therefore, a higher olefin yield in the MTO path, and consequently a higher difference in the product yields can be expected if the carbon capture rate is improved.

4.1.1.2 Side Product Yield

The results from the simulation regarding the yields of the side product fractions are shown in Figure 59. It is important to remark, that the methane, ethane, and propane fraction in the pyrolysis path have to be used as a fuel for the reactor, while in the MTO path it is possible to obtain these gaseous side products as a product fraction that can be sold or further processed to other chemical feedstocks. For this work, these gaseous fractions are used as a fuel and considered in the energy balance comparison.

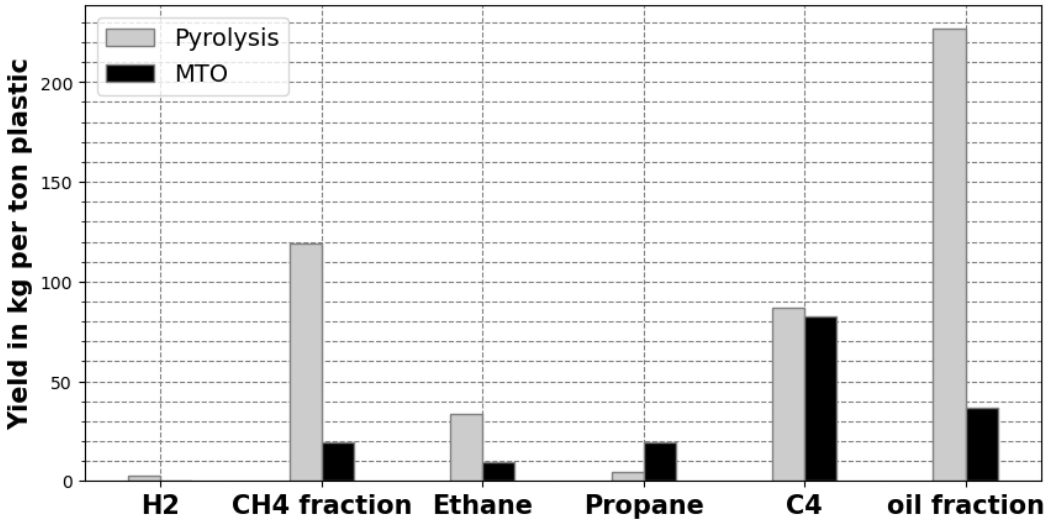

Figure 59: Results for the side products yields for each recycling loop.

As it can be seen in the previous figure, the production of side products in the pyrolysis path is much higher than in the MTO process, which explains the low light olefin selectivity showed in Figure 58. The biggest side product fraction produced in the pyrolysis path is the oil fraction (pyrolysis gasoline), while in the MTO, the C4 fraction has the highest production rate. The production rate for the C4 hydrocarbons is almost the same, with the pyrolysis path fraction being 5% higher than the MTO path.

Additionally, a small amount of hydrogen is obtained as a side product in the pyrolysis path, which is a valuable product that can be used as a feedstock in other chemical processes. The hydrogen production yield depicted in Figure 59 represents 53 % of the total recovered hydrogen from the purification unit, as the remaining 47 % is used as a fuel in the reactor, together with the methane, ethane, and propane fraction.

Regarding the MTO path, no hydrogen is recovered as side product, as no acetylene hydrogenation processes are required. Moreover, the hydrogen content in the feedstock of the MTO product recovery section is much lower than in the pyrolysis path. The main

reason for this is that the whole hydrogen contained in the plastic feed is burned during the combustion process, exiting the loop as water in the flue gas. The hydrogen required for the methanol synthesis is provided externally by the electrolysis unit in stoichiometrically amounts, which leads to almost no hydrogen side product in the main gaseous stream. However, a big fraction of O_2 (2.92 $t/t_{plastic}$) is obtained as an additional side product in the electrolysis unit.

Furthermore, the simulations results for the pyrolysis path show that the yield for the oil fraction is 64 % higher than the propylene fraction, making the second largest product fraction after ethylene in the chemical recycling loop. Although the pyrolysis is a valuable chemical feedstock rich in BTX aromatics, these results show a deviation from the main purpose of the loop, which is the light olefin production. In comparison, the MTO path biggest production fractions are ethylene and propylene, which shows that the MTO path fulfills the aim purpose of the loop better that the pyrolysis path.

4.1.1.3 Carbon Balance and Waste Streams

For comparing the CO2 abatement based on the carbon content of the plastic waste feed in both loops, a carbon balance is performed using in the simulation results. The balance is carried out by comparing the carbon content of the feed and at the outlet waste streams of the process (coming from the feed). The results are shown in Figure 60.

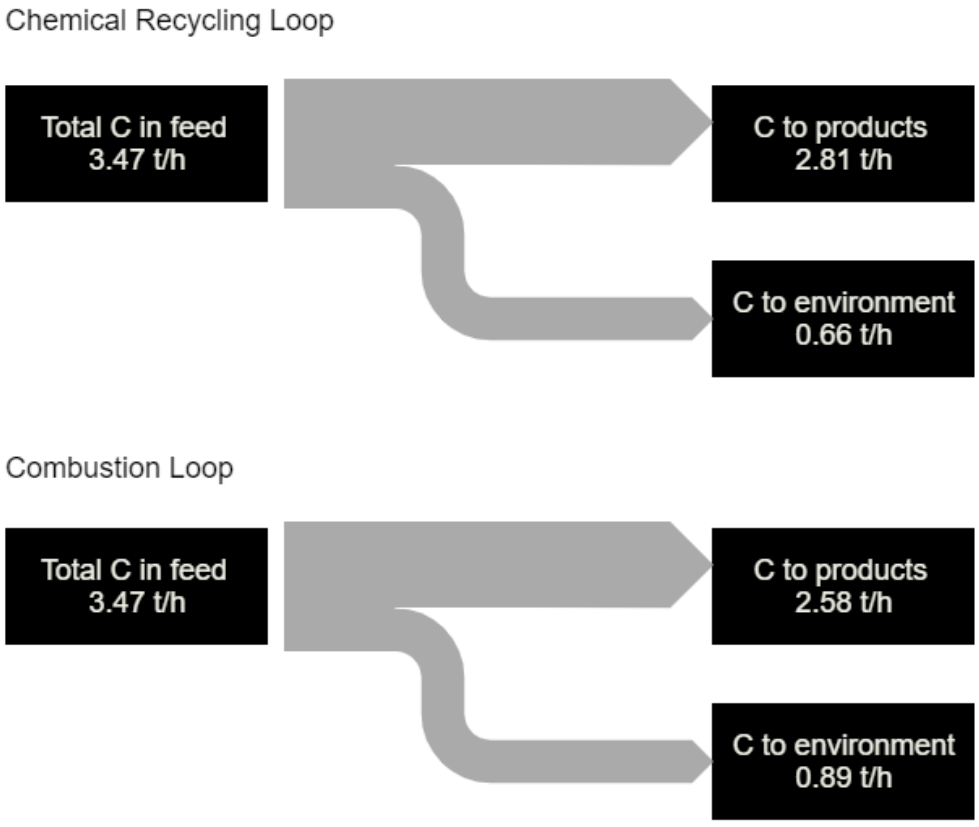

Figure 60: CO_2 abatement/carbon (C) balance for both recycling loops.

The results show that 81 % (2.8 t/h) of the carbon in the feed of the pyrolysis loop is converted to a product or side product, while the remaining carbon exits the loop as CO_2. The main source of CO_2 in the plant comes from the reactor burner. In the combustion loop, this percentage drops to 74 % (2.58 t/h), with main CO_2 source being

the grate firing for the plastic waste combustion. The results from the material balance for the produced waste streams and the carbon footprint (carbon dioxide balance) are shown in Figure 61.

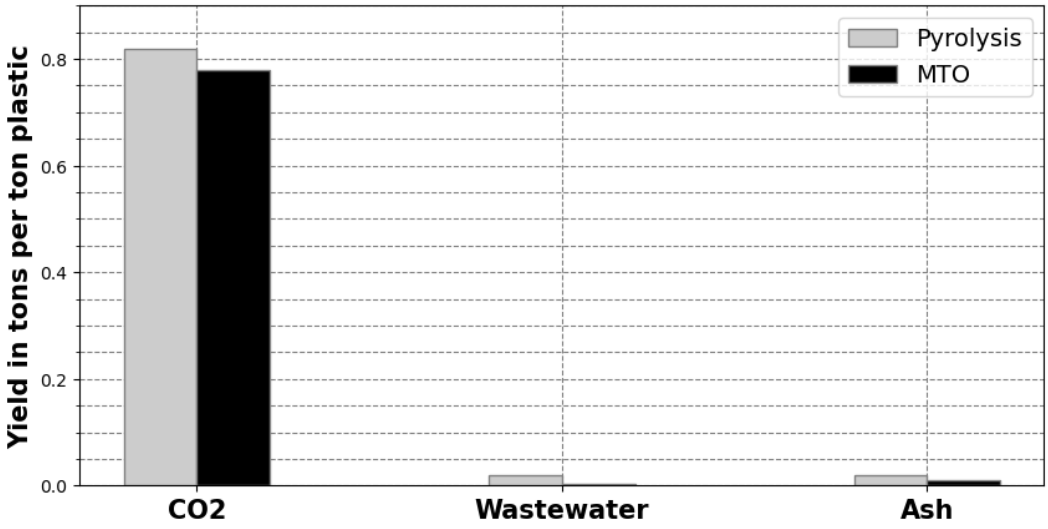

Figure 61: Comparison of the waste streams production for both recycling loops.

As presented in Figure 61, the carbon footprint in the pyrolysis loop (0.82 tons CO_2 per ton plastic) is slightly higher (approx. 4%) than in the MTO path (0.78 tons CO_2 per ton plastic). It is important to remark, that the amount of CO_2 for the MP-steam production in the pyrolysis path was considered additionally, as the energy supply for this process has to be provided externally. It was assumed that the heat for the MP-Steam boiler is provided through natural gas combustion. If the heat for the MP-steam boiler is provided through other sources that don't increase the CO_2-footprint (e.g. renewable energies), the carbon footprint of the MTO-loop turns out higher that in the pyrolysis path.

As an additional remark, the results of the simulation show that the flue gas production of the combustion loop is almost six times the amount of the chemical recycling loop, with 23.61 tons flue gas per ton plastic produced in the MTO path, while only 4.02 tones flue gas per ton plastic feed are produced in the pyrolysis process. However, most of the CO_2 produced in the MTO path is captured in the CCU unit, while this is not the case in the pyrolysis path. Nevertheless, this implies that a bigger effort for the stacks and the fans for the flue gas disposal has to be taken in the MTO path.

Regarding the wastewater production, the simulation results show that the amount of wastewater produced in the pyrolysis path is approx. 1.4 times the amount of the MTO loop. This can be explained when the source of the water contained in the gaseous stream is considered. The water content in the pyrolysis loop comes from the dilution steam, which is added in a 1.9 mass ratio to the plastic feed. In the MTO path, the water content emerges as a side product during the methanol synthesis and the MTO reaction, which means that its formation is delimited to the amount of CO_2 in the gas stream and therefore to the carbon content in the plastic feed.

However, several amounts of condensed water are recovered during the combustion loop, especially during the flue gas condensation (0.77 $t/t_{plastic}$) and the water quench tower section (2.04 $t/t_{plastic}$). Although these streams are recovered as pure water in the simulation, in reality, the water would contain small amounts of pollutants and dissolved gases, which would imply a further treatment for using this fraction in other processes.

In case this fraction is also disposed as wastewater, the wastewater fraction in the MTO path would increase drastically, resulting in the MTO wastewater fraction being 137 times higher than in the pyrolysis path (0.08 $t/t_{plastic}$).

Regarding the production of solid residues (ash fraction), the pyrolysis path produces 43% more ash than the MTO loop. This can be explained considering the HCl absorption with CaO, which produced an extra solid residue that is removed in the cyclone located at the outlet of the pyrolysis reactor. This would make the solid disposal in the pyrolysis loop slightly more difficult than in the MTO loop. Furthermore, the simulation shows that a pollutant concentration (11 % vol O_2 basis) of 0.4 mg/Nm³ and 0.13 mg/Nm³ for ash and HCl respectively, are achieved at the outlet of the flue gas purification process, which lie below the emission limits presented in Table 2.

In summary, it can be said that the combustion loop performs much better in the product yield, carbon footprint and waste streams production as the pyrolysis loop, as it has a much higher selectivity of light olefin product and a slightly less production of CO_2 during the process. Although the chemical recycling loop has apparently a better CO_2 abatement respecting the carbon usage of the feed, the results turn out different when the extra produced CO_2 for the medium pressure steam generation is considered.

The only aspect in which the MTO path has a clear disadvantage over the pyrolysis loop is in the wastewater production. This applies only if no further treatment or use for the recovered water in the flue gas condensation and the water quench section in the MTO unit is applied.

4.1.2 Energy Balance

The aim of the energy balance is to portray the thermal heat and power demand for the investigated recycling loops. Regarding the required power for the overall process, the compressor power (e.g., multistage compression) and the mechanical power for the cryogenic process (assuming vapor compression refrigeration) are considered. Additionally, the required power for the pumps in the different energy recovery cycles (Rankine cycles) and for the compression of the feed water for the dilution steam generator are accounted.

4.1.2.1 Power Balance

The power required for pressure losses in fans and other pumps are neglected (excepting the loop compressor in the methanol synthesis loop). The potential available power coming from the energy recovery in the Rankine cycles is considered in the analysis as well. The results for both loops are summed up in Figure 62.

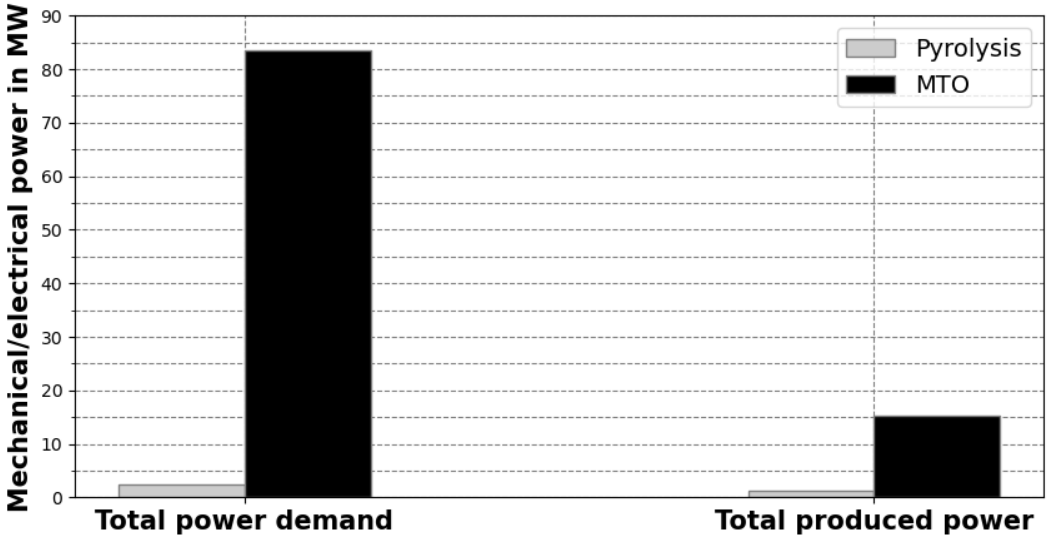

Figure 62: Simulation results for the total power demand and the total produced power for both recycling loops.

As shown in Figure 62, the power demand for the MTO loop is by far higher, representing approx. 32 times the amount of energy required for the pyrolysis loop. This significant difference in the power demand is caused by the electrolysis unit, which consumes 80.52 MW electrical power during the hydrogen production for the CO_2 hydrogenation, making it by far the most power consuming unit in both loops. As it was assumed that this unit uses renewable energy, this would mean that 96% of the total power demand for the combustion loop have to be provided externally by a stable renewable energy source.

Regarding the available power in the loops, the produced power in the energy recovery section is approx. 13 times higher in the MTO path. When comparing the power demand and the produced power for the MTO loop, it results in additional 68 MW that have to be provided externally. Regarding the pyrolysis path, 1.33 MW are still needed to cover the power demand in the pyrolysis loop. This means that only 46 % of the power demand can be covered through internal energy recovery. The reaming 54 % have to be provided externally.

Comparing both loops while considering the produced power, the results show that the MTO loop requires 52 times additional electrical power that the pyrolysis loop. Under these conditions, the pyrolysis path is by far superior to the MTO loop regarding the power balance.

4.1.2.2 Heat Balance

For the analysis of the thermal energy demand in the loops, the amounts of available energy and required external energy are analyzed. For the comparison, the thermal duty obtained from the simulation was divided into four levels, depending on the final cooling/heating temperature of the thermal unit: cryogenic heat (CRY) for $\vartheta < 25°C$, low temperature heat (LT) for $\vartheta < 50°C$, medium temperature heat (MZ) for $\vartheta < 100°C$, and high temperature heat (HT) for temperatures of 100°C and above.

The cryogenic cooling demand of the plant was already considered in the power demand comparison, assuming a vapor compression refrigeration system. Therefore, only the cryogenic heating demand is considered in the thermal analysis. The results for both loops are shown in Figure 63.

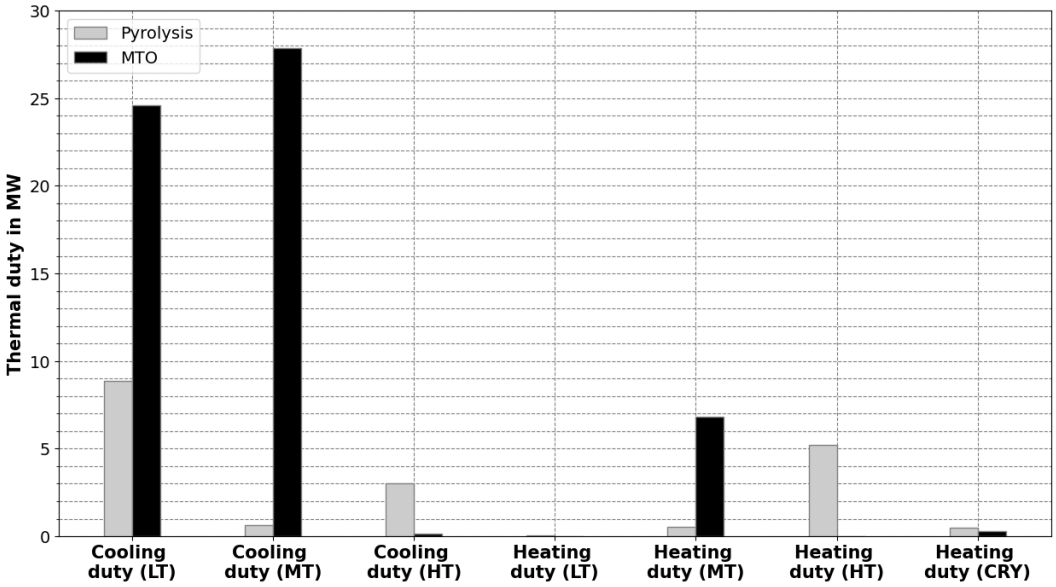

Figure 63: Results for the thermal duty of both recycling loops.

As presented in Figure 63, the biggest amount of thermal heat available in the amount correspond to the cooling duty at low and medium temperature levels in the MTO loop. Concerning the MT cooling duty, 99 % of the heat comes from the turbine steam condenser in the Rankine cycle of the combustion chamber. In case of the LT cooling duty, the heat comes from several units of the loop, with the crude methanol condenser and the water quench tower having the biggest cooling demand, with 9.32 and 6.38 MW respectively. A small amount of high temperature heat (0.15 MW) can be obtained from the cooling of the outlet flue gas from the catalyst regenerator in the MTO unit.

Regarding the heating demand, it can be seen that, for the MTO path, both heating duties (medium temperature and cryogenic) can be fully covered by the available cooling duty in the plant, as only 25 % of the MT and 1 % of the LT cooling duty are needed for the MT and the cryogenic heating demand, respectively. Approximately 80 % of the MT heating duty comes from the reactor feed evaporator in the MTO unit (5.57 MW), while the cryogenic heat demand comes from the hydrocarbon fractionation section. No low temperature heating is required in the MTO path.

In case of the pyrolysis path, the biggest amount of cooling demand comes from the LT level, with most of the cooling duty coming from the quench water tower (62 %, 5.52 MW) and the steam turbine condenser of the TLE heat recovery section (23 %, 2.05 MW). Additionally, 0.16 MW MT and 3.16 MW HT level heat are available. The medium temperature heat comes from the cooling of the flue gases before exiting the stack, while the high temperature heat comes from the tar burner and the primary fractionation of the product recovery section.

Concerning the heating demand of the pyrolysis path, it has a lower MT level heat demand (0.54 MW) in comparison with the MTO loop, with 54 % of the heat demand coming from the C3-splitter reboiler in the hydrocarbon fractionation section. The available MT and HT level cooling duty (3.78 MW in total) is sufficient to cover the MT heat demand, leaving 3.24 MW for other heating purposes in the plant.

In contrast to the MTO path, in which no HT level heat is needed, 5.03 MW HT heat are required for the pyrolysis loop, with the MP-steam generator being the biggest HT heat

consumer (4.42 MW) in the loop. As it can be seen in Figure 63, the available cooling duty in the pyrolysis loop is not sufficient for covering the heating demand in the loop.

Although the internal heat recovery in a conventional steam cracking plants is very efficient [14, p. 513], this seems not to be the case if plastic is used instead of naphtha. Possible reasons for this are the higher steam to feed ratio in the pyrolysis reactor and higher pyrolysis heat demand for plastic waste. Therefore, the remaining heat demand, especially for the MP-steam generator, has to be supplied externally. For the simulation, a heat supply through natural gas burner was assumed. The resulting carbon footprint for the combustion was considered in the material balance. The remaining heat (0.72 MW) can be covered by the available HT cooling duty (3.16 MW).

In summary, the combustion loop has a better performance in comparison to the pyrolysis loop with respect to the energy demand. Although the MTO has higher heating demand, these are in a lower temperature level, and they can be fully covered by the available cooling duty in other parts of the process. This is not the case for the pyrolysis path, which requires external heating resources due to its HT heat demand. However, the LT and MT cooling duties in the MTO path are very high, which could lead to expensive cooling systems if there is no possibility to use the heat for other external processes (e.g., district heating or heat pumps).

Comparing both thermal duty and power demand in both loops, it can be said that the combustion loop has a better performance regarding the thermal energy demand but requires by far more external power than the chemical recycling loop. Although the heating demand can be fully covered by the available cooling duty, the MTO path requires additional 68.33 MW electrical power, while the pyrolysis path additional energy requirements are only 1.32 MW and 4.42 MW (MP-steam generator) for the power and thermal duty respectively.

4.1.3 Technology Readiness Level

The results for the evaluation of the TRL of the recycling loops is presented in Table 13. The technologies present in the loops were rated separately and three representative numbers for each loop were obtained.

Table 13: Results of the TRL evaluation for the investigated recycling loops.

Pyrolysis	TRL	MTO	TRL
Pyrolysis reactor	3	Grate firing	9
TLE	9	Flue gas purification	9
Quench section	9	CCU	9
Compression section	9	Methanol synthesis loop	9
Hydrocarbon fractionation	9	MTO section	9
		Compression section	9
		Hydrocarbon fractionation	9
Min TRL	**3**	**Min TRL**	9
Max TRL	**9**	**Max TRL**	9
Average TRL	**7.8**	**Average TRL**	9

As shown in Table 13, the TRL results for the chemical recycling loop (pyrolysis path) are lower than the numbers in the combustion loop. The main reason for this is the pyrolysis reactor in the chemical recycling loop, which, in the particular case of plastic

pyrolysis with steam and at the current date of this work, exits only at laboratory scale. In comparison, the employed technologies used for the combustion loop exist in a plant scale already, with the methanol synthesis loop with CO_2 hydrogenation being the newest one.

In conclusion, it can be said that the chemical recycling loop technology maturity is lower than in the combustion loop, principally due to the chosen technology for the pyrolysis reactor. However, this only applies for the one step pyrolysis of plastic waste. Regarding the two-step plastic pyrolysis described in chapter 2.5.1.1, projects have been carried out in the recent years, e.g., the quanta fuel project for plastic recycling with pyrolysis [85]. As stated in previous chapters, the one step pyrolysis process was chosen to maximize the olefin production. Therefore, a bigger gap in the product yield between the loop should be expected, if the two-step pyrolysis alternative is selected.

Additionally, it is important to remark that although all technologies in the MTO process have been individually successfully applied as plant projects, some of the technologies, such as the electrolysis unit and the methanol synthesis through CO_2 hydrogenation, have not been yet fully optimized and require further development.

4.2 Economical Evaluation

The results for the capital costs of the equipment are presented in this chapter. For visualization purposes, the costs for each loop are divided into different sections. The chemical recycling loop is divided into 5 sections. The reactor section contains the cost for the pyrolysis reactor, the cyclone and the TLE. The quenching section consist of both the oil and water quench plus the dilution steam cycle. The compression section comprises the compressors in the DWSIM simulation (purification unit). The hydrocarbon fractionation consists of the 6 distillation columns, the PSA hydrogen purification unit, and the acetylene reactor. The energy recovery costs consider the tar burner and the TLE steam turbine. The results for the chemical recycling loop are depicted in Figure 64.

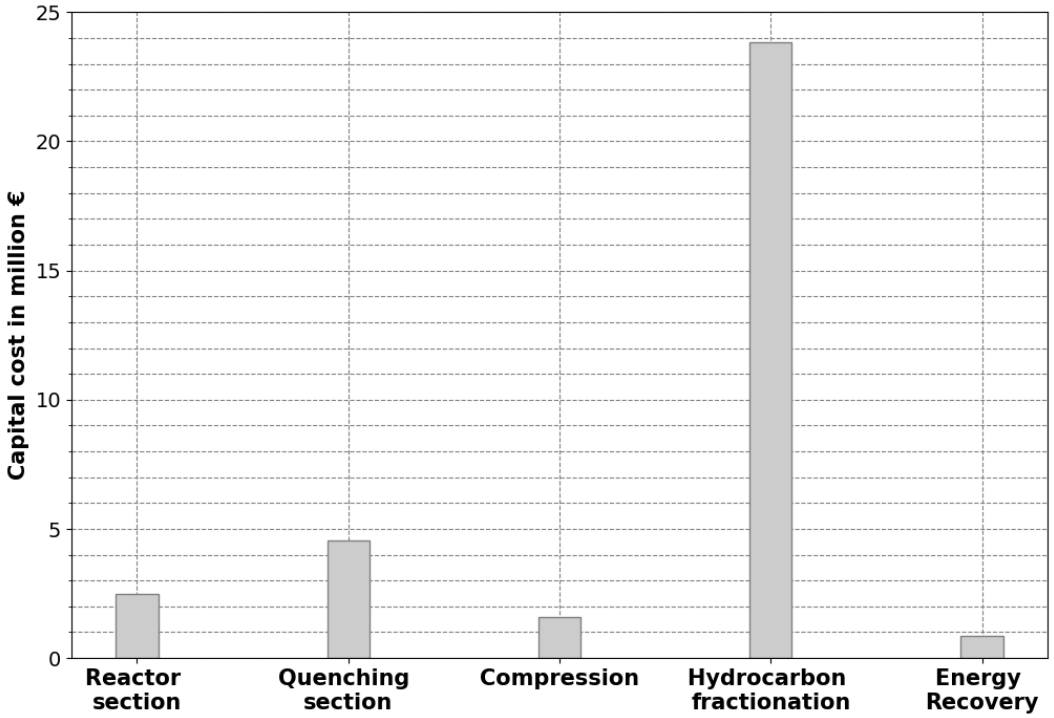

Figure 64: Capital cost for the different sections in millions € for the chemical recycling loop.

As presented in Figure 64, the major capital costs for the chemical recycling loop come from the hydrocarbon fractionation section (23.83 million €), which represents 71 % of the total costs of the loop, with the C3-splitter distillation column being the most expensive equipment in the section (8.54 million €). The second largest capital cost comes from the quenching section, with 4.56 million €.

For the combustion loop, the costs are divided according to the different unit operations in the EBSILON simulation. Additionally, the MTO unit was divided into the MTO section (reactor and regenerator), and the water quench section (water quench tower plus steam stripper). Analogous to the chemical recycling loop, the purification unit was divided into compression section and hydrocarbon fractionation. The energy recovery costs comprise the additional gas burners and the steam turbines.

The results for the capital cost of the combustion loop equipment are presented in Figure 65.

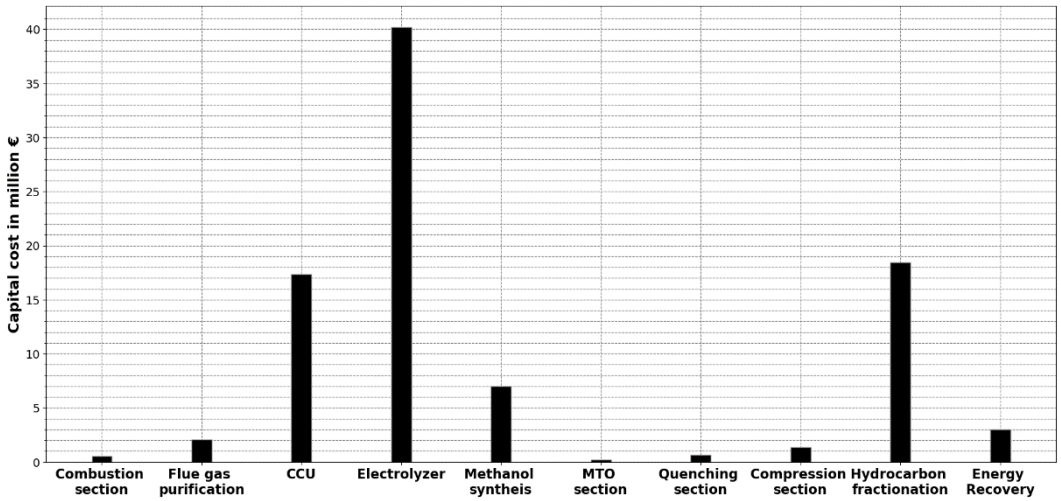

Figure 65: Capital costs in the different sections of the combustion loop in million €.

Regarding the investment costs in the combustion loop, the electrolysis unit has the highest capital cost (40.17 million €), making 41 % of the total capital cost of the loop, followed by the hydrocarbon fractionation section, with 18.45 million € equipment capital cost. In contrast to the chemical recycling loop, the most expensive unit in the combustion loop is the most energy consuming as well (see chapter 4.1.2).

For comparison of both recycling loops, the total capital cost of the plant equipment is considered. Additionally, the equivalent sections of both loops (quenching, compression, hydrocarbon fractionation and energy recovery) are compared separately. These sections have very similar equipment and process layout in both loops. The results for these sections for the two investigated loops are presented in Figure 66.

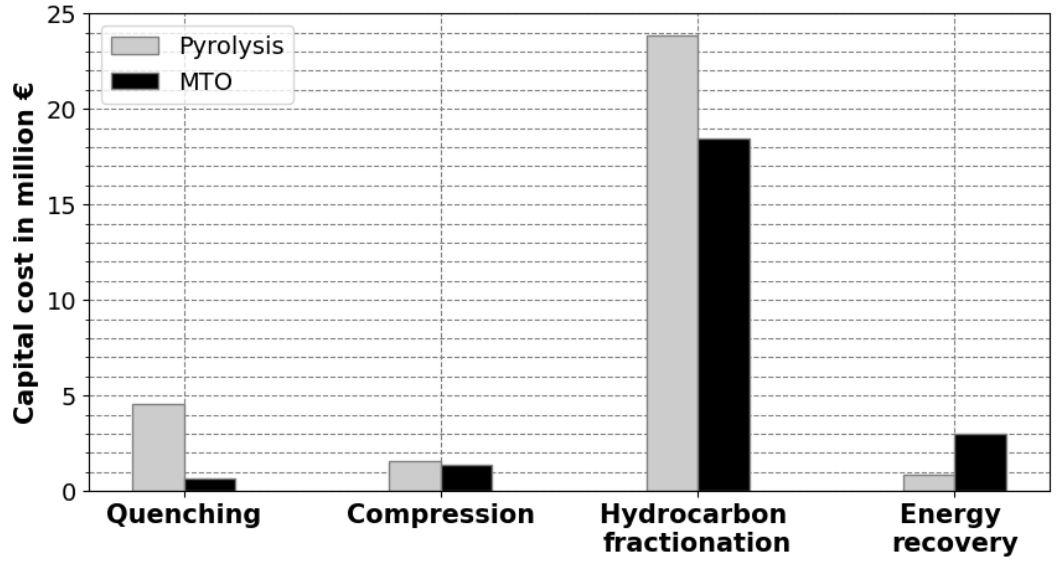

Figure 66: Comparison of the capital cost for the equivalent sections in both recycling loops.

When comparing the cost of the equivalent sections of both loops, it can be seen that the costs in the chemical recycling loop are higher, excepting the energy recovery section. The biggest difference can be found in the hydrocarbon fractionation and the quenching section, with a difference of 5.37 and 4.05 million € respectively. Regarding

the quenching section, the difference relies in the complexity of the pyrolysis quenching, as a primary fractionation and the dilution steam cycle are required. These processes are not present in the MTO unit of the combustion loop.

Respecting the hydrocarbon fractionation, the same explanation applies, as this process requires additional units in the pyrolysis loop (hydrogen purification, acetylene reactor, debutanizer column) that are not presented in the MTO path. Furthermore, as the product from the MTO reactor has higher concentrations of olefins, the distillation columns are smaller than in the chemical recycling loop. In case of the Energy recovery section, the higher price in the MTO path is caused by the higher amounts of available energy for recovery, which results in higher sizes and costs for the turbines in the Rankine cycles.

The results for the total capital costs of both loops are depicted in Figure 67.

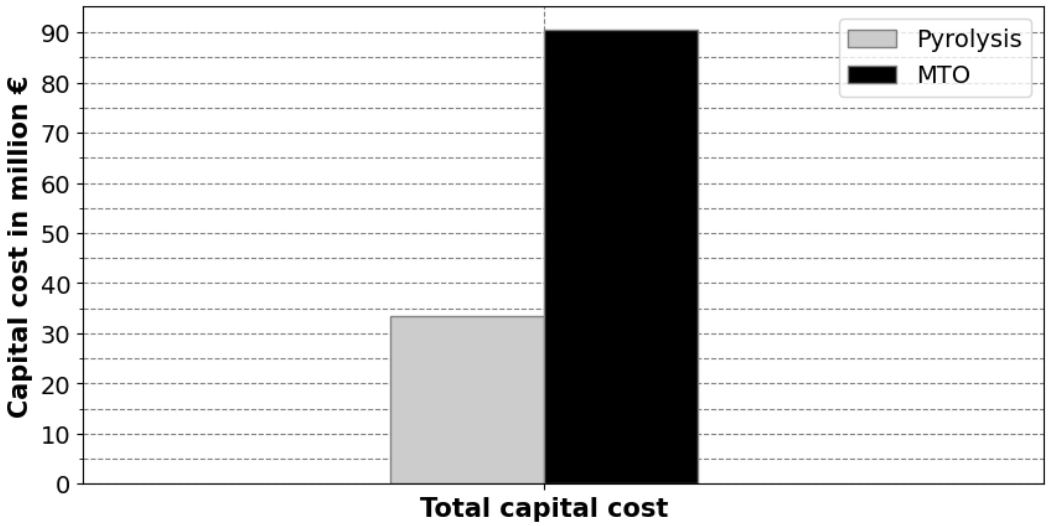

Figure 67: Comparison of the total capital cost and their cost reduction alternatives for both recycling loops.

As it can be seen in Figure 67, although the comparison for the equivalent loop sections results in lower costs for the MTO path, the results for the total capital costs show that the investment for the combustion loop is almost 3 times the amount of the cost for the chemical recycling loop, with a difference of 57.33 million €.

To sum up, it can be said that regarding the investment costs, the chemical recycling loop is by far more feasible than the combustion loop. Reason for this is the higher complexity of the combustion loop, which combines 4 different processes (combustion, carbon capture, methanol synthesis and MTO), while the chemical recycling loop consists only of one single process (steam cracking of plastic). Additionally, it has to be pointed out that the pyrolysis loop requires additional pretreatment (e.g. shredding, washing) before entering the first unit operation, which is not the case of the combustion loop. The consideration of these additional units could decrease the economical and energetical gap between the loops. However, as these units are outside the system boundary, they were not considered in this work.

5 Conclusions and Outlook

Two different recycling loops are compared in this work. The main aspects for the comparison were the product yield, the energy demand, the capital cost and the TRL. The basis for the comparison, are the results obtained in the process simulation, which was performed in EBSILON und DWSIM. The summary of the comparison is presented in Table 14. The "+" sign represents that the loop has an advantage in the regarding criterion, while the "-" sign means a disadvantage. The sign "++" is placed in case that the difference in the criterion is very notorious.

Table 14: Summary of the comparison between the two investigated recycling loops.

Criteria	Chemical recycling loop	Combustion loop (with electrolysis)
Product yield	-	+
Energy demand	++	-
Carbon footprint	-	+
Capital cost	++	-
TRL	-	+

As the overall ratings are quite balance, it is not quite clear which alternative is absolutely better. The combustion loop is superior to the chemical recycling loop regarding the product yield and the carbon footprint, although the difference between both loops is not very significant as in other aspects. It is important to remark that the chemical recycling loop has a very poor propylene product yield compared to the combustion loop. In case of ethylene, the yields are in a close range, although the combustion loop yield remains higher.

The biggest differences between the loops appear in the energy demand and the capital costs, in which the chemical recycling loop requires by far less energy and less investment compared to the combustion loop. The main reason for this is the big hydrogen demand for the CO_2 hydrogenation in the combustion loop. The hydrogen production through electrolysis requires high amounts of energy and is the most expensive unit in the loop.

Some alternatives to reduce the cost and energy demand in the loops are briefly mentioned. Regarding the combustion loop, the main issue is the hydrogen demand in the loop. A potential alternative to the CO_2 hydrogenation for the methanol synthesis could be the gasification of plastic. This technology would allow to use the hydrogen contained in the plastic feed by producing syngas, which is wasted in the combustion process as it is oxidized to water. By using this alternative, the external hydrogen demand could be suppressed (or at least reduced).

Another advantage of implementing this variant is the presence of CO in the syngas, which would avoid the reduction of the catalyst activity during the methanol synthesis. Furthermore, as the methanol synthesis is carried out usually with syngas, it would be theoretically possible to use current methanol plants for feedstock recycling of plastic, assuming that the quality of the syngas is suitable for the process.

Regarding the cost and energy reduction in the chemical recycling loop, the costs can be reduced if existing installations for the hydrocarbon fractionation in a steam cracking plant are used, as this section has by far the highest investment costs in the loop. Alternatively, the high temperature pyrolysis process could be replaced by a two-step pyrolysis process as described in chapter 2.5.1. This would allow to produce a naphtha-

like pyrolysis product, which could be further processed in a conventional steam cracking plant. However, as a gaseous fraction would be produced as a side product during the first pyrolysis step, the effort would be mitigated by reducing the product yield, which would increase the gap between the loops in favor of the combustion loop.

Regarding the technology maturity of the processes used in the loops, it indicates that the TRL of the combustion loop is better than in the chemical recycling loop. This occurs mainly due to the fact that every single technology used in the MTO process has been already applied at plant scale. This is not the case with the chemical recycling loop, in which the main technology (pyrolysis reactor using steam) has been tested just until laboratory scale (although plant and pilot scale projects have been executed for other alternatives of the process).

Summarizing, the combustion loop is superior that the chemical recycling loop regarding the product yield, the carbon footprint, and the technology maturity. The chemical recycling loop has lower costs and energy consumption. However, it is important to remark that the difference between the energy demand and the investment costs between the loops are very high, resulting in better product yield and less carbon footprint at the expense of a higher energy consumption, higher investment costs and more complexity in the process development.

References

[1] V. Voet, J. Jager and R. Folkersma, Plastics in the Circular Economy, Berlin: Walter de Gruyter GmbH, 2021.

[2] J. Aguado and D. P. Serrano, Feedstock Recycling of Plastic Wastes, Cambridge: The Royal Society of Chemistry, 1999.

[3] Plastics Europe, "The Circular Economy for Plastics," Plastics Europe AISBL, Brussels, 2022.

[4] A. Buekens, "Introduction to Feedstock Recycling of Plastics," in *Feedstock Recycling and Pyrolysis of Plastic Waste*, Chichester, John Wiley & Sons Ltd, 2006, pp. 1-43.

[5] R. Sadeghbeigi, Fluid Catalytic Cracking Handbook, Oxford: Elsevier Inc., 2020.

[6] E. Breitmaier and G. Jung, Organische Chemie, Stuttgart: Georg Thieme Verlag, 1978.

[7] U. R. Chaudhuri, Fundamentals of Petroleum and Petrochemical Engineering, Boca Raton, Florida: CRC Press, 2011.

[8] A. Ashraf and A. Aftab, "Distillation process of Crude oil," *Research Gate,* 14 04 2014.

[9] A. Nag, Hydrocarbon Processing, Boca Raton, Florida: CRC Press, 2023.

[10] D. Seddon, Petrochemical Economics, London: Imperial College Press, 2010.

[11] B. Crynes, L. F. Albright and L.-F. Tan, "Thermal Cracking," in *Encyclopedia of Physical Science and Technology*, California, USA, Academic Press, 2003, pp. 613-626.

[12] P. Tian, Y. Wei, M. Ye and Z. Liu, "Methanol to Olefins (MTO): From Fundamentals to comercialization," *ACS Catalysis,* vol. 5, pp. 1922-1938, 2015.

[13] M. Regel-Rosocka, "Technology of simple hydrocarbon intermediates," in *Chemical Technologies and Processes*, Berlin,Boston, Walter de Gruyter, 2020, pp. 65-101.

[14] H. Zimmermann and R. Walzl, "Ethylene," in *Ullman's Encyclopedia of Industrial Chemistry*, vol. 13, Weinheim, Wiley-VCH Verlag, 2012, pp. 465-529.

[15] T. Ren, M. Patel and K. Blok, "Olefins from conventional and heavy feedstocks: Energy use in steam cracking and alternative processes," *Energy,* vol. 31, pp. 425-451, 2006.

[16] K. Kolmetz, "Ethylene quench water tower selection, sizing and troubleshooting," *Research Gate,* 2014.

[17] K. Kolmetz, C. D. Nolidin and Z. Mustaffa, "Improve the Reliability of High Flux Reboilers, A Treatment Approach for Dilution Steam Generator (DSG) Reboilers in Ethylene Plants," *Research Gate,* 2018.

[18] O. D. Khold, M. Parhoudeh and M. R. Rahimpour, "A new configuration in the tail-end acetylene hydrogenation reactor to enhance catalyst lifetime and performance," *Journal of the Taiwan Institute of Chemical Engineers,* vol. 65, pp. 8-21, 2016.

[19] C. D. Chang, "Methanol to Gasoline and Olefins," in *Methanol Production and Use*, New York, Basel, Hong Kong, Marcel Dekker, Inc., 1994, pp. 133-175.

[20] M. R. Gogate, "Methanol-to-olefins process technology: current status and future prospects," *Petroleum Science and Technology,* vol. 37, no. 5, pp. 559-565, 2019.

[21] F. J. Keil, "Methanol-to-hydrocarbons: process technology," *Microporous and Mesoporous Materials,* vol. 29, pp. 49-66, 1999.

[22] M. Ye, H. Li, Y. Zhao, T. Zhang and Z. Liu, "MTO Processes Development: The Key of Mesoscale Studies," *Advances in Chemical Engineering,* vol. 47, pp. 279-335, 2015.

[23] B. V. Vora, T. L. Marker, P. T. Barger, H. R. Nilsen, S. Kvisle and T. Fuglerud, "Economic Route for Natural Gas Conversion to Ethylene and Propylene," in *Natural Gas Conversion IV*, Amsterdam, ELSEVIER SCIENCE B.V. , 1995, pp. 87-99.

[24] P. Eisele and R. Killpack, "Propene," in *Ullmann's Encyclopedia of Industrial Chemistry*, vol. 30, Weinheim, Wiley-VCH Verlag, 2012, pp. 281-293.

[25] R. Klein, Laser Welding of Plastics, Weinheim: Wiley-VCH Verlag & Co. KGaA, 2012.

[26] Plastics Europe, "Polyolefins," 2023. [Online]. Available: https://plasticseurope.org/plastics-explained/a-large-family/polyolefins-2/. [Accessed 26 02 2023].

[27] D. B. Malpass, Introduction to Industrial Polyethylene, Massachusetts: Scrivener Publishing LLC., 2010.

[28] N. Rudolph, R. Kiesel and C. Aumnate, Understanding Plastics Recycling, Munich: Carl Hanser Verlag, 2017.

[29] M. E. Callapez, "History of the beginnings of the plastics industry in Portugal," *ChemTexts,* vol. 7, p. 17, 2021.

[30] Plastics Europe, "Plastics- the Facts 2022," PlasticsEurope AISBL, Brussels, 2022.

[31] M. Negrete-Cardoso, G. Rosano-Ortega, E. Alvarez-Aros, M. E. Tavera-Cortés, C. A. Vega-Lebrún and F. J. Sánchez-Ruíz, "Circular economy strategy and waste management: a bibliometric analysis in its contribution to sustainable development, toward a post-COVID-19 era," *Environmental Science and Pollution Research ,* p. 61729–61746, 12 01 2022.

[32] Ellen MacArthur Foundation, "Towards a Circular Economy: Business Rationale For an Acelerated Transition," 2015. [Online]. Available: https://ellenmacarthurfoundation.org/towards-a-circular-economy-business-rationale-for-an-accelerated-transition. [Accessed 01 03 2023].

[33] L. Wolters, J. van Marwick, K. Regel, V. Lackner and B. Schäfer, Eds., Kunstoff Recycling, München: Carl Hanser Verlag, 1997.

[34] C. M. Simon, W. Kaminsky and B. Schlesselmann, "Pyrolysis of polyolefins with steam to yield olefins," *Journal of Analytical and Applied Pyrolysis,* vol. 38, pp. 75-87, 1996.

[35] J. Scheirs, "Overview of Commercial Pyrolysis Processes for Waste Plastics," in *Feedstock Recycling and Pyrolysis of Waste Plastics*, Chichester, John Wiley & Sons Ltd, 2006, pp. 383-435.

[36] W. Kaminsky, "The Hamburg Fluidized-bed Pyrolysis Process to Recycle Polymer Waste and Tires," in *Feedstock Recycling and Pyrolysis of Waste Plastics*, Chichester, John Wiley & Sons Ltd, 2006, pp. 475-493.

[37] W. Kaminsky, "Pyrolyse von Kunstoffabfällen und Altreifen," in *Pyrolyse von Abfällen*, Berlin, EF-Verlag, 1985, pp. 166-195.

[38] F. Joos, Technische Verbrennung, Berlin, Heidelberg: Springer-Verlag, 2006.

[39] R. Günther, Verbrennung und Feuerungen, Berlin, Heildelberg: Springer Verlag, 1974.

[40] M. Kranert and K. Cord-Landwehr, Einführung in die Abfallwirtschaft, Wiesbaden: Vieweg+Teubner Verlag, 2010.

[41] Europäische Kommission, "SCHLUSSFOLGERUNGEN ZU DEN BESTEN VERFÜGBAREN TECHNIKEN (BVT) FÜR DIE ABFALLVERBRENNUNG," in *DURCHFÜHRUNGSBESCHLUSS (EU) 2019/2010 DER KOMMISSION vom 12. November 2019 über Schlussfolgerungen zu den besten verfügbaren Techniken (BVT) gemäß der Richtlinie 2010/75/EU des Europäischen Parlaments und des Rates in Bezug auf die Abfallverbrennung*, Brüssel, Amtsblatt der Europäischen Union , 2019, pp. 56-92.

[42] M. Schultes, Abgasreinigung, Berling, Heidelberg: Springer Verlag, 1996.

[43] J. M. Ketzer, R. S. Iglesias and S. Einloft, "Reducing Greenhouse Gas Emissions with CO2 Capture and Geological Storage," in *Handbook of Climate Change Mitigation*, New York, Springer Science+Bussines Media, 2012, pp. 1407-1443.

[44] L. E. Øi, "CO2 removal by absorption: challenges in modelling," *Mathematical and Computer Modelling of Dynamical Systems,* vol. 16, no. 6, pp. 511-533, 2010.

[45] U. Desideri and A. Paolucci, "Performance modelling of a carbon dioxide removal system for Power Plants," *Energy Conversion & Management,* vol. 40, pp. 1899-1915, 1999.

[46] D. Wappel, G. Gronald, R. Kalb and J. Draxler, "Ionic liquids for post-combustion CO2 absorption," *International Journal of Greenhouse Gas Control,* vol. 4, pp. 486-494, 2010.

[47] P. Markewitz and R. Bongartz, "Carbon Capture Technologies," in *Carbon Capture, Storage and Use*, Switzerland, Springer International Publishing, 2015, pp. 13-47.

[48] R. Sakwattanapong, A. Aroonwilas and A. Veawab, "Behavior of Reboiler Heat Duty for CO2 Capture Plants Using Regenerable Single and Blended Alkanolamines," *Industrial & Engineering Chemistry Research,* vol. 44, no. 12, pp. 4465-4473, 2005.

[49] M. Fang and D. Zhu, "Chemical Absorption," in *Handbook of Climate Change Mitigation*, New York, Springer Science+Business Media, 2012, pp. 1441-1515.

[50] M. Rzelewska-Piekut and M. Regel-Rosocka, "Technology of large volume alcohols, carboxylic acids and esters," in *Chemical Technologies and Processes*, Berlin,Boston, Walter de Gruyter, 2020, pp. 101-147.

[51] R. J. Da Silva and C. J. A. Mota, "CO2 Hydrogenation to Methanol and Dimethy Ether," in *Carbon dioxide Utilization*, Berlin, Boston, Walter de Gruyter, 2019, pp. 345-361.

[52] J. R. LeBlanc, R. V. Schneider and R. B. Strait, "Production of Methanol," in *Methanol Production and Use*, New York, Marcel Dekker, 1994, pp. 51-133.

[53] D. Mignard, M. Sahibzada, J. M. Duthie and H. W. Whittington, "Methanol synthesis from ue-gas CO2 and renewable electricity: a feasibility study," *Inernational Journal of Hydrogen Energy,* vol. 28, pp. 455-464, 2003.

[54] É. S. Van-Dal and C. Bouallou, "Design and simulation of a methanol production plant from CO2 hydrogenation," *Journal of Cleaner Production,* vol. 57, pp. 38-45, 2013.

[55] J. Q. Chen, A. Bozzano, B. Glover, T. Fuglerud and S. Kvisle, "Recent advancements in ethylene and propylene production using the UOP/Hydro MTO process," *Catalysis Today,* vol. 106, pp. 103-107, 2005.

[56] D. Luna Victoria Torres, "Erstellung eines Modells für die Abfallverbrennung mit sauerstoffangereicherter Luft," HAW-Hamburg, Hamburg, 2021.

[57] Aero Check, "Die relative Luftfeuchtigkeit in Deutschland (mit Tabelle)," Monocal OÜ, 2023. [Online]. Available: https://aero-check.de/luftfeuchtigkeit/deutschland/. [Accessed 21 05 2023].

[58] G. Erfani, C. Lowe and J. Mayourian, "Ethylene Production Plant Design," Cooper Union for the Advancement of Science and Art, New York, 2014.

[59] W. Jerzak, M. Reinmöller and A. Magdziarz, "Estimation of the heat required for intermediate pyrolysis of biomass," *Clean Technologies and Environmental Policy,* vol. 24, p. 3061–3075, 2022.

[60] K. Lucas, Thermodynamik, Berlin, Heidelberg: Springer Verlag, 2006.

[61] AFRY Deutschland, "Reference Project (confidential)," AFRY Deutschland, Hamburg, 2023.

[62] S.-Y. Lee, J.-M. Lee, D. Lee and I.-B. Lee, "Improvement in Steam Stripping of Sour Water through an Industrial-Scale Simulation," *Korean Journal of Chemical Engineering,* vol. 21, no. 3, pp. 549-555, 2004.

[63] B. Lohrengel , Einführung in die thermischen Trennverfahren, München: Oldenbourg Wissenschaftsverlag, 2012.

[64] M. Nitsche, Kolonnen-Fibel, Berlin, Heidelberg: Springer Verlag, 2014.

[65] E. A. Porter, "DISTILLATION," THERMOPEDIA A-to-Z Guide to Thermodynamics, Heat & Mass Transfer, and Fluids Engineering, 02 02 2011. [Online]. Available: https://www.thermopedia.com/content/703/. [Accessed 15 06 2023].

[66] A. K. Coker , Ludwig's Applied Process Design for Chemical and Petrochemical Plants, Oxford: Elsevier, 2015.

[67] Impact Energy, "Kälteanlagen in der Industrie," 2022. [Online]. Available: https://www.topmotors.ch/sites/default/files/2018-08/D_MB_27_Kaelteanlagen.pdf. [Accessed 26 05 2023].

[68] W. L. Luyben, "Comparison of a conventional two-column demethanizer/deethanizer configuration requiring refrigerated condensers with a nonconventional column/rectifier configuration," *Journal of Chemical Technology and Biotechnology,* vol. 91, pp. 1688-1696, 2016.

[69] F. M. Fabrega, J. S. Rossi and . J. V. d'Angelo, "Exergetic analysis of the refrigeration system in ethylene and propylene production process," *Energy,* vol. 35, pp. 1224-1231, 2010.

[70] A. Anand, V. Kumar and N. Kaistha, "Vapor Recompression C3 Splitter: Design and Control," *International Federation of Automatic Control,* vol. 53, no. 1, pp. 117-122, 2020.

[71] O. Schmitz, Modellbasierte Untersuchung der CO2-Abscheidung aus Kraftwerksabgasen, Wiebaden: Springer Fachmedien, 2016.

[72] A. Schönbucher, Thermische Verfahrenstechnik, Grundlagen und Berechnungsmethoden für Ausrüstungen und Prozesse, Berling, Heidelberg: Springer-Verlag, 2002.

[73] F.-Y. Jou, A. E. Mather and F. D. Otto, "The Solubility of CO2 in a 30 Mass Percent Monoethanolamine Solution," *The Canadian Journal of Chemical Engineering,* vol. 73, no. 1, pp. 140-147, 1995.

[74] K.-E. Wirth, "Druckverlust in durchströmten Schüttungen," in *VDI-Wärmeatlas*, Düsseldorf, VDI-Verlag, 2013, pp. 1275-1279.

[75] L. Chen, Q. Jiang, Z. Song and D. Posarac, "Optimization of Methanol Yield from a Lurgi Reactor," *Chemical Engineering Technology,* vol. 34, no. 5, pp. 817-822, 2011.

[76] J. Zhou, . J. Zhao, J. Zhang, T. Zhang, M. Ye and Z. Liu, "Regeneration of catalysts deactivated by coke deposition: A review," *Chinese Journal of Catalysis,* vol. 41, pp. 1048-1061, 2020.

[77] G. A. Buchner, K. J. Stepputat, A. W. Zimmermann and R. Schomäcker, "Specifying Technology Readiness Levels (TRL) for the Chemical Industry," *Industrial & Engineering Chemistry Research,* vol. 58, p. 6957–6969, 2019.

[78] D. E. Garrett, Chemical Engineering Economics, New York: Van Nostrand Reinhold 1989, 1989.

[79] J. M. Douglas, Conceptual Design of chemical processes, New York: McGraw-Hill, 1988.

[80] M. S. Peters and K. D. Timmerhaus, Plant Design and Economics for Chemical Engineers, New York: McGraw-Hill, 1991.

[81] G. Di Marcoberardino, D. Vitali, F. Spinelli, M. Binotti and G. Manzolini, "Green Hydrogen Production from Raw Biogas: A Techno-Economic Investigation of Conventional Processes Using Pressure Swing Adsorption Unit," *Processes,* vol. 6, no. 19, 2018.

[82] "Techno-economic study of CO2 capture from an existing coal-fired power plant: MEA scrubbing vs. O2/CO2 recycle combustion," *Energy Conversion and Management,* vol. 44, pp. 3073-3091, 2003.

[83] R. Turton, J. A. Shaeiwitz and D. Bhattacharyya, Analysis, Synthesis, and Design of Chemical Processes, Boston: Pearson Education, 2018.

[84] Chemical Engineering, "Economic Indicators," *Chemical Engineering,* p. 48, 2020.

[85] Quantafuel, "Our Technology," [Online]. Available: https://www.quantafuel.com/our-solution/technology. [Accessed 20 06 2023].

Annex 1

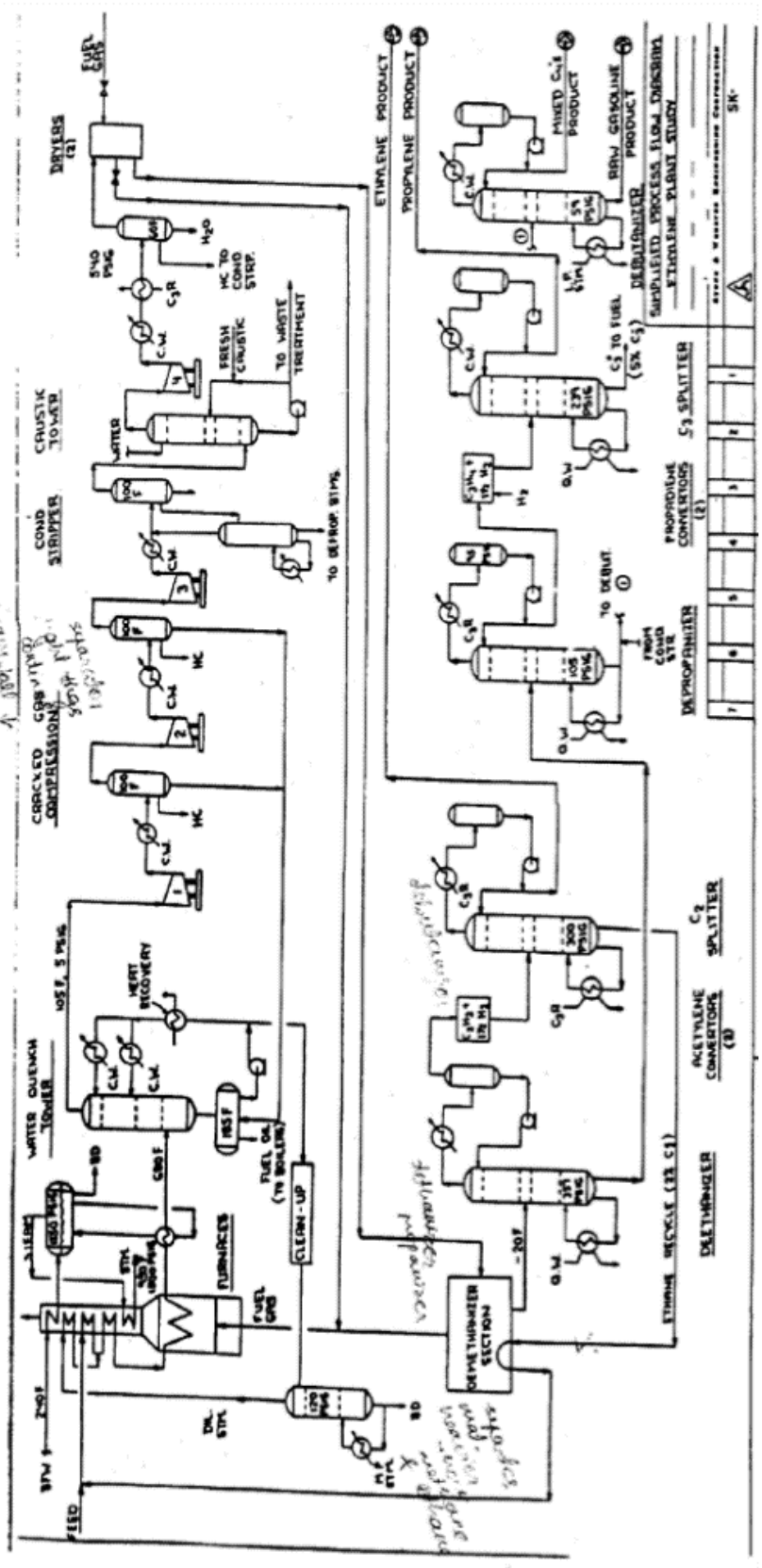

Annex 1: Process flow diagram of an ethylene plant (steam cracking) [57, p. 2].

Annex 2

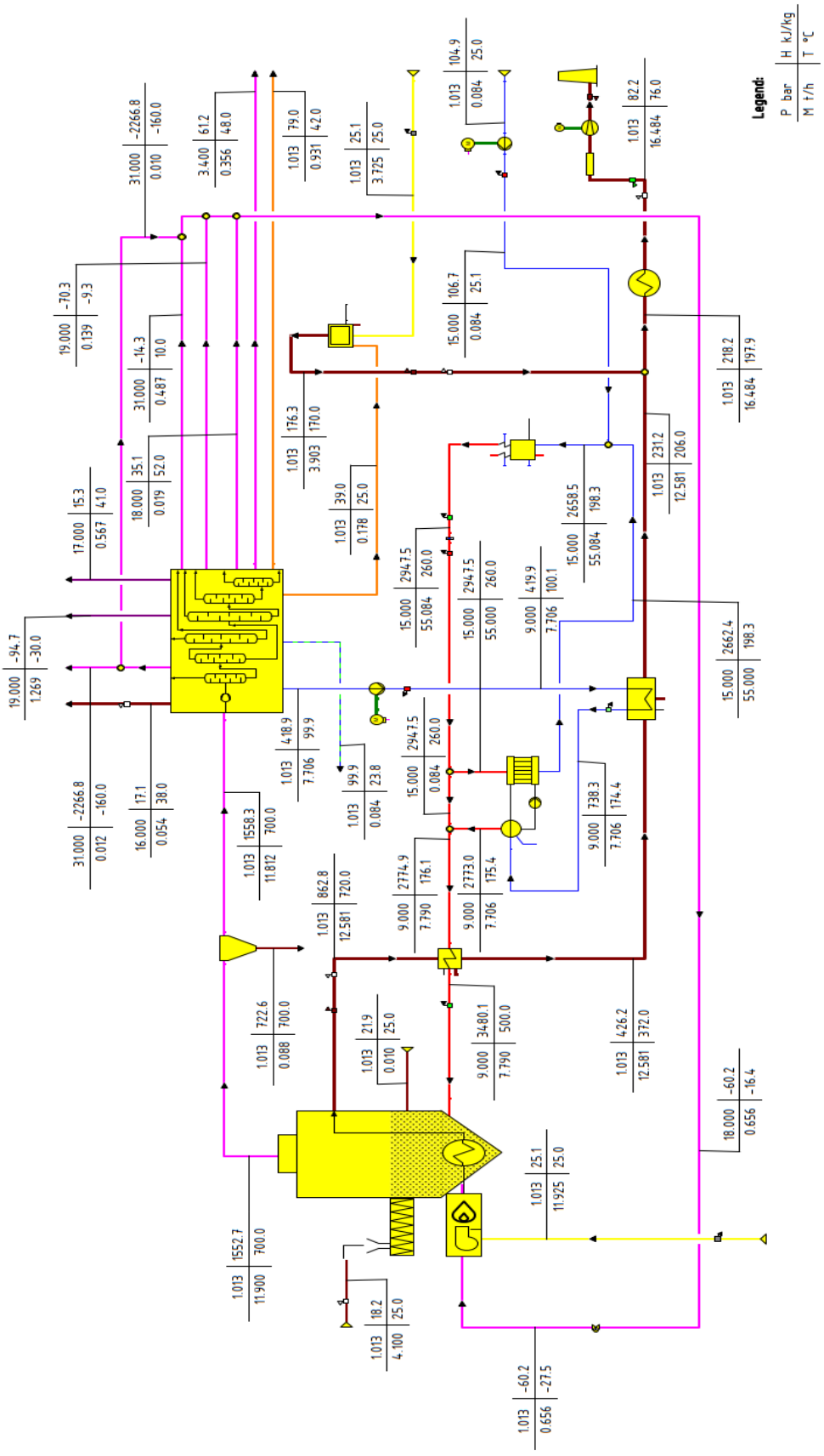

Annex 2: EBSILON simulation results for the chemical recycling loop.

Annex 3

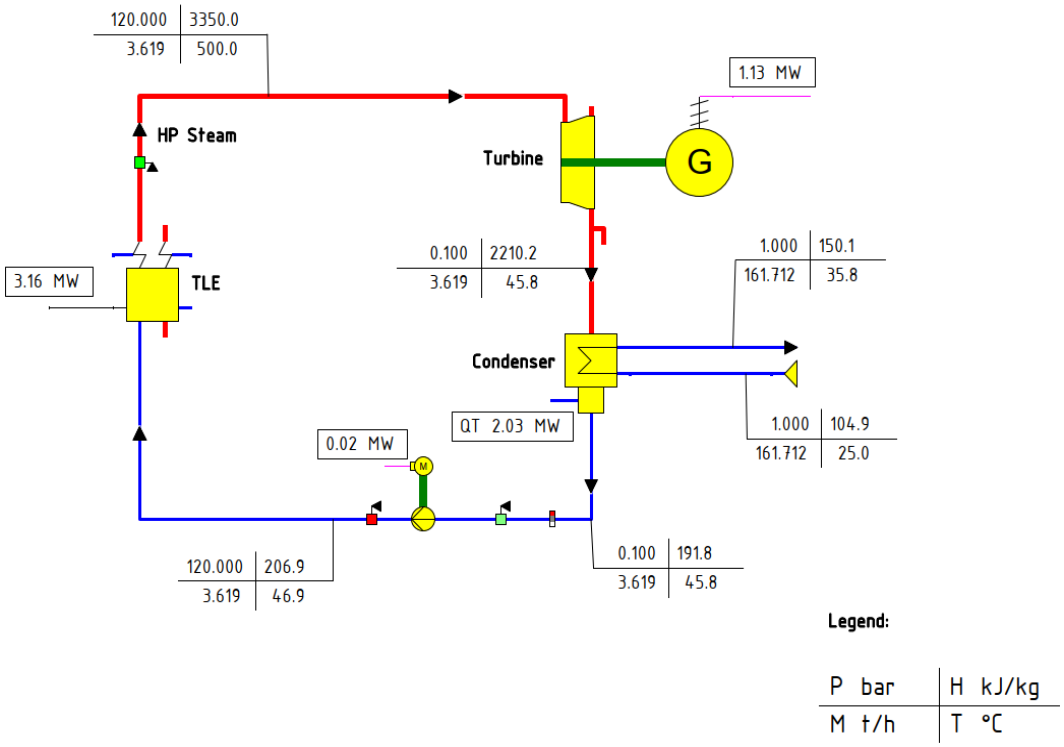

Annex 3: EBSILON simulation results for the TLE heat recovery in the chemical recycling loop.

Annex 4

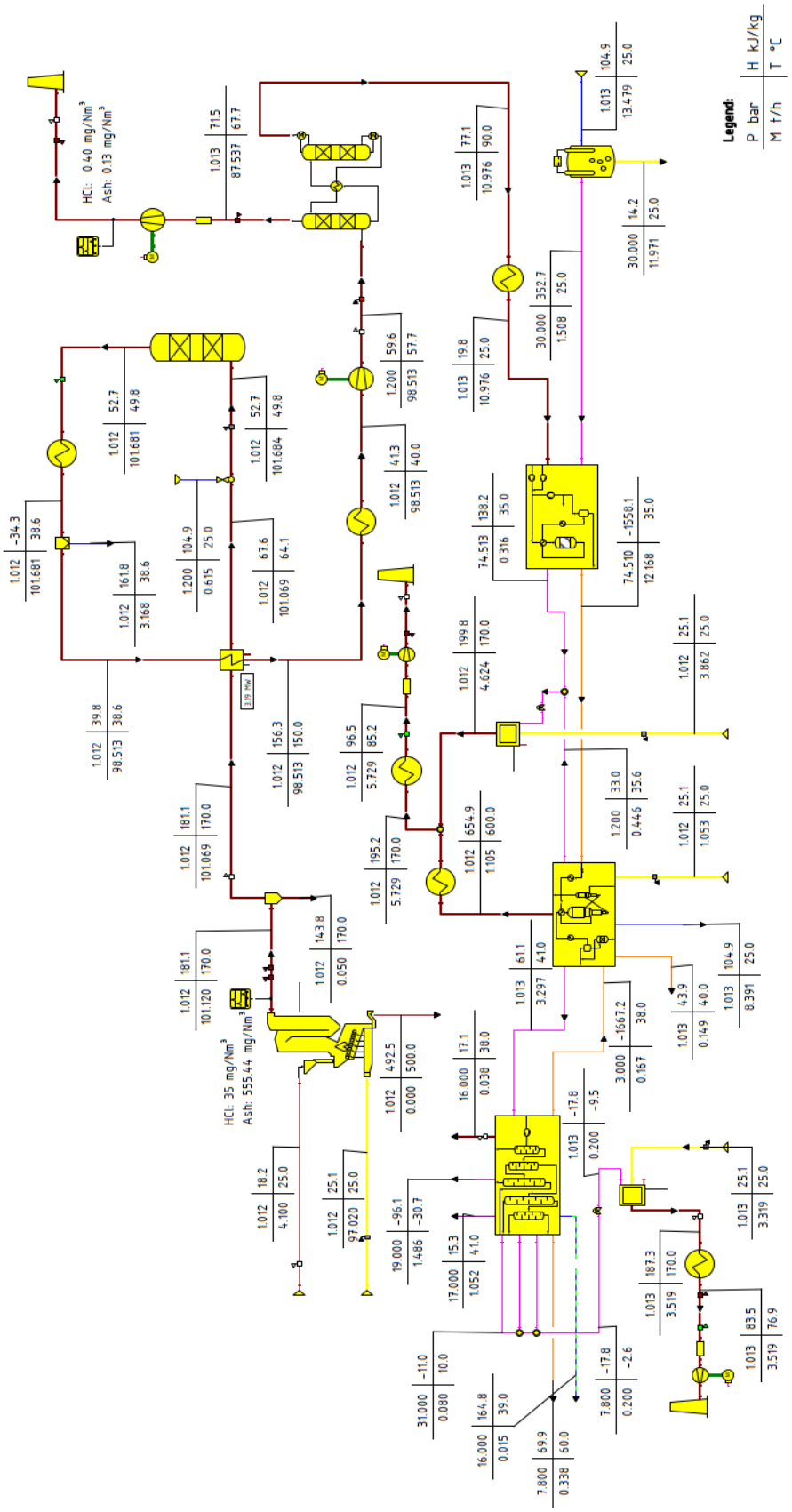

Annex 4: EBSILON simulation results for the combustion loop.

Annex 5

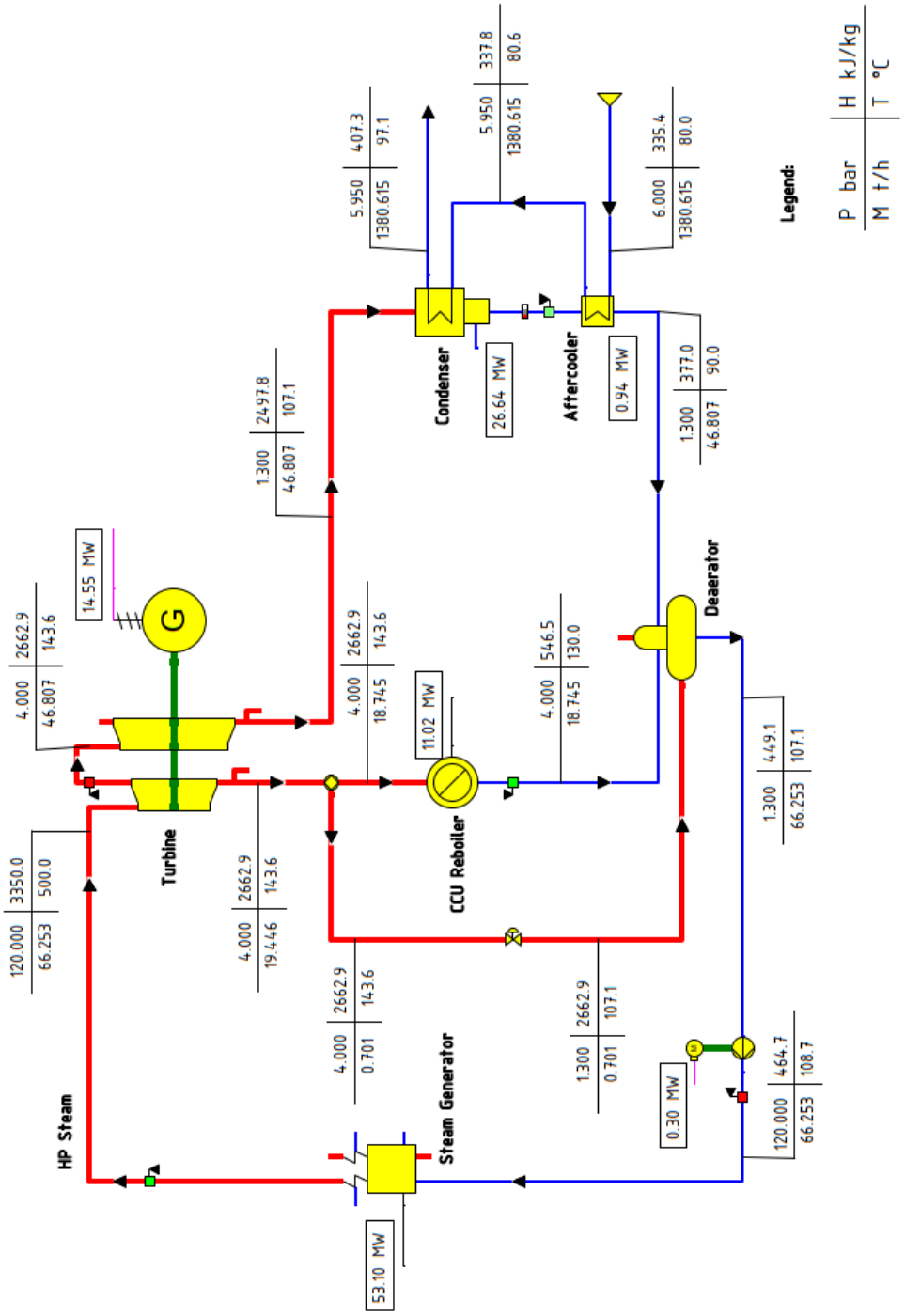

Annex 5: EBSILON simulation results for the combustion loop HRSG.

Annex 6

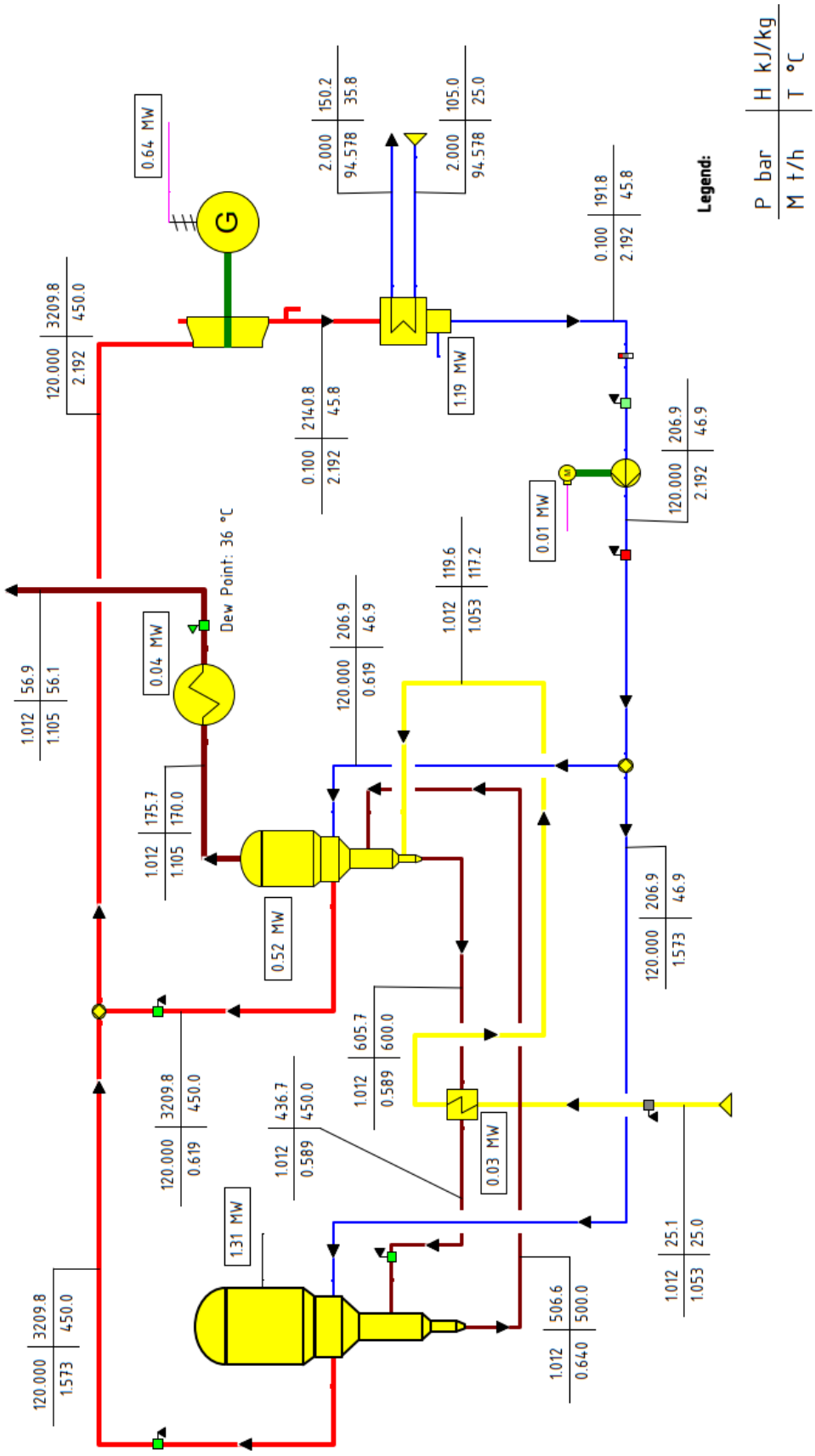

Annex 6: EBSILON simulation results for the MTO reactor and regenerator energy recovery.